

**An investigation of polyamide 6 and 12 synthesis  
in an oscillatory baffled reactor**

**Ross David Frank Laska**

**Thesis submitted for the degree of Doctor of Philosophy  
Centre for Oscillation Baffled Reactor Applications (COBRA)  
School of Engineering and Physical Sciences  
Heriot-Watt University  
March 2019**

The copyright in this thesis is owned by the author. Any quotation from this thesis or use of any of the information contained in it must acknowledge this thesis as the source of the quotation or information.

## Abstract

This work focuses on the investigation of the synthesis of polyamide-12 (PA-12) particles in an oscillatory baffled reactor (OBR) and was funded by Polymer Technology Ltd (PTL). Despite considerable usage in industry, there is very little information available for both synthesis and reaction kinetics of PA-12 synthesis. As a result, the initial effort was directed to the study and the understanding of reaction kinetics and parameters affecting kinetics for the PA-6 synthesis, a sister reaction, for which there are some literature and recipes on public domain.

For the PA-6 reaction, the effects of various operational conditions on molecular weight, particle size and melting point were investigated using the design of experiment (DOE) technique. The results of the DOE studies indicated that temperature, the rate of chain initiator injection and agitation speed had the most influence over specifications of PA-6 particles. A new method for measuring reactant concentration by FTIR was devised, allowing reaction kinetics to be extracted. By switching from a batch to a semi-continuous reactor, the reaction order could change from 1<sup>st</sup> to zeroth, depending on the injection rate and reaction temperature. The biggest deviation from batch conditions was that monomer to catalyst ratio in the semi-continuous reactor did not have any effect over polymer properties.

From the learning of PA-6 synthesis, the PA-12 recipe was formulated and tested. By using continuous injection of the chain initiator and by adding small amounts of caprolactam and N, N-Ethylene bis(stearamide), PA-12 particles were successfully synthesised. As with PA-6, reaction temperature, injection rate and stirring rate had a strong influence over PA-12 particle properties. However, while increasing the injection rate lead to an increase in the size of PA-12 particles it caused PA-6 particles to decrease in size. Provided that the reaction recipe can be developed further to stop the build-up of material between baffle columns the next steps would be study the reaction under continuous conditions.

## Acknowledgements

There are many people I need to thank who have helped me with my research. Without their assistance, this project would not have been a success.

Firstly, I thank my doctoral advisor, Professor Xiongwei Ni for his constant direction, support, patience and for the chance to carry out this enterprise. Furthermore, I need thank the other members in the COBRA group: Juliet Adelakun, Guillermo Jimeno Millor, Meifen Jiang, Arabella, McLaughlin and Francisca Navarro Fuentes for their help and friendship over the course of the project.

Thanks to the technicians, Richard Kinsella and Douglas Wagener for their assistance with experimental apparatus and their friendship. Additionally, thanks to Arno Kraft for allowing me to borrow his spare Schlenk line. Thank you to Cameron Smith for his help in obtaining and ordering the necessary equipment and supplies. Thanks to Andrew Haston for his help with electronic apparatus and in the development of the syringe heater. Additionally, I need to thank Dr Stephen Mansell and Rob Newland for their assistance in teaching me air sensitive chemistry techniques. Thanks to Dr Florin Dan for his invaluable advice in creating a working synthetic route for PA-12. Thank you to Warren Thompson for his help in learning the statistical software Minitab. And thank you to Professor Graeme White for allowing me to borrow his Fume hood.

For making sure that I kept a good balance between work and life I thank Rick, Tom and Murray. And, finally, thanks to my family and my girlfriend Tatiana for their constant backing, encouragement and love throughout this project.

## Research Thesis Submission

Please note this form should be bound into the submitted thesis.

Name:	Ross David Frank Laska		
School:	Engineering and Physical Sciences		
Version: <i>(i.e. First, Resubmission, Final)</i>	Final	Degree Sought:	Doctor of Philosophy, Chemical Engineering

### **Declaration**

In accordance with the appropriate regulations I hereby submit my thesis and I declare that:

1. The thesis embodies the results of my own work and has been composed by myself
2. Where appropriate, I have made acknowledgement of the work of others
3. The thesis is the correct version for submission and is the same version as any electronic versions submitted\*.
4. My thesis for the award referred to, deposited in the Heriot-Watt University Library, should be made available for loan or photocopying and be available via the Institutional Repository, subject to such conditions as the Librarian may require
5. I understand that as a student of the University I am required to abide by the Regulations of the University and to conform to its discipline.
6. I confirm that the thesis has been verified against plagiarism via an approved plagiarism detection application e.g. Turnitin.

### **ONLY for submissions including published works**

Please note you are only required to complete the Inclusion of Published Works Form (page 2) if your thesis contains published works)

7. Where the thesis contains published outputs under Regulation 6 (9.1.2) or Regulation 43 (9) these are accompanied by a critical review which accurately describes my contribution to the research and, for multi-author outputs, a signed declaration indicating the contribution of each author (complete)
8. Inclusion of published outputs under Regulation 6 (9.1.2) or Regulation 43 (9) shall not constitute plagiarism.

\* Please note that it is the responsibility of the candidate to ensure that the correct version of the thesis is submitted.

Signature of Candidate:		Date:	
-------------------------	--	-------	--

### **Submission**

Submitted By <i>(name in capitals)</i> :	ROSS DAVID FRANK LASKA
Signature of Individual Submitting:	
Date Submitted:	

**For Completion in the Student Service Centre (SSC)**

Limited Access	Requested	Yes		No		Approved	Yes		No	
<i>E-thesis Submitted (<b>mandatory for final theses</b>)</i>										
Received in the SSC by ( <i>name in capitals</i> ):						Date:				

# Table of Contents

Abstract.....	I
Acknowledgements.....	II
Thesis Submission Form.....	III
Table of Contents.....	V
List of Tables.....	VIII
List of Figures.....	X
Nomenclature.....	XIII
Acronyms.....	XV
Chapter 1 – Introduction.....	1
1.1-Basis of research.....	1
1.2-Research objectives.....	2
1.3-Structure of the thesis.....	3
Chapter 2 – Literature Review.....	4
2.1-Polymers.....	4
2.1.1-Polymerisation mechanisms.....	6
2.1.1.1-Condensation polymerisation.....	6
2.1.1.2-Chain-Growth Polymerisation.....	6
2.1.2-Methods of Polymerisation.....	7
2.1.2.1-Bulk Polymerisation.....	8
2.1.2.2- Solution/precipitation polymerisation.....	8
2.1.2.3-Suspension polymerisation.....	9
2.1.2.4-Emulsion polymerisation.....	10
2.1.3-Nylon.....	11
2.1.4-Lactam-polymerisation mechanisms.....	13
2.1.5-Anionic Polymerisation mechanism.....	14
2.1.6-Anionic Polymerisation methods.....	19
2.1.7-Reaction kinetics.....	21
2.1.8-Nylon Particle synthesis.....	26
2.1.9-Polymer development.....	27
2.1.10-Morphology.....	30
2.2-Oscillatory Baffled Reactors.....	33
2.2.1-Background.....	33

2.2.2-Mixing in an OBR.....	34
2.2.3-Fluid mechanics.....	35
2.2.4-Polymerisation using Oscillatory Baffled Reactor.....	39
2.2.5-Power consumption.....	41
Chapter 3 - Experimental setup and procedure.....	43
3.1-Experimental Apparatus.....	43
3.1.1-The Stirred Tank Reactor (STR).....	43
3.1.2-The Oscillatory Baffled Reactor.....	44
3.1.3-The set up for PA-6 equimolar kinetic measurements.....	45
3.2-Reagents.....	46
3.3-Experimental procedures.....	46
3.3.1-Recipe and Procedure for PA-6 synthesis within STR.....	46
3.3.2-Procedure for PA-6 kinetic study in an OBR.....	47
3.3.3- Procedure for equimolar kinetics measurements.....	48
3.3.4-Recipe and Procedure for PA-12 synthesis.....	49
3.4-Measurement tools.....	51
3.4.1-Melting point analysis.....	51
3.4.2-Particle size analysis.....	53
3.4.3-Molecular weight analysis.....	54
3.4.4 Morphology analysis.....	57
3.5-Kinetics study.....	58
Chapter 4 - PA-6 synthesis and kinetics.....	61
4.1 - PA-6 synthesis.....	61
4.1.1-Introduction.....	61
4.1.2-Factorial Design.....	62
4.1.3-Experimental design.....	64
4.1.4-Interpretation of DOE data.....	65
4.1.5 Results and discussion.....	68
4.1.5.1-Effect of factors on the molecular weight.....	68
4.1.5.2-Effect of factors on the melting point.....	72
4.1.5.3-Effect of factors on mean particle size.....	76
4.2-Reaction Kinetics.....	82
4.2.1-Introduction.....	82

4.2.2-Analytical methods.....	83
4.2.3-Results and discussion.....	85
4.2.3.1-Effect of Chain initiator and catalyst concentration.....	94
4.2.3.2-Effect of temperature on reaction kinetics.....	99
4.2.3.3-Effect of mixing on kinetics.....	102
4.3-Conclusions.....	107
4.3.1-Plackett-Burman design conclusions.....	107
4.3.2-Kinetic measurement conclusions.....	107
4.4.-Problems.....	108
4.4.1-PA-6 synthesis.....	108
4.4.2 Kinetics measurements.....	109
Chapter 5 - PA-12 synthesis.....	111
5.1-Introduction.....	111
5.2-Results and discussions.....	111
5.2.1-Development of synthesis route.....	111
5.2.2-Effect of experimental parameters on molecular weight.....	115
5.2.3-Effect of experimental parameters on mean particle size.....	117
5.2.4 Effect of experimental parameters on melting point.....	119
5.2.5 Morphology.....	120
5.3 Conclusions.....	122
5.4 Problems, observations and solutions.....	123
Chapter 6-Conclusions and future work.....	125
6.1 Conclusions.....	125
6.2 Future research.....	128
References.....	131



## List of Tables

Table 2.1 Table of potential catalysts, chain initiators and solvents.....	15
Table 3.1 Physical properties of reagents for PA-6 synthesis.....	46
Table 3.2 Reaction conditions for PA-6 synthesis within OBR.....	48
Table 3.3 The reaction conditions for kinetics studies under equimolar conditions.....	49
Table 3.4 Recipe and physical properties of reagents for PA-12 synthesis.....	49
Table 3.5 PA-12 synthesis reaction parameters.....	50
Table 3.6 Table of CI mixture constituents.....	51
Table 3.7 Particle size distributions of PA-6 and PA-12 samples.....	54
Table 3.8 Molecular weights of PA-6 and PA-12 samples.....	57
Table 3.9 Summary of the calibration curve data.....	60
Table 4.1 List showing how many experiments are required to carry out a full factorial analysis depending on how many variables are present.....	63
Table 4.2 List of different factorial designs and required experiments that can be used to analyse 6 factors.....	64
Table 4.3 Table of variables values and desired responses.....	65
Table 4.4 Plackett-Burman screening design with six variables generated using Minitab software.....	68
Table 4.5 Summary of each model studying the influence of various factors over molecular weight.....	69
Table 4.6 Summary of each model studying the influence of various factors over melting point model.....	73
Table 4.7 Model summaries for each mean particle size model.....	77
Table 4.8 Table of all p-values for all models.....	81
Table 4.9 Table of raw data from DOE investigations (results are not presented in their initial randomised order).....	82
Table 4.10 Table of CI injection rates with corresponding reaction orders and rate constants.....	96
Table 4.11 Table of catalyst volumes with corresponding reaction orders and rate constants.....	99
Table 4.12 Table of reaction temperatures with corresponding reaction orders and rate constants.....	99

Table 4.13 Oscillatory Reynolds numbers for the corresponding oscillation frequency	104
Table 5.1 Percentage yield of PA-12 after 2 hours using different masses of EBS and caprolactam contents. Reaction considered a failure if uncontrollable agglomeration occurred.....	114
Table 5.2. Table displaying the influence of CI injection rate, temperature and mass of EBS on the molecular weight.....	116
Table 5.3 Table displaying the influence of CI injection rate, reaction temperature and mass of EBS on the PA-12 particle size.....	118
Table 5.4 Influence of variables on the PA-12 melting point and degree of crystallinity.....	119

## List of Figures

Figure 2.1 Diagram of suspension polymerisation in action.....	10
Figure 2.2 Representation of emulsion polymerisation in action.....	11
Figure 2.3 Anionic Initiation and Propagation reactions in the polymerisation of un-substituted lactams.....	17
Figure 2.4 Example of potential side reactions that can take place during polymerisation.....	18
Figure 2.5 Adiabatic conversion of nylon-6 with an initial polymerization temperature of 136°C and caprolactam magnesium bromide concentration of 108mmol L <sup>-1</sup> . Isophthaloyl-bis-caprolactam concentrations used were 40mmol L <sup>-1</sup> (lower line), 70mmol L <sup>-1</sup> (middle line) and 100mmol L <sup>-1</sup> (upper line).....	23
Figure 2.6 Adiabatic conversion of nylon-6 experimental data for initial polymerization temperature of 135C with isophthaloyl-bis-caprolactam (chain initiator) concentration of 70mmol <sup>-1</sup> and caprolactam magnesium bromide of 108mmol <sup>-1</sup> (lower curve) and 150mmol <sup>-1</sup> (higher curve).....	25
Figure 2.7 Illustration of the various phases of polymer particle development.....	30
Figure 2.8 SEM image of PA-6 particles: a) PA-6 with defined spherulites resultant from the use of a quick/slow CI/catalyst combination <sup>6</sup> b) PA-6 with a macroporous continuous network resultant from the use of slow/slow or a slow/quick CI/catalyst combination.....	31
Figure 2.9 Eddy formation within an OBR.....	34
Figure 2.10 Flow within a tube with diameter D.....	35
Figure 2.11 Oscillatory motion applied to flow in a tube.....	36
Figure 2.12 Oscillatory baffled flow.....	36
Figure 2.13 Effect of oscillation frequency on mean particle size with a fixed amplitude and baffle width.....	40
Figure 2.14 Effect of amplitude on mean particle size at a fixed frequency and baffle width.....	41
Figure 3.1 Setup for STR. Note that in this setup a syringe was used instead of Teflon tubing. Schlenk line connector not shown.....	43
Figure 3.2 Setup of oscillated baffled reactor, for simplicity the Schlenk line, hairdryer and various seals used were not displayed.....	45
Figure 3.3 In-depth look at the syringe pump and baffle.....	45

Figure 3.4 DSC spectrum showing melting point of all substances in the reaction mixture.....	52
Figure 3.5 DSC spectrum comparing melting point of synthesised PA-6 particles and control PA-6.....	52
Figure 3.6 DSC spectrum comparing melting point of synthesised PA-12 particles and control PA-12.....	53
Figure 3.7 a) Particle size distribution of PA-12 synthesised particles b) Particle size distribution of PA-6 synthesised particles.....	54
Figure 3.8 Average molecular weight distributions based upon two scans of various synthesised PA-12 polymer particles.....	56
Figure 3.9 Molecular weight distributions of various synthesised PA-6 polymer particles.....	56
Figure 3.10 Example SEM images of PA-12.....	58
Figure 3.11. a) FTIR spectra of caprolactam dissolved in ethylbenzene at the beginning of the reaction and b) FTIR spectra of caprolactam dissolved in ethylbenzene near the end of the reaction.....	59
Figure 3.12* Calibration curve showing how carbonyl peak height is related to monomer concentration.....	60
Figure 4.1 Pareto graphs of Models 1A (a) 2A (b), 3A(c) and 4A(d).....	70
Figure 4.2 Interaction plot between monomer mass and rate of injection.....	72
Figure 4.3 Cube plot of temperature, the rate of injection and monomer mass relationship effects on molecular weight.....	72
Figure 4.4 Pareto graphs of Models 1B (a) 2B (b), 3B(c) and 4B(d).....	74
Figure 4.5 Interaction plot between solvent volume and temperature for model 3B....	75
Figure 4.6 Cube plot of temperature and solvent volume effects on 2 <sup>nd</sup> melting point..	76
Figure 4.7 Pareto graphs of Models 1C (a) 2C(b), 3C(c) and 4C(d).....	77
Figure 4.8 Interaction plot between stirring speed and monomer mass for model 4d...	79
Figure 4.9 Cube plot of monomer mass, the rate of injection and stirring speed relationship effects on molecular weight.....	80
Figure 4.10 Caprolactam consumption with time and the corresponding integrated rate plots for one-shot injection of CI.....	87
Figure 4.11 Caprolactam consumption with time and the corresponding integrated rate plots for continuous injection of CI at a rate of 40µL/min.....	88

Figure 4.12 Potential reaction mechanism for caprolactam reacting with octadecyl isocyanate.....	88
Figure 4.13 a) OI consumption against time for single injection with a reaction temperature of 70°C and corresponding integrated rate order plots.....	89
Figure 4.14 OI consumption against time for continuous injection at 70µL/min and 70°C and corresponding integrated rate plots.....	90
Figure 4.15 OI consumption against time for one-shot injection at 40°C and corresponding integrated rate order plots.....	91
Figure 4.16 a) OI consumption against time for continuous injection at 70µL/min and 50°C and corresponding integrated order rate plots.....	92
Figure 4.17 a) OI consumption against time for continuous injection (35µL/min) at 80 C, b) Zero-order integrated rate plot.....	93
Figure 4.18 Caprolactam consumption at injection rates of 40µL/min, 30µL/min and 20µL/min and corresponding integrated rate order plots for all injection rates.....	95
Figure 4.19 Caprolactam consumption with catalyst volumes of 2mL, 4mL and 6mL and corresponding integrated rate order plots for all catalyst volumes.....	97
Figure 4.20 Caprolactam consumption at temperatures 80°C, 90°C and 100°C. All three experiments were carried out with an injection rate of 20µL/min.....	100
Figure 4.21 a) Order tests for reaction temperatures of 80°C, 90°C and 100°C.....	100
Figure 4.22 Concentration profiles at different oscillation frequencies and corresponding integrated rate order plots.....	103
Figure 4.23 OI consumption under equimolar at stirring speeds 400, 600, and 800rpm and corresponding integrated rate order plots.....	106
Figure 5.1 The build-up of oligomer on the baffle.....	112
Figure 5.2 Micrograph of PA-6 particles formed using a ‘slow-slow’ CI/catalyst system.....	121
Figure 5.3 Micrographs of Nylon-12 particles formed using a slow/slow CI/catalyst combination at a magnification of a)x1811 and b) x5000.....	121

## Nomenclature

<b><u>Symbol</u></b>	<b><u>Definition</u></b>	<b><u>Units</u></b>
[A]	Chain initiator concentration	(mol <sup>-1</sup> L)
[C]	Catalyst concentration	(mol <sup>-1</sup> L)
$A_o$	Response constant	Varies
$A_{PIPE}$	Cross-sectional area of pipe	(m <sup>2</sup> )
$A_{PISTON}$	Cross-sectional area of piston	(m <sup>2</sup> )
b	Autocatalytic term	(l mol <sup>-1</sup> )
$C_A$	Reactant concentration and at point in time	(mol L <sup>-1</sup> )
$C_{A0}$	Initial concentration of material	(mol L <sup>-1</sup> )
$C_D$	Discharge coefficient	(--)
$C_V$	Fractional conversion	(--)
D	Pipe diameter	(m)
$D_0$	Orifice diameter	(m)
$D_s$	Diameter of stirrer	(m)
F	Oscillating frequency	(Hz)
H	Half channel width	(m)
$H_{max}$	Max channel width	(m)
K	Pre-exponential factor	Varies
k	Number of variables within the model	(--)
l	Mixing length	(m)
L	Baffle spacing	(m)
$M_0$	Monomer concentration	(mol <sup>-1</sup> L)
N	Number of baffles per unit length	(m <sup>-1</sup> )
N	Number of points within the data sample	(--)
P/V	Power density	(W m <sup>-3</sup> )
$P_o$	Power number	(--)
Q	Volume flow rate	(V min <sup>-1</sup> )
R	Universal gas constant	(J mol <sup>-1</sup> K <sup>-1</sup> )
$R^2$	Percentage of variation in response	(--)
$R^2(adj)$	$R^2$ value adjusted to account for different predictors in model	(--)

$r_A$	Reaction rate	Varies
$Re$	Reynolds Number	(--)
$Re_n$	Numerical Reynolds number	(--)
$Re_{op}$	Orifice plate Reynolds number	(--)
$Re_p$	Pulsating Reynolds number	(--)
$St_f$	Strouhal number	(--)
$T$	Temperature	(K)
$U$	Activation energy	(J mol <sup>-1</sup> )
$u_0$	Velocity	(ms <sup>-1</sup> )
$u_p$	Pulsating flow velocity	(ms <sup>-1</sup> )
$u_{peak}$	Peak velocity maximum channel width	(ms <sup>-1</sup> )
$u_{ref}$	Velocity reference	(ms <sup>-1</sup> )
$V$	Dynamic viscosity	(Pa.S)
$V_L$	Volume	(m <sup>3</sup> )
$X$	Variation of displacement	(m)
$X_c$	Degree of crystallinity	(--)
$x_o$	Centre-to-peak oscillation amplitude	(m)
$Y$	A response	Varies
$Z$	An individual factor in a response	Varies
$\alpha$	Baffle free area ratio	(--)
$\beta$	Ratio of the orifice to pipe diameter	(--)
$\Delta H_c$	Enthalpy of crystallisation	(J/g)
$\Delta H_{c(100\%)}$	Heat of fusion for 100% crystalline polymer	(J/g)
$\Delta H_m$	Enthalpy of melting	(J/g)
$\rho$	Density	(kg/m <sup>3</sup> )

## Acronyms

### Name

### Definition

ANOVA

Analysis of variance

ATR-FTIR

Attenuated Total Reflection-Fourier Transform Infrared

CI

Chain Initiator

CST

Continuously stirred tank

DOE

Design of Experiment

DSC

Differential Scanning Calorimeter

FFD

Fractional factorial design

GC

Gas Chromatography

HFIP

Hydrofluoroisopropanol

HPLC

High Performance Liquid Chromatography

HT-GC

High Temperature Gas Chromatography

IDI

Isophorone Diisocyanate

MMA

Methylmethacrylate

OBF

Oscillatory Baffled Flow

OBR

Oscillating Baffled Reactor

OI

Octadecyl Isocyanate

PB

Plackett-Burman

PIB

Polyisobutene

POF

Pure oscillatory flow

PS

Polystyrene

PTFE

Polytetrafluoroethylene

PVC

Poly(vinyl) chloride

RBF

Round bottom flask

ROAP

Ring-opening Anionic polymerisation

RTD

Residence time distribution

SEM

Scanning electron microscope

STR

Stirred Tank Reactor

TGA-MS

Thermal-gravimetric analysis-Mass spectroscopy

THF

Tetrahydrofuran

TVA

Thermal Volatilisation Analysis



# Chapter 1 - Introduction

This chapter discusses the purpose and inspiration of the research.

## 1.1-Basis of research

Nylon is the name given to a range of polymers consisting of aliphatic and/or semi-aromatic polyamides. Nylons are thermoplastics known for their high heat, wear and chemical resistances. Since the initial creation by Wallace Carothers in 1935 at the DuPont research facility, nylons have found usage in a vast range of applications including but not limited to stockings, parachutes, toothbrushes and kitchen utensils. Originally nylons were synthesised via a condensation reaction between a diamine and a dicarboxylic acid<sup>1</sup>. Later devised methods involved the hydrolytic or anionic polymerisation of lactams. These methods were initially developed to prevent patent violations<sup>2</sup> and are still in use today. Unusually, anionic polymerisation requires both a catalyst and chain initiator (CI) for a successful reaction.

Nylon powders (specifically nylon-6) were first synthesised by Chrzczonowicz in 1955 through the anionic precipitation polymerisation of caprolactam<sup>3</sup>. Since then nylon particles have found usage in flame-spraying<sup>4</sup>, electrostatic coating<sup>5</sup> and as lacquer binders<sup>6</sup>. Normally the chain initiator is added in a single injection but as indicated by Florin and Grolier<sup>7</sup> that adding the CI continuously over a period improves the control over the reaction. However, little research and publications are available on this very subject, the one-shot injection has been the prescribed method in the production of nylon-6 alike. The impact of injection methods on key process and polymer properties, such as melting point, molecular weight, particle size and reaction kinetics, has not been investigated.

One of the derivatives to Nylon-6 (PA-6 from now) is Nylon-12 (PA-12 from now), which is of key interest in this PhD work. Multiple different routes to synthesise PA-12 in a powdered form already exist but the working recipes are company heirlooms and not available for public viewership. Between Arkema, Evonik and UBE approximately 600,000 tons of Nylon-12 is produced each year, most of which is used in cosmetic and powder coating industries. However, these companies do not change the chemical or mechanic properties of

their products without substantial incentive. Often only small quantities of the material (< 250 kg per month) are required for a particular industrial sector, manufacturing could only be possible if high sale price is warranted, commonly above £15/kg. This limits the applications and developments of such materials. The grinding process currently used for customisation, in addition to being expensive, produces a wider distribution of particle sizes. The ground material must go through a sieving procedure in order to produce the correct distribution. It is not unusual for more than 30% of the ground material to be discarded in the form of ‘fines’ or oversized particles. The latter polymer beads would go through further grinding, while the former presents significant hazards in storage and transportation.

This leaves a gap in the market, in which PA-12 could be produced in relatively small quantities with customers tailored parameters at a lower cost. The continuous baffled oscillatory reactor (COBR) provides uniform mixing, enhanced mass<sup>8</sup> and heat transfer<sup>9</sup> rates that give better control over droplet/particle size and molecular weight distributions and is a viable alternative to the traditional stirred tank reactors. Additionally, nylon particle formation can take several hours and can be very power intensive. COBR’s can achieve maximum conversion rates at much lower power densities than traditional stirred tanks, lowering production costs. Finally, linear scale up relationships would make it easy to go from lab to industrial scale relationships<sup>10</sup>.

Reaction kinetics and parameters affecting the kinetics of PA-6 synthesis under semi-continuous conditions have not been investigated; understanding PA-6 reaction kinetics is also the prologue for creating a synthesis route for PA-12 that is not available in public domain. These are the motivations of this PhD work.

## **1.2-Research objectives**

The following is the list of objectives for this thesis work:

- Develop an in-depth understanding of how reaction conditions affect properties of PA-6, e.g. molecular weight, particle size and melting point;

- Develop an understanding of how reaction kinetics are influenced by adding the chain initiator continuously;
- Develop a reproducible method to synthesise PA-12 within an OBR;
- Develop an understanding of how PA-12's properties are affected by changes in reaction temperature, injection rate and additive concentration.

### **1.3-Structure of the thesis**

The thesis is divided into six chapters. After this introduction in Chapter two, there is a literature review of current knowledge on nylon particle synthesis, properties and the OBR.

Chapter three describes the experimental set-ups, procedures and analytical methods applied to accomplish research goals. Chapter 4 presents the work carried out on PA6. Firstly, the factors affecting the desired polymer properties were analysed. This was followed by the study of the reaction kinetics.

Chapter five describes how the synthesis route for the production of PA-12 was developed and discuss how various factors affected polymer properties. Chapter 6 summarises major findings from this work and recommends future research to be carried out based upon the results of this PhD work.

## Chapter 2 - Literature review

This chapter reviews background literature relevant to the synthesis of nylon particles and the design and operation of the OBR.

### 2.1-Polymers

Polymers (also known as a class of macromolecules) are a class of large molecule synthesised through the covalent bonding of many chemical units. These units are called monomers. For a chemical to be considered a monomer it must possess two or more sites where bonding can take place. A polymer does not have to be synthesised from only one monomer it can be made from multiple different monomers. When a polymer is synthesised from only one monomer, it is called a homopolymer. Should two monomers be used then the resultant polymer is called a copolymer; and in rare cases when three monomers are used, the resultant polymer is called a terpolymer. Copolymerisation is often used to improve the properties of existing homopolymers. This is done by choosing monomers with separate desired characteristics where these two different monomers can be arranged in four different ways along the chain, depending on the desired properties of the polymer.

A polymer can display a range of different characteristics, with many different parameters affecting polymer properties. In general, the four most important ones are 1) Polymer size, as in molar mass and chain length; 2) Chemical composition, this determines the strength of intramolecular and intermolecular bonding; 3) Polymer structure and architecture, whether the material is made from branched or only single polymer chains, do chains bond together to form networks? 4) Polymer shape, the degree of twisting, coiling, chain entanglements etc. Through the manipulations of these characteristics, there are many different potential properties that a polymer may possess. A polymer may have a high modulus, preventing deformation; others will easily be deformed and capable of being severely elongated but still capable of returning to their initial shape. More recent developments have shown that polymers have possible applications in heterogeneous catalysts<sup>11</sup>, photovoltaic cells<sup>12</sup>, molecular sensing<sup>13</sup> and gas storage<sup>14</sup>.

There are multiple different ways to classify polymers; one of the more common ones is based upon their group structure. Most synthetic plastics can be categorised into 3 groups: plastics, fibres and elastomers but there is no set line between these groups. Plastics can also be further subdivided into two other categories: thermoplastics and thermosets. The key difference between the two is that thermoplastics soften upon heating and are capable of being reshaped, becoming rigid again when cooled. In contrast, when a thermoset has been heated above a set temperature they will become permanently solid and will not soften or change shape upon being reheated.

Elastomers are easily deformed and capable of undergoing substantial elongations while being able to recover their starting shape. A common example of this is an elastic band. Flexible plastics usually have moderate to high tensile strength and modulus but also capable of recovering its original shape after small deformations. Fibres and rigid plastics are characterised by a high resistance to being deformed and high tensile strength. Kevlar is a key example of a synthetic fibre; its high tensile strength allows it to be used in a range of applications, the most famous of which is body armour. Owing to its exceptional stiffness, Kevlar can also be used as a plastic reinforcement in aeroplanes, boat hulls etc. The difference between fibre and rigid plastics is that fibre is a polymer that has been melted down and drawn into a filament. This process involves stretching the polymer, uncoiling the polymer chains and aligning them parallel to the direction of stretching. Such properties are called anisotropy. This orientates the polymer along with an axis, making the fibre much stronger along the axis than across it.

To summarise, polymers have a multitude of properties that allow them to be found in a range of applications, with more waiting to be found.

### ***2.1.1-Polymerisation mechanisms***

#### ***2.1.1.1-Condensation polymerisation***

Condensation polymerisation reactions are classified as polymerisation reactions involving the elimination of a smaller molecule, such as water or hydrochloric acid. Because of this elimination, the polymer will lack some of the atoms present within the monomer. A condensation reaction is a form of step-growth polymerisation that is a reaction with bifunctional (or multifunctional) chains in a stepwise fashion. For example, any two species can react with each other; two monomers react to form a dimer, a dimer and a monomer form a trimer, two dimers can react and so forth. As a result, while the monomer is used up very quickly, the degree of polymerisation increases very slowly and so does molecular weight. As a consequence of this, molecular weight distributions are usually broad and average molecular weights are often lower than those of other methods. Molecular weights can be increased by removing side product during the reaction and by ensuring an exact 1:1 ratio between functional groups. Despite these disadvantages, condensation reactions are still used extensively in industry, owing to their versatility. Examples include the production of Kevlar, Nomex and polyimides. Furthermore, unlike addition polymers, a polymer formed through condensation polymerisation may be biodegradable owing to the innate reversibility of the condensation reaction.

#### ***2.1.1.2-Chain-Growth Polymerisation***

Chain-growth polymerisation is a method of polymerisation in which an unsaturated monomer, which can be vinyl or cyclic in nature, adds itself onto a growing chain's active site<sup>15</sup>. Depending on the functionality of the monomer in question, the growth of the polymer can occur at one end only or at different ends. Chain-growth polymerisation methods are superior to step-growth polymerisation methods if polymers with high molar masses are desired. Additionally, unlike in step polymerisation where each individual monomer within a polymer chain is a residue of its monomer, in chain-growth polymerisation, the polymer has the same chemical composition of the monomer pre-polymerisation. The 3 most common forms of chain growth polymerisation are free-radical, cationic and anionic. All three methods are comprised of 3 individual stages: 1) *initiation*, where the active site is formed through the use of an

initiator; 2) *propagation*, where the active site created in the initiation step begins to grow into a macromolecular chain via a kinetic chain mechanism, defined by a repeating sequence of a monomer being added to the growing chain; and the final stage is 3) *termination*, where the growth of a chain has stopped, either caused by the neutralisation of the active site or the transfer of said site. There is no elimination of a small molecule during the polymerisation process. This is crucial for potential applications within an OBR, as mixing could be affected by the addition of small molecules.

Anionic polymerisation is a form of chain growth polymerisation that while somewhat difficult to carry out experimentally, does have advantages over free-radical polymerisations. In free-radical polymerisations, it is very easy for two growing polymer chains to react together, either through recombination or disproportionation (a redox reaction in which a chemical substrate undergoes oxidation and reduction reaction simultaneously to give two different products, causing chain growth to terminate) reaction. In anionic (and cationic) polymerisation, such terminations are not possible, as the negatively (positive in the case of cationic polymerisation) charged ends repel each other electrostatically. Termination via chain transfer is also highly unlikely as this requires a hydride ( $H^-$ ) to be transferred from a growing chain onto a monomer; such a transfer is energetically unfavourable.

To summarise, there are multiple different ways that polymerisation can be undertaken, choosing the correct mechanism is vital to polymer is synthesised with the desired properties in the most efficient manner.

### **2.1.2-Methods of Polymerisation**

There are many methods for chain addition polymerisation, such as bulk, solution, suspension etc. Each of the relevant methodologies will be described in the following sections. In addition, two step-growth polymerisation methods, condensation and evaporation will also be examined.

### ***2.1.2.1-Bulk Polymerisation***

Bulk polymerisation, also known as mass polymerisation, is a method where an initiator is added to the molten monomer, for successful polymerisation the initiator must be soluble in the monomer<sup>16</sup>. As there is no need for a dispersant or other solvent, the resultant polymer is very pure, temperatures required are relatively high in comparison to other methods and molecular weight distribution of products can easily be changed via the addition of a chain transfer agent<sup>17</sup>. However, during bulk polymerisation, the rate of polymerisation increases, instead of decreasing as would be expected, this leads to auto-polymerisation (i.e. acceleration of reaction) or the so-called Tromorsdorf effect<sup>16</sup>. This is caused by an increase in viscosity of the system as the reaction progresses. While the increase in viscosity decreases as the number of termination steps takes place within the system<sup>17, 18</sup>, the increase in viscosity and the Tromorsdorf effect make heat transfer and mixing challenging as the reaction proceeds. Broader molecular weight distributions and low molecular weights of resultant polymers are the direct outcomes. For these reasons, bulk polymerisation is not often used in industry. Notable exceptions including the production of poly(ethylene), poly(styrene) and poly (methyl methacrylate).<sup>17</sup>

### ***2.1.2.2- Solution/precipitation polymerisation***

Solution polymerisation can either be a homogeneous or heterogeneous (depending on whether the polymer remains in solution) method of polymerisation. Should the polymer be soluble in the solvent, it is called a lacquer or varnish<sup>19</sup>. If only the monomer is soluble, then the polymer will precipitate as it's formed<sup>19</sup>. Should a precipitate be formed the method is called precipitation polymerisation. The monomer is dissolved within an inert solvent; catalyst can then be added or can already be present within the solvent. Similar to bulk polymerisation, solution polymerisation also experiences the Tromorsdorf effect but thermal control is better as the solvents act as a diluent<sup>16</sup>. Additionally, the solvent lowers the viscosity of the solution, allowing for easier processing. If the final product is in pearl/bead/powder form, isolation of the product is very easy<sup>19</sup>. However, like bulk polymerisation, molecular weights of products tend to be low due to chain transfer to the solvent, but high molecular weights can be achieved with longer durations. In addition, it is impossible to completely eliminate chain transfer, as no solvent is entirely inert<sup>19</sup>. Solvent removal is then the problem as it can be expensive, very



difficult to be done fully<sup>19</sup> and can cause the degradation of polymer properties. Finally, the polymer produced is not as pure as that by bulk polymerisation. Polymers formed by this method include polyacrylic acid and polyacrylonitrile.

### ***2.1.2.3-Suspension polymerisation***

Suspension polymerisation is a heterogeneous polymerisation technique where a monomer that is (mostly) insoluble in water(or other polar liquid) is dispersed within the liquid in the form of droplets, as shown in Figure 2.1<sup>20</sup>. A steric stabilizer is usually included within the system to stop coalescence and an initiator is also added to the system. The initiator must be non-reactive towards the solvent and be soluble in the monomer. The major aim is to form a uniform dispersion of monomer droplets within the aqueous phase and to control the coalescence of droplets during polymerisation. Reverse phase suspension polymerisations are also possible where a hydrophilic polymer and catalyst are held within an aqueous phase which is dispersed in a non-polar organic layer<sup>20</sup>. Suspension polymerisation does not have a problem with heat control, viscosity or chain transfer but like solution polymerisation, the polymer must be purified because it is not as pure as that achieved from bulk polymerisation<sup>19</sup>. An additional problem is that if the monomer is rather soluble in water, the system would have to be vigorously stirred to prevent agglomeration. Agglomeration is also a problem in the synthesis of tacky polymers<sup>17</sup>. Despite this, suspension polymerisation has been used to synthesise poly(vinyl) chloride (PVC) industrially, amongst others.

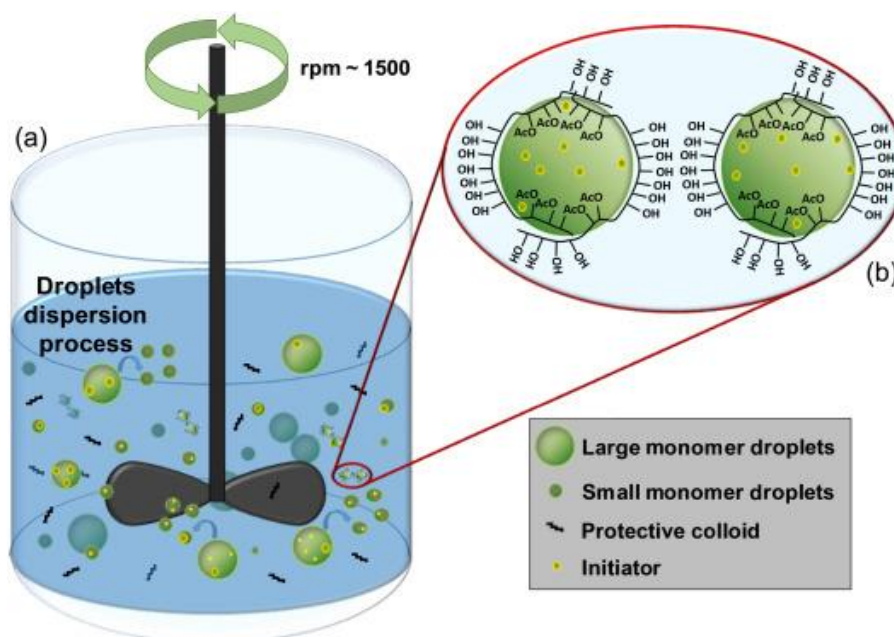


Figure 2.1 Diagram of suspension polymerisation in action<sup>21</sup>

#### 2.1.2.4-Emulsion polymerisation

Emulsion polymerisation is like suspension polymerisation in that it is a heterogeneous polymerisation technique. The name is a misnomer as polymerisation does not occur in emulsion droplets but in latex particles that are formed at the beginning of the process<sup>22, 23</sup>. Emulsion polymerisation requires a monomer with little to no water solubility, a water soluble initiator and a surfactant<sup>24</sup>. The surfactant acts as an emulsifier for the monomer within the continuous phase. The initiator and surfactant are not absolutely necessary to form the latex required but it is uncommon for them to be absent<sup>24</sup>. Once all parts of the system have been added a new phase will form as a polymer colloid, a dispersion of discrete, colloiddally stable latex particles<sup>24, 25</sup>. The mechanism of emulsion polymerisation is illustrated in Figure 2.2. These latex particles are made up of many polymer chains. The surfactant prevents these latex particles from coagulating together. Through emulsion polymerisation, polymers with high molecular weights can be synthesised quickly and like with suspension polymerisation, emulsion polymerisation does not have problems with heat control, viscosity or chain transfer<sup>23</sup>.

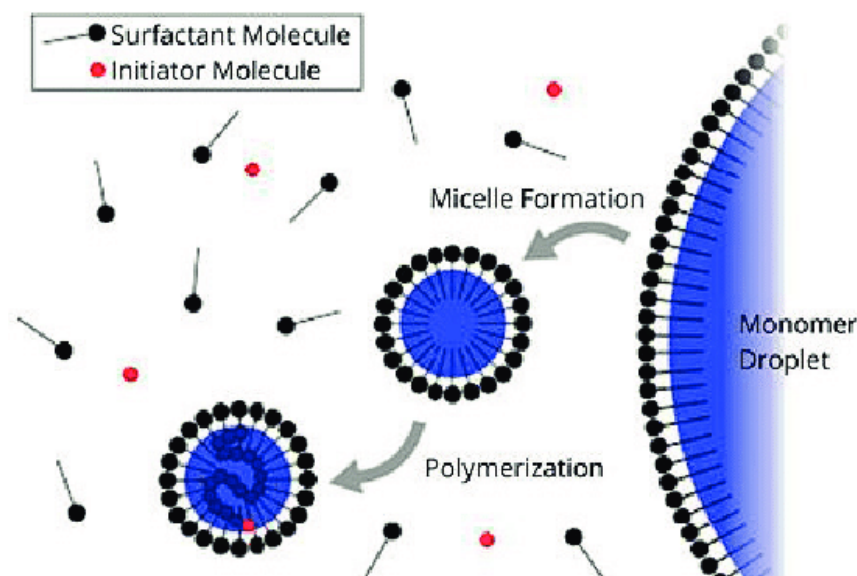


Figure 2.2 Representation of emulsion polymerisation in action <sup>26</sup>

In summary, there are numerous methods available to synthesise polymers, each with its own advantages and disadvantages. Choosing the right method to create a viable synthetic route for PA-12 particles is crucial.

### 2.1.3-Nylon

Nylon is the label given to a range of polymers, specifically aliphatic and semi-aromatic polyamides (a polymer where the monomer units are bonded together via an amide bond). It was the first commercially successful thermoplastic. Nylons are known for their high heat, chemical and wear resistance. In addition, nylons are good at absorbing water from their surroundings<sup>27</sup>. This absorption of water will affect the mechanical properties of the nylon; improve the impact resistance and flexibility of the nylon at the cost of strength and stiffness. Also, it is also an electrical insulator. These various characteristics have allowed nylons to be useful in a range of applications including cable ties, fluid reservoirs, fishing lines, sporting equipment, low voltage switch gears, carpets and a host of others<sup>18, 28</sup>.

The two main methods to synthesise nylons are either via a condensation reaction between diamines and dicarboxylic acids or through the addition polymerisation of lactams or

amino acids with themselves. The first nylon used for industrial applications was synthesised by Wallace Carothers at the DuPont research facility on February 28th 1935 via a step-growth polymerisation reaction with adipic acid and hexamethylenediamine<sup>1</sup>. The first variant of nylon was initially titled fibre-66, due to both the acid and the amine possessing 6 carbons. As there were two separate monomers being used in the production of this variant of nylon, it is a copolymer. Using the same condensation technique but with different substrates, a whole range of different nylons can be produced. Today Nylon is synthesised via a range of techniques including rotational moulding, casting, injection moulding or extrusion into film or fibre, depending on the desired shape and properties. While nylon first found usage as the bristles in toothbrushes, the main goal was for nylon to be a replacement for silk, specifically in woman's hosiery. This proved to be very successful and by 1941 30% of all hosiery was made from nylon<sup>29</sup>. However, with the advent of WW2, all nylon production went to towards the war effort.

As mentioned before lactams can also be used in the synthesis of nylons, however, this route was not investigated by Carothers but by Paul Schlack, working for IG Farben. Schlack attempted to reproduce the synthesis of nylon 6,6 without impeding on any patents<sup>2</sup>. Schlack showed that via ring-opening polymerisation caprolactam can be polymerised to form a nylon<sup>1</sup>. As caprolactam consists of 6 carbons, the new carbon is labelled nylon-6, because only one monomer is used in the production of this polymer, nylon-6 is a homopolymer. These two polymers are the two most commercially used nylons<sup>27</sup>. It must be noted that the method of polymerisation has a substantial impact on polymer properties, with the melting point of nylon-6,6 having a melting point of  $\sim 270^{\circ}\text{C}$  while the melting point of nylon-6 is only  $\sim 220^{\circ}\text{C}$ , despite having the same molecular structure.

Nylons have a range of desirable properties and can be synthesised either by condensation or chain-growth polymerisation. Due to the lack of eliminated molecule during the polymerisation process the chain-growth method is the most suitable method.

#### 2.1.4-Lactam-polymerisation mechanisms

There are multiple routes in which a lactam can be polymerised into its corresponding polyamide including anionic and cationic<sup>30, 31</sup> polymerisations, together with acidolytic<sup>32, 33</sup>, aminolytic<sup>33, 34</sup> and hydrolytic<sup>33, 35</sup> processes. Initially, Schrock synthesised nylon-6 by heating caprolactam to approximately 250 °C with up to 10% water present<sup>2</sup>. It should be noted that polymerisation can occur without a catalyst present, however, this process is incredibly slow and so does not contribute to polymer synthesis<sup>36</sup>.

Later work showed that lactam polymerisation could be performed using amines (aminolytic process) and carboxylic acids (acidolytic process). The aminolytic process involves the protonation of the lactam, however, the protonation happens in a very low amount leading to long polymerisation times, even at temperatures above 200°C. Polymerisation times under the acidolytic process are even longer. Hydrolytic polymerisation has been used in industry to produce nylon-6 fibres<sup>37</sup>. However, hydrolytic polymerisation requires a very high reaction temperature of ~250°C and extended reaction times. PA-12 has also been successfully synthesised under hydrolytic conditions, requiring reaction temperatures of ~260°C<sup>38</sup>. The cationic process has potential, but it does not produce polymers in such a high yield or with as high molecular weights as the anionic method does. This is mostly due to the electron withdrawing nature of the lactam functional group, which will stabilise the negative charge required<sup>39</sup>.

The method with the most potential is anionic polymerisation; there is a substantial amount of literature, both in journals and in patents detailing the usage of procedures in producing PA-6 and various other polyamide derivatives using this method, including PA-12<sup>40-44</sup>. Based upon literature surveyed, anionic polymerisation is one of the most used in modern polyamide production methods: however, this does not preclude older techniques being used<sup>45</sup>.<sup>46</sup> Anionic polymerisation requires lower reaction temperatures than other methods, has faster reaction times<sup>47</sup> and produces polymers with low polydispersity. And crucially, no literature has been found where nylon-6 particles have been synthesised by any other method other than anionic polymerisation.

To summarise, due to the substantially lower reaction temperatures required and that it is the only addition polymerisation mechanism that has been proven to make polyamide particles, anionic polymerisation seems the best mechanism for developing a synthesis route for PA-12.

### **2.1.5-Anionic Polymerisation mechanism**

Anionic polymerisation of lactams requires a “two” catalyst system consisting of a catalyst (also known as an Initiator) and a chain initiator (also known as a co-catalyst or activator)<sup>39, 48</sup>. What is named a catalyst can be more accurately described as a pre-catalyst. The ‘catalyst’ will react with the lactam monomer to form an anionically activated monomer complex. It is this complex that is the actual catalyst. The chain initiator acts as a growth centre for the growing chain. Catalysts can be separated into three major groups: metal alkyl lactamates; strong bases reacting with lactams to yield lactamates in irreversible or reversible reactions and substances that have low to medium basicity initially but form strong bases in reaction conditions<sup>39</sup>. Catalyst concentration is usually between 0.8 and 3 moles per 100 moles of lactam<sup>49, 47</sup>. There are an array of catalysts and chain initiators to choose from when devising a synthetic route, see Table 2.1 for potential catalysts and chain initiators.

Monomer	Catalyst (Initiator)	Activators (Cocatalyst)	Solvent
Dodecalactam	Alkali metals <sup>50</sup>	CO <sub>2</sub>	Decane
	Metal Halides <sup>51</sup>	N-acyllactams e.g	Ethylbenzene
	Metal alkoxides <sup>52</sup>	Acyl chlorides	THF
	Grignard Reagents <sup>53</sup>	Ureas	
	Pentamethylene guanidine <sup>54</sup>	Anhydrides	
	Quaternary ammonium salts <sup>55</sup>	Esters	
	Phosphazene <sup>56</sup>	Amides	
	Carbenes <sup>57</sup>	Diacylalkylamines	
	Bicyclic ‘superbase’ protophosphatranes <sup>58, 59</sup>	Acylating agents with a slow acylating action	
		Isocyanates e.g Octadecylisocyanate	
		HCl: Hexamethylene diisocyanate	
		Imides e.g. DCI: N,N'- dicyclohexylcarbodiimide or DICI N,N'-Diisopropylcarbodiimide	

Table 2.1 Table of potential catalysts, chain initiators and solvents

The full reaction for the anionic polymerisation of lactams is not completely understood but the mechanism can be split into five steps. Figure 2.3 gives an in-depth mechanism for these five steps. An unusual aspect of this reaction is that there are two ‘initiation’ stages. The first initiation step in the polymerisation process is the formation of the anionically active monomer through treatment with the chosen catalyst. For simplicity the first initiation step is called the activation step. The first step is the creation of the anionically active monomer by treating the monomer with the chosen catalyst(see step 1 in Figure 2.3).

Once the anionically activated monomer has been formed there are two possible limiting situations that can take place<sup>60</sup>: a) acylation of the monomer by the active species; and b) addition of chain initiator. In the case of a) the dimerisation of monomer is a slow reaction because dimerization requires a substantial induction period as lactams are only moderately good acylating agents. The chain initiator can either be formed in situ or added to the reaction mixture pre-formed. The initiation step is the anionically active monomer reacting rapidly with the chosen chain initiator via nucleophilic attack of the electron deficient carbon atom on the CI<sup>36</sup> (see step 2 in Figure 2.3). It is the resulting complex that is the true initiator of this polymerisation. During this process a proton-exchange reaction will regenerate the active monomer and protonate the negatively charged nitrogen atom on the chain end to complete the cycle (step 3 in Figure 2.3). The propagation step is very similar to the initiation stage. The difference is that following the nucleophilic attack of the ring of the previously added lactam is broken open as shown in step 4. As with the initiation step a proton exchange reaction regenerates the active monomer and the pattern will begin anew. Depending on chain initiator the initiation mechanism may change somewhat but the core process will remain the same.



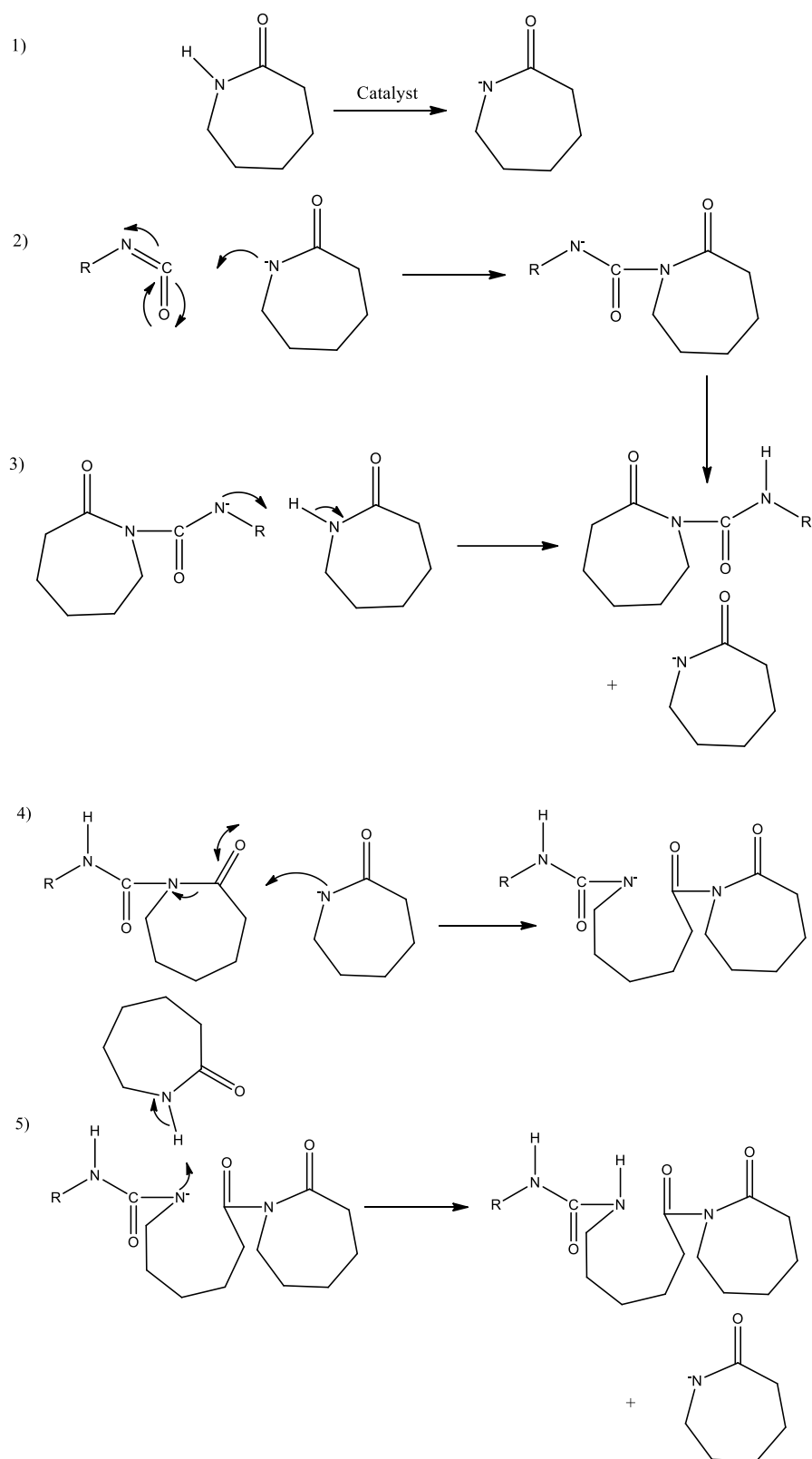


Figure 2.3 Anionic Initiation and Propagation reactions in the polymerisation of unsubstituted lactams<sup>36</sup>

As with any polymerisation process, there are multiple potential side reactions that can take place. Two undesired disproportionation reactions involving polymer amide and amide anions can potentially occur (see Figure 2.4)<sup>36</sup>. Undesired transacylation reactions can also occur, causing depolymerisation of the integration of a single monomer unit (see Figure 2.4). These are a small example of the potential side reactions that can take place, many others can potentially occur, particularly at elevated temperatures.

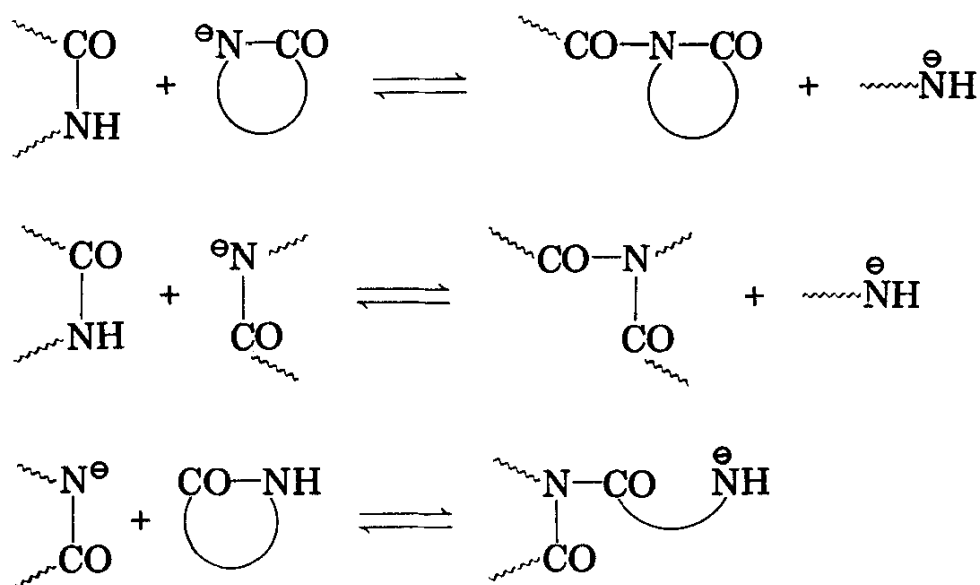


Figure 2.4 Example of potential side reactions that can take place during polymerisation<sup>36</sup>

If care is taken any potential termination step can be avoided and ‘living’ polymerisation can be achieved. This would lead to polydispersities very close to one being attained. However, as carbanions are very sensitive to moisture, oxygen and other potential protic (a solvent which has a hydrogen atom attached to either an oxygen or nitrogen atom) impurities, anionic polymerisation must be carried out under nitrogen in thoroughly dried equipment and solvents, conditions for ‘living’ anionic polymerisation are more difficult to achieve.

In summary, while the mechanism behind the anionic polymerisation of lactams is not completely understood, there is a great deal of literature on the subject. However, the mechanism may vary substantially depending on reaction conditions and the combination of catalyst and CI used. Such variations can influence reaction kinetics.

#### **2.1.6-Anionic Polymerisation methods**

As mentioned previously anionic polymerisation must take place in an inert atmosphere, free of moisture, and unfortunately, this does add complications for the implementation into a continuous reactor. The four main potential methods to achieve anionic polymerisation of a lactam into polyamide particles include polymerisation in suspension, emulsion, precipitation and using a polystyrene (PS)/polyamide blend. One other possible method to make polyamide particles exists, but involves dissolving the premade polymer and then expanding the solution through various nozzles into the anti-solvent CO<sub>2</sub><sup>61</sup>. This method is used to make particles from polymers that are formed by condensation polymerisation such as nylon-6/6. This system would be very difficult to adapt to a tubular reactor and unnecessarily expensive as the other methods form particles directly from the monomer.

A novel method to synthesise polyamides from lactams is through the formation of a polystyrene /polyamide blend, via the inversion of phase morphology caused by these blends at low PS concentrations<sup>62, 63</sup>. Firstly, styrene is polymerised using the lactam as a solvent via a free-radical polymerisation reaction to give polystyrene which surrounds the lactam. This is then followed by the polymerisation of the lactam to its respective nylon variant via anionic polymerisation. Resultant polyamide is in a mini-spherical form surrounded by PS. PS can be dissolved via the addition of tetrahydrofuran (THF) to isolate the polyamide in a powdered form. This method has potential, however, takes a great deal of time, with polymerisation of styrene alone taking 24h and presently, the spread of the distribution of particle sizes available by this method is quite small with sizes only ranging from 7µm to 80µm but are easily reproducible<sup>62</sup>. Several years later work carried out by *Wu et al*<sup>64</sup> used this method to successfully synthesis PA-12 particles. They employed a more updated method where the polystyrene was polymerised pre-reaction, drastically shortening the reaction time. Neither the

molecular weight nor particle size was analysed in their report but based on scanning electron microscopy (SEM) images the particle size was approximately 20 $\mu$ m. Unfortunately, such a polymerisation method would be very difficult to adapt to a tubular reactor and even harder to make into a continuous system.

The polymerisation of caprolactam in suspension has been achieved<sup>65</sup> requiring temperatures of 180°C for polymerisation. The research<sup>65</sup> showed that, while high temperatures were required and at present no suspension stabiliser has been found, the technique gave control over molecular weight and particle size. Suspension polymerisation of dodecalactam would be harder to do than that of caprolactam as the technique requires the monomer to be in the molten state, caprolactam melts at ~70°C while dodecalactam melts ~150°C. Molten solutions generally have higher viscosity, impacting flowability. In addition, there is no way of knowing if the suspending media of low molar mass polyisobutenes (PIB's) would work as efficiently. Additional problems include that PIB's are extremely sticky, which would make it extremely difficult, if not impossible, to use in any tubular reactor. The polymerisation of caprolactam has also been achieved through emulsion polymerisation,<sup>66</sup> one method necessitates the use of very high temperatures ~210°C for up to 22 hours. The other emulsion polymerisation method requires plenty of pre-reaction processing<sup>66</sup>. Despite these shortcomings, both emulsion methods do have potential as a viable route for the polymerisation of caprolactam and dodecalactam, however further work would be required to make either method be viable for industry scale synthesis. As with emulsion and suspension polymerisation method precipitation polymerisation has been used to produce nylon particles. Nearly all literature and patents concerning nylon particle synthesis uses the precipitation method and required reaction temperatures to synthesis PA-12 are lower than those required for emulsion and suspension methods as the monomer is not required to be kept in the molten state.

In summary, a catalyst and chain initiator are required for successful polymerisation. Multiple different anionic polymerisation methods are available, but the precipitation polymerisation was considered the best to develop a synthesis route for PA-12.

### 2.1.7-Reaction kinetics

The chemical kinetics behind anionic polymerisation of a lactam is a complex process due to the multiple irreversible and reversible reactions in which the active species of the reaction are both spent and revived<sup>67</sup>. Information on the kinetics of nylon-6 particle synthesis is very limited and no information is available in the public domain for the synthesis of PA-12 particles. However, there is a substantial volume of literature for bulk reaction kinetics that can be used to enhance what little literature on particle synthesis is available.

Two approaches are taken to create a kinetic model: mechanistic models<sup>68-70</sup> and overall models<sup>71-73</sup>. A mechanistic model is ideal as it attempts to account for all possible reactions, however, in the case of ROAP of lactams not all these reactions are understood, this leads to the mechanistic approach being impractical. As such, overall models, in which all reactions steps that happen within the system are accounted for by a single reaction step, are more practical at this time<sup>67</sup>.

Numerous models have been proposed throughout years however the autocatalytic model developed by Malkin<sup>72</sup> is commonly used as a basis to understand nylon synthesis kinetics. However, there is one substantial limitation to this model. It is only valid when the catalyst and CI are of equal concentration. Following this, Bolgov et al<sup>67</sup> then developed a modification of this model that takes into account unequal amounts of catalysts and chain initiators (see equation 2.1). It must be noted that it appears that only fast acting chain initiators were used when developing this model. It is unknown if this model is valid when slow acting CIs are used.

$$\frac{dX}{dT} = K \exp \left( \frac{U}{RT} \right) \frac{[A][C]}{[M_0]} (1 - C_V) \times \left\{ 1 + \frac{b}{[A][C]^{\frac{1}{2}}} \right\} \quad (2.1)$$

where  $C_V$  is the fractional conversion,  $T$  is the temperature (K),  $K$  is the pre-exponential factor ( $\text{l mol}^{-1} \text{s}^{-1}$ ),  $U$  is the activation energy ( $\text{J mol}^{-1}$ ),  $R$  is the universal gas constant ( $\text{J mol}^{-1} \text{K}^{-1}$ ),  $[A]$  is chain initiator concentration ( $\text{mol L}^{-1}$ ),  $[C]$  catalyst concentration ( $\text{mol L}^{-1}$ ),  $M_0$  is the initial monomer concentration ( $\text{mol L}^{-1}$ ),  $b$  is the autocatalytic term ( $\text{l mol}^{-1}$ )<sup>67</sup>.

Investigations carried out by Davé, et al<sup>67</sup> confirmed the kinetics of anionic polymerisation of caprolactam through the use of an adiabatic reactor. These studies showed that reaction temperature has a very strong effect on polymerisation. Going from a starting polymerisation temperature of 117°C to 136°C showed a substantial increase in reaction rate and conversion, however, increasing from 136°C to 157°C there is very little difference. Crystallisation rate is at its maximum rate at 140-145°C. At lower temperatures, the polymerisation rate is low due to growing polymer chains beginning to crystallise, limiting the movement of the active site and ultimately suppressing the propagation of the growing chain. At elevated temperatures equilibrium conversion had already been reached and so increasing the temperature had no further impact on reaction kinetics.

As previously noted, the CI/catalyst combination has a very strong impact on polymerisation kinetics. When a quick-quick or a quick-slow combination is used the formation of the carbanion active species (the initiation step) is much faster, by several orders of magnitude than the propagation step. The chain initiator only aids in the initiation of the reaction and has no known involvement in the propagation step, however as the propagation step can only take place post initiation the CI has a strong influence over kinetics. Figure 2.5 shows that altering the chain initiator concentration had a substantial effect on adiabatic conversion, however only to a point, after which increasing concentration CI had little effect<sup>74</sup>. Molecular weight has an inverse relationship with chain initiator concentration, the lower the CI concentration, the larger the molecular weight of the resultant polyamide. When polymerisation rate is slow long polymer chains can become entangled. This entanglement

creates a gel-like structure that can force the reaction to shift from a kinetic mechanism to a diffusion one.

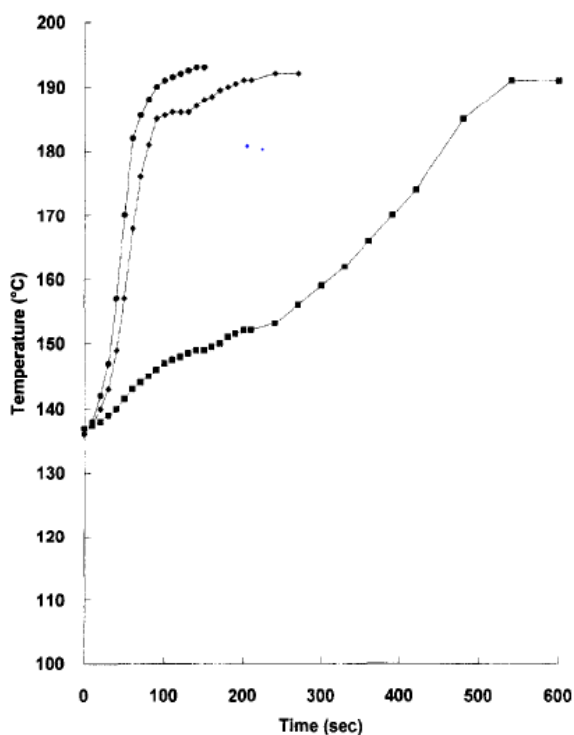


Figure 2.5 Adiabatic conversion of nylon-6 with an initial polymerization temperature of  $136^{\circ}\text{C}$  and caprolactam magnesium bromide concentration of  $108\text{mmol L}^{-1}$ . Isophthaloyl-bis-caprolactam concentrations used were  $40\text{mmol L}^{-1}$  (lower line),  $70\text{mmol L}^{-1}$  (middle line) and  $100\text{mmol L}^{-1}$  (upper line)<sup>67</sup>

These findings were substantiated by the work of Zhang et al<sup>75</sup>. The investigations carried out by Zhang et al studied the synthesis of nylon-3 copolymers. Like with PA-6 particle synthesis the reaction starts in a homogeneous medium but unlike PA-6 particle synthesis the product, PA-3 remains in solution. Regardless these experiments found that there was a first-order rate dependence on monomer and chain initiator concentration.

Investigations carried out by Stratula-Vahnoveanu et al<sup>76</sup> is one of the few studies looking at the kinetics of nylon particle synthesis. Their work showed that for the most part, the reaction follows pseudo-first-order kinetics, but at later stages the reaction slows down, causing the reaction to deviate from first order kinetics. This was partly attributed to precipitated polymer causing the mobility of CI to decrease. In conjunction, the polymer particles hinder the ability of the activated monomer to reach the active site of the growing chain. As with bulk polymerisation increasing the temperature lead to a substantial increase in reaction rate. Unlike bulk polymerisation, equilibrium conversion is not reached with increasing temperature, but reaction temperatures above 140°C lead to the formation of large aggregates that cling to the reactor wall.

The impact of mixing intensity has on chemical kinetics has been studied for decades<sup>77</sup> and in nylon particle synthesis mixing intensity has a normal influence over reaction kinetics. The mixing intensity has less influence on reaction rate than temperature and increasing the mixing intensity past a certain point has no further influence on the reaction rate. Interestingly, at low mixing rates, the reaction order can seemingly change from pseudo first order to pseudo-zero-order reaction. The reason for this is not completely understood but it may be caused due to a change in the hydrodynamic regime<sup>76</sup>.

The results from Stratula-Vahnoveanu and Vasiliu-Oprea was corroborated by the work of Dan and Grolier<sup>7</sup>. Their investigation made no mention to the order of the reaction however studies into mixing effects and temperature reported similar results to work carried out by Stratula-Vahnoveanu.

The CI/catalyst combination also brings in another complication, depending on the combination used the rate determining step can be altered. When both the catalyst and CI are considered slow-acting, the rate determining step is the ‘initiation’ step between the CI and the catalyst<sup>78</sup>. Therefore, the overall rate equation would be second order. In most literature, the propagation step is considered the rate-determining step and most kinetic models are based on this. There is, however some disagreement with this consensus. Work done by Ueda et al stated



that even the concentrations of the catalyst and chain initiator can cause the rate equation to change<sup>79</sup>. It should also be noted that these observations were made using a far more efficient catalyst and a CI that would be considered fast acting, so how valid such observations would be for a slow acting catalyst/CI combination is questionable.

The catalyst concentration, despite being key to the propagation step, was found to have to no effect on the adiabatic conversion (see Figure 2.6), at least within the concentrations tested. Again, these results were backed up by Zhang et al<sup>43</sup>. They observed a zero-order rate dependence on the catalyst concentration.

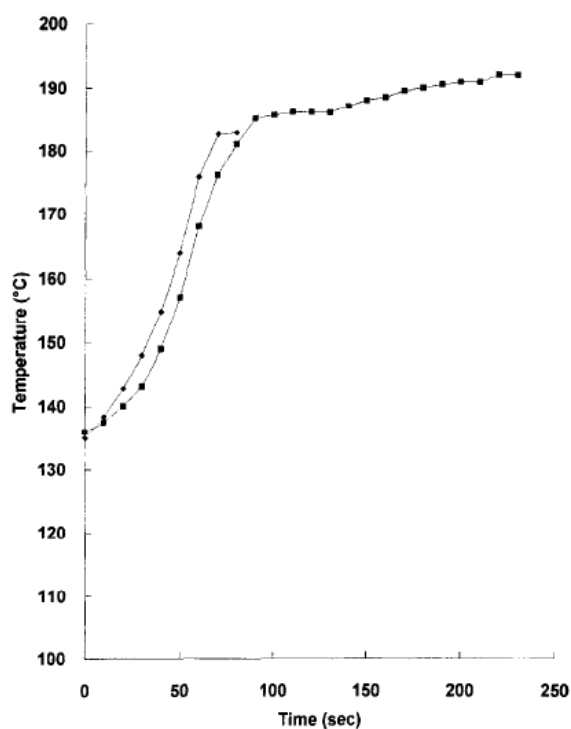


Figure 2.6 Adiabatic conversion of nylon-6 experimental data for initial polymerization temperature of 135C with isophthaloyl-bis-caprolactam (chain initiator) concentration of 70mmol<sup>-1</sup> and caprolactam magnesium bromide of 108mmol<sup>-1</sup> (lower curve) and 150mmol<sup>-1</sup> (higher curve)<sup>67</sup>

In summary, the reaction kinetics reported differ, there have been very few published works on both synthesis and kinetics in PA-6 and PA-12.

### ***2.1.8-Nylon Particle synthesis***

The methodology to synthesise nylon (nylon-6) particles was developed by the pioneering research done by Chrzczonowicz<sup>3, 80-82</sup>. Initially, the particles were formed using a CI/catalyst combination of carbon dioxide and sodium caprolactamate. Following this research, a host of different catalysts and chain initiators was used to produce particles of various molecular weights, particle sizes and morphologies. Regardless of the combination used, these nylon-6 particles are characterised as having high homogeneity and high molecular weight.<sup>83, 84</sup>. These particles have an array of uses including but not limited to flame spaying<sup>4</sup>, electrostatic coating<sup>5</sup>, thickener<sup>85, 86</sup> and lacquer binders<sup>6</sup>. In comparison to bulk polymerisation, lower basicity and milder temperatures are required for successful polymerisation as this limits the formation of branching polymers. The result of this leads to polymers with greater structure regularity and molecular weight homogeneity. Providing that the end product is stable, this method can be used to synthesise a host of different nylon powders.

The synthesis of nylon particles is a complex process with many competing factors. The most important of these factors include temperature, the initial concentration of monomer, amount of catalyst and activator/catalyst ratio<sup>60</sup>. Temperature increases conversion, the degree of polymerisation and particle size. The effect of temperature is limited and after a certain point increasing temperature any further only gives negligible improvements. The monomer to solvent ratio is in a delicate balance. If too much solvent is used, then the rate and degree of polymerisation are poor. If too little solvent is used, then the degree of polymerisation decreases as the mixture takes on more bulk-like characteristics. For numerous reasons a substantial amount of catalyst is required to carry out polymerisation and much like the monomer/solvent ratio, the monomer/catalyst is in a delicate balance. The combination of catalyst and chain initiator is a vital part (perhaps the most important) of the synthesis as it has a huge influence on particle size, molecular weight, product yield and morphology. Both the catalyst and the chain initiators can broadly be put into two categories: “slow” and “fast” acting<sup>6</sup>. The catalysts are characterised by their nucleophilicity: quick acting reagents such as alkali metal caprolactamates (formed by reaction between monomer and sodium hydride) are highly nucleophilic while slow acting reagents have a lower nucleophilicity. It is hypothesised that for slow-acting catalysts electron donating substituents decrease the nucleophilicity. Thus,

there are four different combinations that can be used to induce polymerisation: a) quick-quick; b) quick-slow; c) slow-quick, and d) slow-slow. When a quick-quick combination is used polymerisation becomes more bulk-like in nature and product yields, particle sizes and molecular weights are high. Conversely, product yields, particles sizes and molecular weights are significantly smaller for slow-slow and slow-quick chain initiator/catalyst systems. The quick-slow chain initiator/catalyst combination results in polymers with intermediate properties.

In summary, many different factors influence the properties of nylon particles. How adding the chain initiator continuously affects polymer properties has not been investigated in literature. The correct choice of CI/catalyst combination is of vital important for the development of a PA-12 synthesis route.

### **2.1.9-Polymer development**

The polymerisation takes place mainly in a heterogeneous mixture consisting of, paradoxically the lactam acting as a “solvent” and the hydrocarbon as the nonsolvent<sup>60</sup>. The liquid medium enables the movement of monomer and catalytic components to the growing polymer. The growing macromolecule has the greatest opportunity to grow when the mixture remains homogeneous. As such, polymerisation is the fastest at the very beginning of the reaction. As the caprolactam is consumed the reaction medium becomes poorer. This leads to phase separation, indicated by of opalescence of the reaction mixture. Phase separation can occur in different ways and is dependent on the concentration of the polymer.

When the concentration of polymer is high within the homogeneous phase (specifically between binodal and spinodal lines), these conditions are usually met when a quick-slow CI/catalyst combination is used, the growing polymer precipitates to form nuclei after a short period of time. As there is no stabiliser used in this process the assumption is that polymer chains within the nuclei are orientated with the hydrophobic end of the chain initiator are facing outwards, to the non-polar solvent while the reactive growth centre faces inwards. As such, the

stability of these primary particles could be partially explained by the external non-polar groups.

As the reaction progresses these individual droplets can collide with each other, causing these two droplets to coalesce, creating a dispersed “polymer” phase and a solvent rich phase. The monomer, pre-existing oligomer chains and catalyst are then absorbed from the solution into these droplets. It is within these monomer-rich droplets (the polymer phase) where the majority of polymerisation takes place. There will be growth centres near the surface of the growing particle allowing polymerisation to occur on the external surface of these particles.

As the reaction continues within these monomer-rich particles they will increase in size and viscosity. Following this, two different phenomena occur essentially at the same time: further collisions causing the growing droplets to cement together to form aggregates caused by the outer hydrophobic groups no longer being able to stabilise the growing droplet and the subsequent solidification of these agglomerates. These aggregates can then hinder the access of the activated monomer to the growing chain. This hindrance can result in the premature cessation of the reaction. Unfortunately, this causes polymer conversion and average molecular weight to diminish when compared to results gained from bulk polymerisation. The final step in this process is the crystallisation via undercooling and the establishment of granular structure<sup>86</sup>.

The second liquid-liquid phase separation method occurs when active sites are generated gradually, this allows the growing chains to spend longer in the homogeneous phase. Active sites are generated gradually when slow acting CI's and catalysts are used. Thus, when phase separation occurs the concentration of the polymer is lower than the previous method. Within the homogeneous phase, the initial increase in viscosity is caused by the formation of lactam salts<sup>87</sup>. Once again demixing occurs and a polymer rich phase and solvent rich phase are created, with the polymer-rich phase in the form of droplets. Each droplet is taken to be an isolated system unlike the previous method, these drops do not undergo collisions. The droplets do not undergo collisions due to the gradual generation of the active sites. At any point in time the number of growing particles is limited, therefore decreasing the probability of collisions.

If each polymer droplet contains a growing polymer, monomer and solvent and in such a composition that a tiny increase in the polymer concentration will cause spinodal decomposition, bicontinuous structures of both phases are gained. If the effective reaction temperature is substantially lower than the polymer melting point and polymer phase will then crystallise, causing a cessation in phase separation. The overall multiphase process is shown in Figure 2.7. The crystallised polymer is a continuous structure, granting the polymer powder unity.

Overall polymer development is a highly complex process with many individual phases that overlap each other. How polymer development may be affected by the continuous addition of the chain initiator has not been studied in the literature.

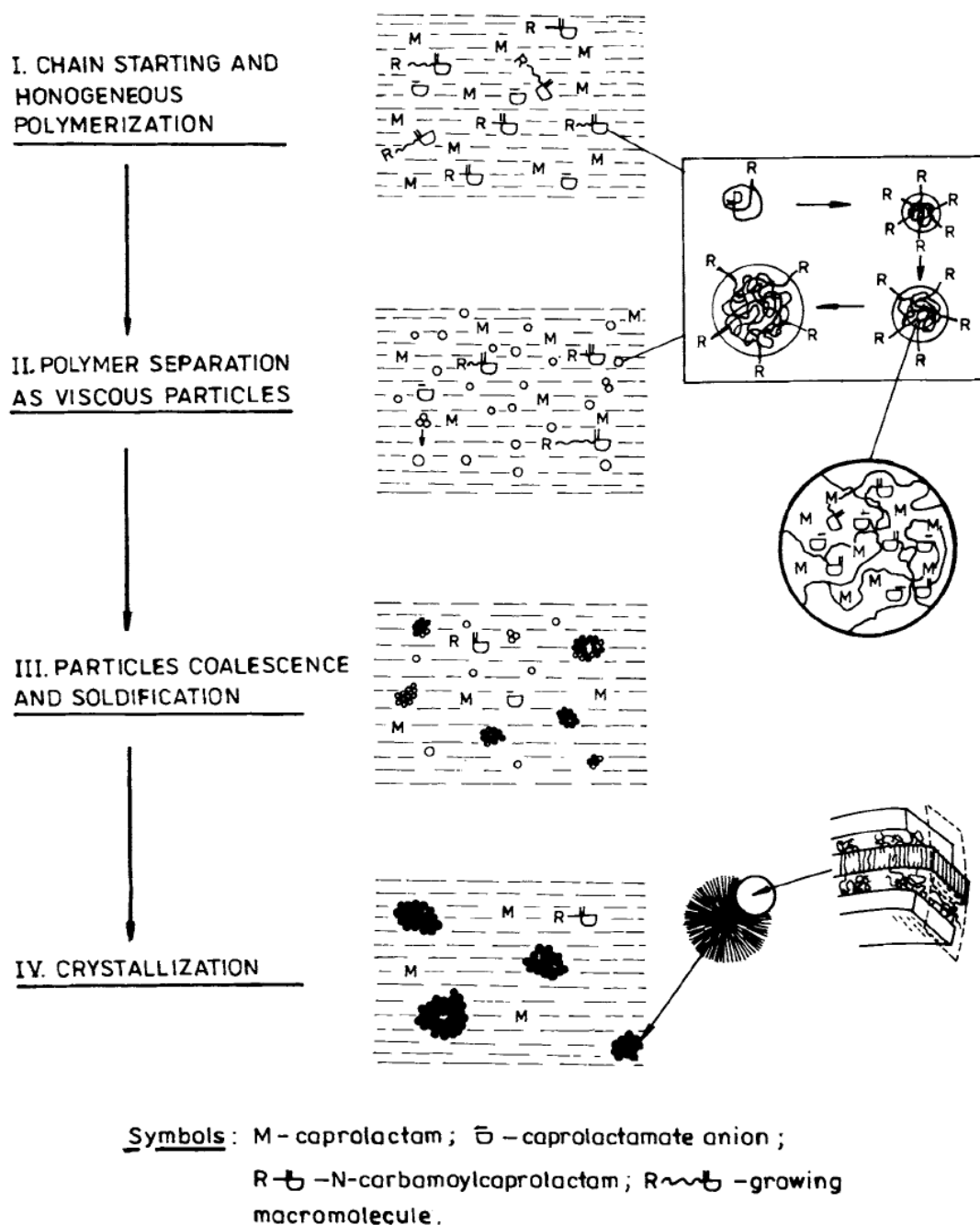


Figure 2.7 Illustration of the various phases of polymer particle development<sup>86</sup>

### 2.1.10-Morphology

The morphology of polymer particles is controlled by a complex array of competing components such as phase separation and crystallisation. As mentioned previously the choice of chain initiator/catalyst has a strong influence on the morphology of polymer particles. For

the quick-quick combination three different chain initiators were investigated by Dan et al<sup>6</sup> and all resulted in fused agglomerates made from smaller individual particles. The shape of these individual particles was found to become more irregular as the efficiency of the chain initiator increased, even for chain initiators of the same class. Increasing the chain initiator efficiency naturally increases the number of polymer rich domains. The higher number of domains causes the reaction medium to favour the coalescence of liquid droplets, this results in irregular particles with a cactus-like structure<sup>6</sup>.

The inner structure of these individual particles changes from a more solid spherulitic structure to a crudely spherical globular morphology as the efficiency of the chain initiator decreases. For the highly efficient CIs the spherulitic structure has a densely packed core with lamellae radiate along the spherulite radius (see Figure 2.8). As CI efficiency decreases the lamella become less advanced. Additionally, growing polymer chains can be captured by existing particles, forming lamellae on the surface.

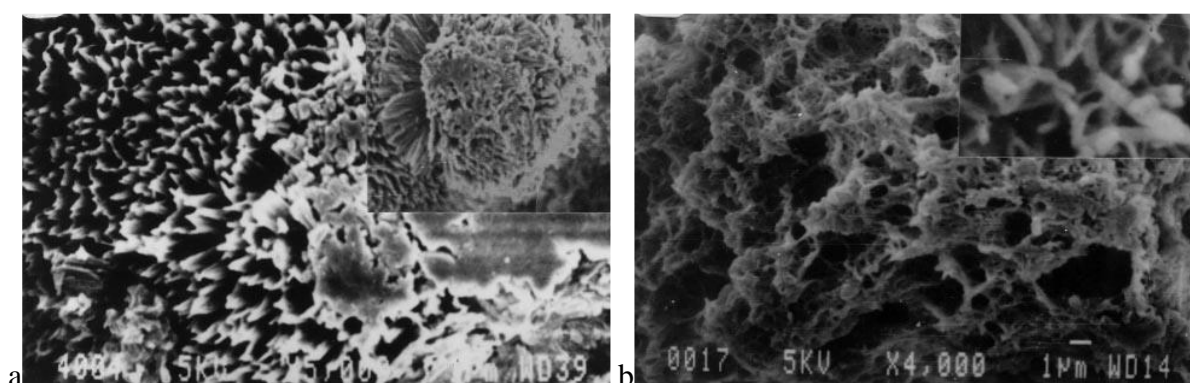


Figure 2.8 SEM image of PA-6 particles: a) PA-6 with defined spherulites resultant from the use of a quick/slow CI/catalyst combination<sup>6</sup> b) PA-6 with a macroporous continuous network resultant from the use of slow/slow or a slow/quick CI/catalyst combination<sup>6</sup>

For both slow-quick and slow-slow CI/catalyst combinations morphologies are quite different. SEM images in Figure 2.9 showed that unlike other combinations the polymer particles were not the result of agglomeration. Instead, it has a bicontinuous network structure.

The network structure is a fibrillar one, with some fibrils interconnected as bundles, it is thought that these bundles form the ‘skeleton’ of the particle. Both individual and bundled fibrils can connect to two or more different fibrils, forming the final morphology of the particle. It was found that using an efficient initiator (for this category) resulted in particles that were flat and ‘disk’-like. As the phase separation time increases the particles become more spherical. Regardless of the CI used the outer surface is rough with a continuous cohesive structure. These are porous particles with the size of the pores dependent on the efficiency of the CI.

Studies into the quick-quick combination found that the increased nucleophilicity of the catalyst causes rapid agglomeration resulting in most of the polymer sticking to the side of the reactors. Very little polymer is produced. The little polymer that was produced is characterised by a strong spherulite structure. Decreasing catalyst concentration was found to decrease the polymer yield but had no effect on particle morphology. Decreasing reaction temperature however did prevent deposition.

To summarise, particle morphology is controlled primarily by the choice of the CI and catalyst. Using more efficient combinations gives ‘spongy’ particles that are made from fused agglomerates. Using less efficient combinations results in individual particles with a structure made from a bicontinuous network, however how the morphology of PA-12 compares to PA-6 has not currently been reported in literature.



## 2.2-Oscillatory Baffled Reactors

### 2.2.1-Background

The research into oscillatory baffled flow (OBF) originated in the 1930s. Van Dijck developed a column of perforated plates which allowed for the mixing of relatively immiscible liquids via oscillatory motion<sup>88</sup>. A later investigation carried out by Sergeev analysed oscillatory motion within smooth-walled pipes.<sup>89</sup> Later Karr carried out research using a reciprocating plate column as an extractor<sup>90</sup>. Following this, it was Bellhouse et al who developed a furrowed membrane that used vortices formed by oscillatory flow to safely enhance the oxygenation of blood for open heart surgery<sup>91</sup>, this was the first usage of oscillatory flow within ducts. However, it wasn't until the 1980s that research into OBF began to see substantial growth. In 1980 Sobey et al conducted further studies on the oxygenator to develop a numerical model of the motion of fluid in both steady and unsteady flow.<sup>92, 93</sup>

The beginning of what would become the oscillatory baffled reactor was introduced by Mackley (1987) through the study of oscillatory baffled tubes<sup>94, 95</sup>. The original study for this came from work done by Knott and Mackley<sup>96</sup> which showed that eddies would form when a periodic flow passes through a sharp edge. The device that Mackley used was a simple cylinder containing periodically placed shape-edge hollow baffles. The fluid oscillates around these baffles. The contact between the baffles and the fluid form vortices that mix said fluid. Further work by Brunold et al investigated what the Reynolds number is required for efficient mixing and initiated studies on what geometries enhanced mixing<sup>97</sup>. It was work carried out by Dickins et al that demonstrated that each baffle cavity acts as a continuously stirred tank (CST). Thus near plug flow residence time distribution (RTD) can be achieved with specific reactor geometries and Reynolds numbers<sup>98</sup>. Throughout the 1990s research continued to flourish. A 30-fold improvement of the Nusselt number over traditional stirred tank reactor (STR) was shown to be achievable<sup>9</sup>. In conjunction, similar improvements in mass transfer<sup>8</sup> and residence time distribution<sup>99</sup>. Significantly, scale-up correlations were found to be linear<sup>8, 10</sup>.

### 2.2.2-Mixing in an OBR

The mixing in an OBR occurs when the fluid oscillation causes liquid to pass through the baffles, generating eddies downstream of each baffle<sup>99</sup>. These vortices draw fluid from the edges of the tubular reactor into the eddy downstream. Upon flow reversal the eddies will then be driven into the centre of the reactor,<sup>97</sup> (see Figure 2.9),<sup>100</sup> creating strong radial motion within the system. The oscillation allows for the continuous creation and destruction of these eddies resulting in flow patterns that lead to efficient radial and axial mixing.

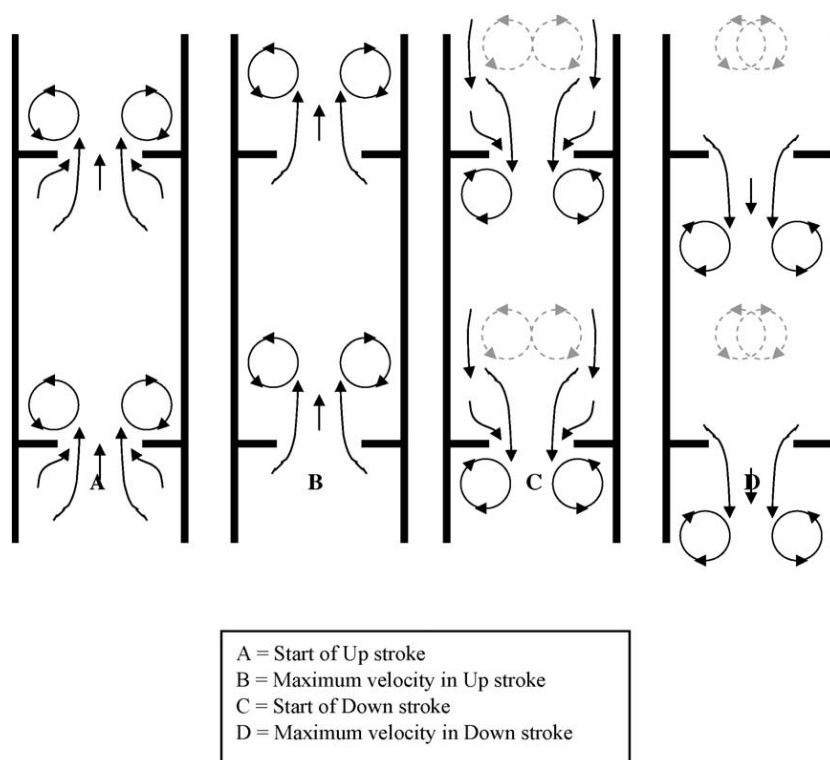


Figure 2.9 Eddy formation within an OBR<sup>100</sup>

Figure 2.9 shows that these eddies cause mixing within each baffle cavity. This allows each baffle cavity to act as a perfectly mixed stirred tank. The formation of these eddies can be achieved by oscillation of the fluid itself or via the oscillation of the baffles. Oscillation of the baffles can be attained via a linear or rotary motor. To oscillate the fluid a piston or bellow is required.

### 2.2.3-Fluid mechanics

The mechanical fluid conditions within any tubular reactor can be described by the Reynolds number that is a ratio of inertial forces within a fluid against the viscous forces within a fluid as seen in Figure 2.10. It is defined by the equations below

$$Re = \frac{\rho D u}{\nu} \quad (2.2)$$

where  $\rho$  is the density of the fluid ( $\text{kg/m}^3$ ),  $D$  is the pipe diameter (m),  $u$  is the velocity of the fluid ( $\text{ms}^{-1}$ ),  $\nu$  is the dynamic viscosity of the fluid (PaS). When the  $Re \leq 2000$  the fluid can be described as laminar. Disregarding the transitional phase when  $Re \geq 2000$  the fluid can be described as turbulent. During turbulent flow eddies can occur, leading to lateral mixing. Simply speaking lamina flow is ‘smooth’ while turbulent flow is ‘rough’. In summary, the Reynolds number is an indicator for the state of flow; describing how ‘smooth’ or ‘rough’ flow it is.



Figure 2.10 Flow within a tube with diameter  $D$ <sup>101</sup>

However, this equation cannot sufficiently describe all the motions a fluid undergoes within a tube when oscillatory motion is applied as shown in Figure 2.11, therefore, an additional dimensionless group is necessary. To account for this a pulsating Reynolds number,  $Re_p$  can be used as

$$Re_p = \frac{u_p D}{\nu'} \quad (2.3)$$

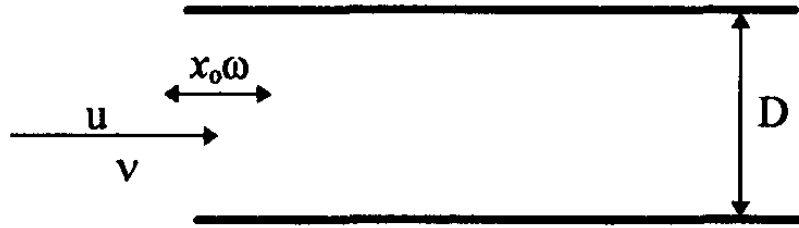


Figure 2.11 Oscillatory motion applied to flow in a tube<sup>101</sup>

Where  $u_p$  is the pulsating flow velocity ( $\text{ms}^{-1}$ ). Work carried out by Sarpkaya<sup>102</sup> defined  $u_p$  as the amplitude of the periodic component of the cross-sectional mean velocity ( $=\pi f x_o A_{piston}/A_{pipe}$ ) where  $f$  is the oscillating frequency (Hz),  $x_o$  is the centre-to-peak oscillation amplitude (m) and  $A_{piston}$  and  $A_{pipe}$  ( $\text{m}^2$ ) are the cross-sections of the piston and pipe respectively. In the majority of cases,  $u_p$  can be simplified to the product of the amplitude of oscillation multiplied by the frequency,  $Re_p = x_o f$ . The  $Re_p$  number describes the oscillatory motion exercised upon a fluid while the  $Re$  describes the state of flow. By combining these two terms all term's important to describing flow can be covered as shown in Figure 2.12.

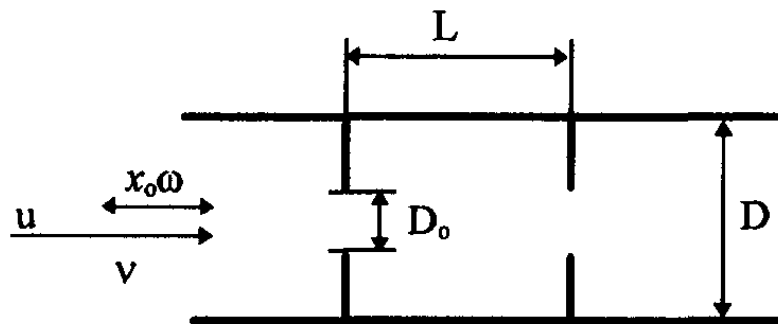


Figure 2.12 Oscillatory baffled flow<sup>101</sup>

However, these two terms do not take into consideration any distortion of the tube's shape or the inclusion of inserts, such as baffles. Under these conditions,  $Re$  and  $Re_p$  are no longer enough to accurately characterise the flow of the liquid. To reconcile this issue, the Strouhal number was brought in. The Strouhal number is defined as:

$$St_f = fH/u_{peak} \quad (2.4)$$

Where  $H$  is the half channel width (m) and  $u_{peak}$  the peak velocity at the maximum channel width,  $H_{max}^{101}$ . It was not until later work done by Sobey<sup>103</sup> that physical meaning for  $St_f$  was provided. The  $St_f$  was defined as the ratio of the scale of channel length to the scale of the fluid particle displacement. Further research carried out in the 1980's investigating unsteadiness in laminar flow<sup>94, 97</sup> demonstrated that when an intermittently reversing flow is applied to a tube that is equipped with equally spaced, transversely mounted orifice-type baffles vortex rings are swept into the cavity between the baffles when flow reverses. The continuous process of vortex creation, growth and ejection results in 'chaotic mixing'.

Brunold et al<sup>97</sup> proposed that the fluid mechanics of oscillatory baffled flow can be described using the following dimensionless groups, the Reynolds number,  $Re_o$  and the Strouhal number as below:

$$Re_o = \frac{u_p H_{max}}{v} = \omega x_o D / v \quad (2.5)$$

$$St = \omega H_{max} / 4\pi x_o \quad (2.6)$$

Further research did illustrate a flaw with these two groups. There was no mention of either baffle spacing or orifice diameter. Both parameters are of crucial importance when discussing OBF. The space between baffles impacts the shape of the eddies created and the orifice diameter controls the size of the vortices within the inter-baffle cavity.

Assuming the same oscillatory Reynolds number (e.g 500) under pure oscillatory flow (Figure 2.11) the mechanical conditions will be primarily axial, while under OBF (Figure 2.12) mixing will be chaotic in nature with a mixture of axial and radial components.

Studies have shown that under oscillatory flow two mixing regimes are possible. For  $Re_o < 250$  mixing intensity is low, and flow is 2D axi-symmetric. This is described as a ‘soft’ mixing regime. Should the  $Re_o > 250$ , the flow becomes increasingly 3D (no axial-symmetry) and chaotic. This allows an OBR to either act as a plug flow reactor when an input and output are imposed or as a device for uniform mixing. However, no single Reynolds number can define two different flow regimes. Under OBF an oscillator usually functions sinusoidally and due to this the variation of displacement,  $x$  and velocity,  $u_0$  takes the form of

$$x = -x_0 \cos(\omega t) \quad (2.7)$$

$$u_0 = x_0 \omega \sin(\omega t) \quad (2.8)$$

Maximum velocity,  $u_0 \max = x_0 \omega$  when  $\sin(\omega t) = 1$ . This indicates that there is no difference in oscillatory velocity for both pure oscillatory flow (POF) and OBF. This means that the input of the system is identical. From this, it can be concluded that  $Re_0$  only defines the strength of input to the system. With regards to fluid mechanical conditions the input is not related to the output.<sup>101</sup>

Using a slightly different type of baffle orifice the research of Jones and Bajura<sup>104</sup> on pulsating laminar flow provided key insights into this problem. Jones and Bajura did not use one, but two Reynolds numbers, the numerical Reynolds number  $Re_n$  and the orifice plate Reynolds number,  $Re_{op}$ .as

$$Re_n = u_{ref} D / 2v \quad (2.9)$$

$$Re_{op} = 4Q / \pi v D_0 \quad (2.10)$$

Where  $u_{ref}$  is the velocity reference ( $\text{ms}^{-1}$ ) and  $Q$  is volume flow rate ( $\text{min}^{-1}$ ). An equation below relates these two equations:

$$Re_{op} = \left( \frac{4}{\beta} \right) Re_n \quad (2.11)$$

Where  $\beta$  is the ratio of the orifice to pipe diameter ( $=D_0/D$ ).

From  $Re_0$  of 100-300, OBF shows plug-flow characteristics. Under these conditions, the vortices are symmetrically generated within the cavity of each baffle. At Reynolds numbers higher than 300, symmetry is destroyed and flow becomes chaotic.

#### **2.2.4-Polymerisation using Oscillatory Baffled Reactor**

One of the first investigations into polymerisation with industrial applications within an OBR was carried out by Ni et al<sup>95</sup>. They studied how the formation of methylmethacrylate (MMA) droplets was affected by varying operational conditions, compared polymers made in an OBR with those from a traditional STR. The weight & number averaged molecular weights and polydispersity were similar to those obtained in the STR<sup>105</sup>, particle size distributions were narrowed due to better and uniform mixing achieved in the OBR.

The influence of frequency of oscillation and oscillation amplitude, as well as baffle width on mean particle size were examined, Ni et al. found that the  $d_{v0.5}$  (the median for a volume distribution) decreased with the increase of the oscillation frequency following a dependence of  $d_{v0.5} \propto f^{-1.39}$  (see Figure 2.13). In addition, increasing oscillation frequency also decreased the particle size distribution. In contrast, the size of particles formed within an STR varied with impeller speeds from power index of -0.3 to -3.3, depending on reaction conditions<sup>106-109</sup>.

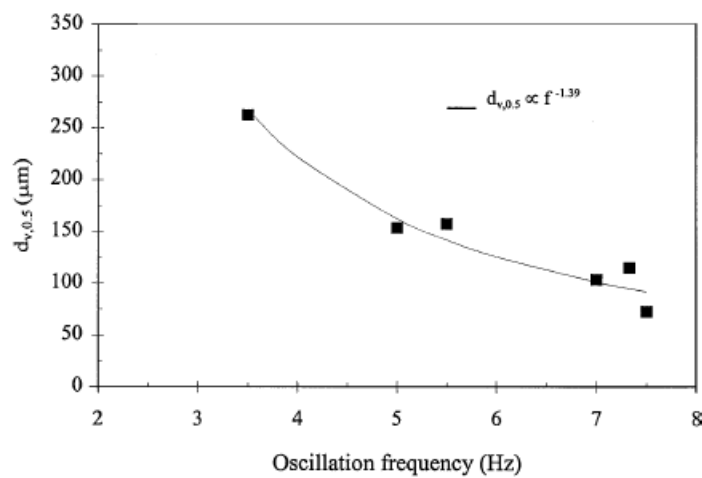


Figure 2.13 Effect of oscillation frequency on mean particle size with a fixed amplitude and baffle width<sup>95</sup>

Much like frequency, increasing the amplitude of oscillation led to a decrease in particle size (see Figure 2.14) with a power index of -1.19. The baffle thickness had little influence over the Sauter mean droplet size; when the baffle width increased from 0.8mm to 3.0mm, the power index was similar from -0.92 to -1.02<sup>95</sup>.



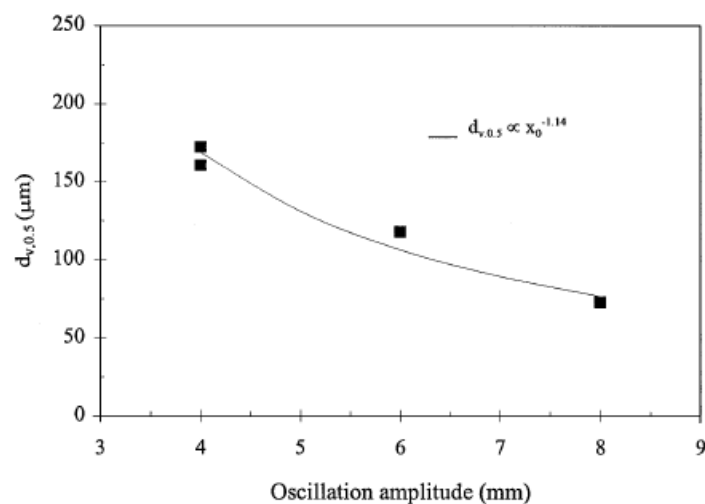


Figure 2.14 Effect of amplitude on mean particle size at a fixed frequency and baffle width<sup>95</sup>

### 2.2.5-Power consumption

When designing a reactor or any sort of mixing device one of the most important parameters to consider is power consumption<sup>110</sup>. How much power a reactor requires is a useful way of determining mixing efficiency and can be used as the basis for comparison of the effectiveness of different types of reactors<sup>111</sup>.

There were two different models for estimating the power density of an OBR: the eddy acoustic model and a quasi-steady flow model. Work carried out by Jealous and Johnson employed the quasi-steady flow method to determine the power density of a pulsed plate column<sup>112</sup>, this has been the basis for the evaluation of the power density in OBR<sup>113, 114</sup> as shown below.

$$\frac{P}{V} = \frac{2\rho N}{3\pi C_D^2} \left( \frac{1 - \alpha^2}{\alpha^2} \right) x_0^3 \omega^3 \quad (2.12)$$

Where  $\rho$  is the fluid density ( $\text{kg m}^{-3}$ ),  $N$  is the number of baffles per unit length of the tube ( $\text{m}^{-1}$ ),  $\alpha$  is the baffle free area ratio and  $C_D$  is a discharge coefficient for the orifice. In the vast majority of cases, the value of  $C_D$  is taken to be 0.7<sup>115-117</sup>.

It must be noted that the quasi-state model is only appropriate for oscillations high amplitudes (5-30 mm) and low frequencies (0.5-2). Beyond these values, the eddy acoustic model appears to become more effective in determining power dissipation<sup>118</sup>. This model is defined as

$$\frac{P}{V} = 1.5 \frac{\rho \omega^3 x_0^2 l}{L \alpha} \quad (2.13)$$

where  $l$  is the mixing length (m) and  $L$  is the baffle spacing (m). Significantly, numerous investigations have shown that OBRs are much more efficient than traditional STRs and in some cases, up to 94%-99% decrease in required power density has been reported<sup>117, 119-121</sup>. Unlike traditional STR, scale-up in OBR did not necessitate an increase in power consumption per unit mass.

Overall, the OBR allows for very efficient scale-up and a substantial decrease in power density when compared to an STR. OBR was chosen as the model reactor for this research.

## Chapter 3 - Experimental setup and procedure

This chapter describes the setup of the experimental apparatus and the procedures of experimental and analytical methods.

### 3.1-Experimental Apparatus

#### 3.1.1-The Stirred Tank Reactor (STR)

Figure 3.1 shows the setup of the STR. The reactor consisted of a round bottom flask (RBF) with a volume of 100mL. The flask was placed within a “polar bear” plus crystal type heating unit. The polar bear heating unit was equipped with a magnetic motor. A 20mm PTFE type magnetic stirrer was placed within the round bottom flask. One port was equipped with a reflux condenser. In turn, the condenser was attached to a Schlenk line. This Schlenk line supplied a constant stream of N<sub>2</sub> to the reactor. The central port was sealed with a glass stopper. Final port is covered with a Suba-seal that equipped with Teflon tubing. Teflon tubing was connected to a 5mL Norm-Ject disposable plastic syringe with an inner diameter of 13.70mm. The syringe was placed upon an NE-1002X Microfluidics syringe pump.

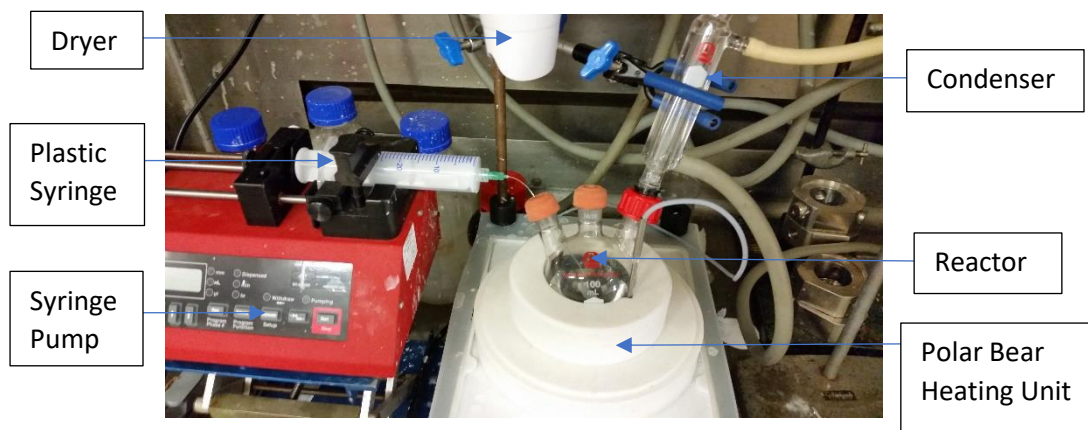


Figure 3.1 Setup for STR. Note that in this setup a syringe was used instead of Teflon tubing.

Schlenk line connector not shown

### 3.1.2-The Oscillatory Baffled Reactor

The OBR consisted of a jacketed glass column with an internal diameter of 50mm and a height of 500mm. Baffle string consisted of four stainless steel baffles with an outer diameter of 48mm, an orifice diameter of 24mm and a thickness of 3mm. The baffles were spaced at 65mm by stainless steel spacers. In all experiments only the first baffle was inserted in the reaction mixture therefore OBR was used as a batch or semi-batch reactor only, not a continuous one. Height of reaction mixture within glass column was ~75mm.

Heating was carried out in a water bath. The heating fluid was water in all cases bar experiments investigating kinetics at 100°C, in those circumstances the heating fluid used was silicon oil. The temperature was checked intermittently using a thermocouple. The baffles were oscillated within the column by a linear motor (Ni-Tech). This motor was held in place by a steel frame above the OBR. The OBR itself was held in place by a plastic frame, seen in Figure 3.2. Frequencies of 0-10Hz and amplitudes of 0-50mm were possible using this setup. The column glass possesses three ports. The first port was connected to a Schlenk line. This Schlenk line supplied a constant stream of N<sub>2</sub>. The second port was covered with a Suba-seal equipped with Teflon tubing. The tubing was connected to a 5mL Norm-Ject disposable plastic syringe with an inner diameter 13.70mm. This syringe was placed upon an NE-1002X Microfluidics syringe pump. The syringe was heated by a hairdryer to keep CI in the liquid state within the syringe and Teflon tubing. The remaining port was closed with a stopper. This port was opened temporarily when withdrawing a sample. A cap was placed on the top of the reactor to ensure that the nitrogen atmosphere was contained. For PA-12 synthesis the syringe was placed within a heated sleeve that is used to keep reaction mixture in the liquid phase (Figure 3.3).

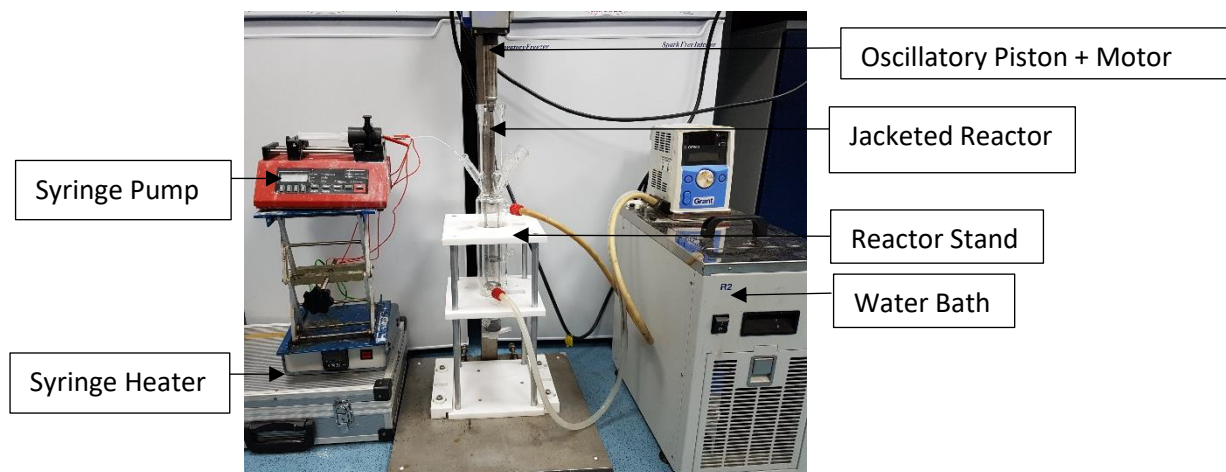


Figure 3.2 Setup of oscillated baffled reactor, for simplicity the Schlenk line, hairdryer and various seals used were not displayed

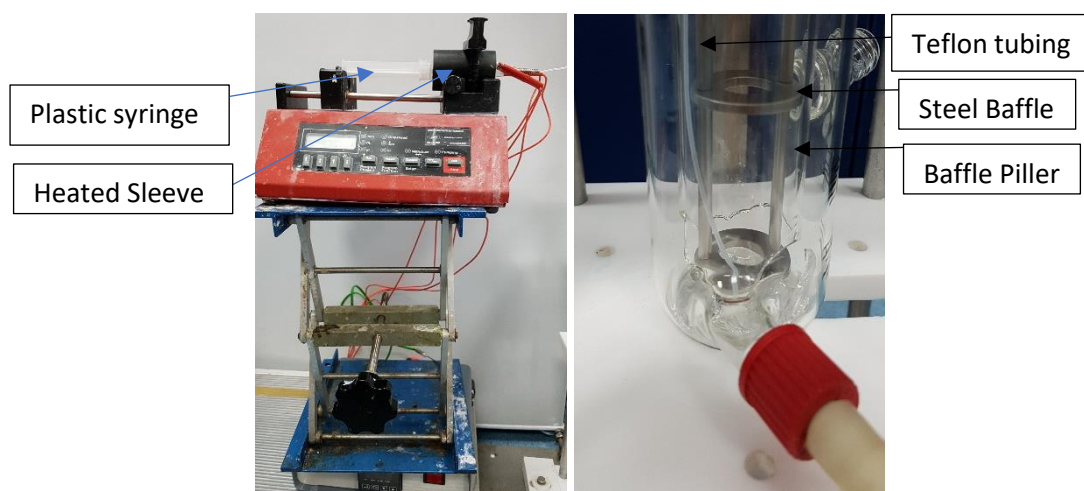


Figure 3.3 In-depth look at the syringe pump and baffle

### 3.1.3-The set up for PA-6 equimolar kinetic measurements

The glassware was left to dry overnight. Jacketed beaker was heated by a water bath via circulated water and placed on the magnetic motor. 20mm PTFE type magnetic stirrer was placed within the round bottom flask. Teflon tubing was connected to a 5mL Norm-Ject disposable plastic syringe with an inner diameter of 13.70mm. This syringe was placed upon an NE-1002X Microfluidics syringe pump. A watch glass was placed on the beaker to prevent the evaporation of ethylbenzene.

### 3.2-Reagents

The laboratory grade caprolactam, dodecalactam, N,N-alkylbisamide, octadecyl isocyanate Red-Al® (determine concentration) and anhydrous grade ethylbenzene were procured from Sigma-Aldrich. The caprolactam and dodecalatam were heated at 50°C overnight before use. Remaining chemicals were used as received.

### 3.3-Experimental procedures

#### 3.3.1-Recipe and Procedure for PA-6 synthesis within STR

The recipe and physical properties of reactants for PA-6 synthesis are shown below in Table 3.1.

Chemical	Molecular mass (g·mol <sup>-1</sup> )	Density at 25C (g/cm <sup>3</sup> )	Melting point (°C)	Boiling point (°C)
Caprolactam	113.16	N/A	68-71	136-138
Ethylbenzene anhydrous, 99.8%	106.17	0.867	-95	136
Octadecyl Isocyanate	295.5	0.847	15-16	172-173
Red-Al® ≥60 wt. % in toluene	202.16	1.036	N/A	110

Table 3.1 Physical properties of reagents for PA-6 synthesis

The procedure involves that the glassware was left to dry overnight. The round bottom flask was then continuously purged with nitrogen and heated with a heat gun to remove moisture. Steam of N<sub>2</sub> was also present until the termination of the reaction. The polar bear heating unit was set to its required temperature and stirring speed and turned on. Once the required temperature had been reached, the apparatus was left for approximately 30 minutes to purge any remaining moisture from the reactor. All but one port of the reactor was then sealed. A syringe was purged with nitrogen and used to transport the ethylbenzene to the reactor. Once the monomer was fully dissolved, a new syringe was purged with nitrogen and employed to

inject the catalyst into the reaction mixture. The catalyst then reacted with the monomer, giving off hydrogen. Once this reaction was completed, indicated by the cessation of hydrogen, the final port was sealed with a Suba-seal. A second syringe purged with nitrogen was loaded with Octadecyl Isocyanate (OI) by gently injecting it into the syringe until the Teflon tubing was filled. The tubing was then used to pierce the Suba-seal, inserted into the reactor and submerged in the reaction mixture. A hairdryer was placed above the syringe, heating the tubing and the syringe to ensure that OI remained in the liquid state within the syringe. An injection rate was chosen and the OI was continuously fed into the reactor. This signalled the beginning of the reaction.

### **3.3.2-Procedure for PA-6 kinetic study in an OBR**

The glassware was left overnight in an oven to remove any moisture from previous cleaning. The OBR was then assembled as shown in Figure 3.2 and purged with a continuous stream of nitrogen. This stream of  $N_2$  is present until the end of the reaction. The water heater was set to its required temperature and turned on. Once the required temperature has been reached, the apparatus was left for approximately 30 minutes to purge any remaining moisture from the reactor. All but one port of the reactor was then sealed. A syringe was purged with nitrogen and used to transport the ethylbenzene to the reactor. Once the monomer was fully dissolved, oscillation frequency and amplitude were selected and the motor turned on. A new syringe purged with nitrogen was employed to inject the catalyst into the reaction mixture. The catalyst then reacted with the monomer, giving off hydrogen, once the reaction was completed the final port was sealed. A second syringe purged with nitrogen was loaded with OI. The syringe was then placed on the syringe pump. Teflon tubing equipped with a Suba-seal was then connected to the loaded syringe and OI was gently injected into the syringe until the tubing was filled. One port on the reactor was then opened allowing the tubing to be placed in the middle of the baffle and the tip was submerged within the reaction mixture. The Suba-seal resealed the reactor. A hairdryer was placed above the syringe and the tubing to ensure that OI remained in the liquid state within the syringe. An injection rate was chosen and the OI then flowed into the mixture. This signals the beginning of the reaction. To remove a sample from the reactor a port was temporarily unsealed. A 1mL syringe equipped with Teflon tubing was used to withdraw approximately 0.3mL of solution from the reactor. The port was then resealed. Teflon tubing was disconnected from the syringe and quenched and cleaned with methanol and placed

within an oven. The sample was then analysed by ATR-FTIR. Table 3.2 lists the reaction conditions.

Conditions	Value
Temperature	90°C
Monomer mass	12g
Ethylbenzene volume	60mL
Catalyst volume	4mL
Octadecyl isocyanate volume (single injection)	2mL
Octadecyl isocyanate injection rate (continuous injection)	20 $\mu$ L/min
Oscillation frequency	1Hz
Oscillation amplitude	32mm

Table 3.2 Reaction conditions for PA-6 synthesis within OBR

### 3.3.3- Procedure for equimolar kinetics measurements

As there was no catalyst used, there was no need to carry out the reaction out under inert conditions. For simplicity, equimolar experiments were carried out in a beaker and not in the OBR. The procedure for the single and continuous injection methods were slightly different. For the single injection, the monomer and ethylbenzene (20mL) was placed within the reactor and the monomer was dissolved in the ethylbenzene. The CI was then added into the mixture in a one-shot fashion. For continuous injection, the CI and ethylbenzene(10mL) were first added to the beaker. The monomer was then dissolved by the remaining ethylbenzene (10mL). The dissolved monomer was loaded onto a syringe. The syringe was equipped with Teflon tubing and placed on the syringe pump. The dissolved monomer was then injected into the mixture at a set rate. Table 3.3 shows the experimental conditions.



Condition	Value
Temperature	70°C
Monomer mass	3g
Ethylbenzene volume	20mL
Octadecyl isocyanate volume using one-shot injection technique	8mL
Octadecyl isocyanate injection rate (continuous injection)	70 $\mu$ L/min
Stirrer Speed	600rpm

Table 3.3 The reaction conditions for kinetics studies under equimolar conditions

### 3.3.4-Recipe and Procedure for PA-12 synthesis

The constituents of the reaction for PA-12 synthesis are shown below in Table 3.4.

Chemical	Molecular mass (g·mol <sup>-1</sup> )	Density at 25°C (g/cm <sup>3</sup> )	Melting point (°C)	Boiling point (°C)
Dodecalactam	197.32	0.973	150-153	348
Caprolactam	113.16	N/A	68-71	136-138
Ethylbenzene anhydrous, 99.8%	106.17	0.867	-95	136
Octadecyl Isocyanate	295.5	0.847	15-16	172-173
Red-Al® ≥60 wt. % in toluene	202.16	1.036	N/A	110
N'-N-Ethylene bis(stearamide)	593.038	N/A	144-146	N/A

Table 3.4 Recipe and physical properties of reagents for PA-12 synthesis

The procedure is very similar to the synthesis of PA-6 within an OBR but with several differences. Pure CI was replaced with a CI mixture. To create the CI mixture, the caprolactam was first dissolved in ethylbenzene. The CI was then melted into a liquid and added to the

mixture. The mixture was stirred vigorously by hand and loaded into a syringe. The syringe was placed within the custom-made syringe heating sleeve (see Figure 3.3). The syringe sleeve was then heated to 55°C for 10 minutes, after which the heat was reduced to 30°C, the syringe heater was left at this temperature for the remainder of the reaction. The syringe and sleeve were then placed on the syringe pump. Teflon tubing equipped with a Suba-seal was connected to the loaded syringe and the CI mixture was gently injected into the syringe until the tubing was filled. One port on the reactor was opened and the tubing was then placed at the side of the baffle within the reactor, next to the reactor wall to prevent the formation of droplets. Tubing must be kept above the reaction mixture. The Suba-seal was used to reseal the reactor. Tables 3.5 and 3.6 contain the operating conditions for the reaction.

Conditions	Value
Temperature	80°C
Dodecalactam (monomer) mass	12g
Ethylbenzene volume	60mL
Catalyst volume	2mL
N,N- Ethylene bis(steramide) mass	0.15g
CI mixture volume (single injection)	2mL
Octadecyl isocyanate injection rate (continuous injection)	15 µL/min
Oscillation frequency	1Hz
Oscillation amplitude	32mm

Table 3.5 PA-12 synthesis reaction parameters

CI Mixture components	Value
Ethylbenzene	10mL
Caprolactam	0.25g
Octadecyl Isocyanate	0.75mL

Table 3.6 Table of CI mixture constituents

### 3.4-Measurement tools

#### 3.4.1-Melting point analysis

The melting point was determined using the Differential Scanning Calorimeter (DSC) 214 polyna. The system was equipped with an intracooling system that could operate between temperatures of -70 to 600°C. Pressurised nitrogen (~2 bar) at flow rates of 40mL/min and 20mL/min was used as the purge gas to prevent sample oxidation. 10-15mg of the sample was weighed and placed into an aluminium container. A pierced lid was used to cover the pan. An empty pan was used as a reference to track the heat flow. Due to the specific heat capacity of the sample, the reference pan usually heats slightly quicker. Upon heating both pans will have parallel heat flow signals until a physical change within the sample occurs. At which point more or less heat will be required to keep sample pan the same temperature as the reference pan. By measuring the difference in the heat flow signals the amount of heat absorbed or released during these transitions can be measured.

Netzsch Proteus© thermal analysis program version 7.0.1 was used for data acquisition and analysis. For PA-6 analysis the sample was heated to 250°C at a rate of 10K/min, then cooled back down to 25°C at the same rate. The resulting melting and cooling curves were used to determine the melting point and crystallisation point. The melting point was considered to be the peak of the curve that was determined using the previously stated software. For PA-12 analysis, the sample was heated to 200°C at a rate of 10K/min, then cooled back down to 25°C at the same rate.

The analysis of the melting points of the product is the means for verification and confirmation of successful synthesis, as both PA-6 and PA-12 have distinct melting points from other substances in the recipes as shown in Figure 3.4. The synthesised particles were then compared to control PA-6 and PA-12 polymers acquired from Sigma Aldrich as shown in Figures 3.5 and 3.6, this confirms if the nylon variant had been successfully synthesised. In both cases, the melting point of the particles is slightly lower than that of the control but still within normal values for PA-6 and PA-12.

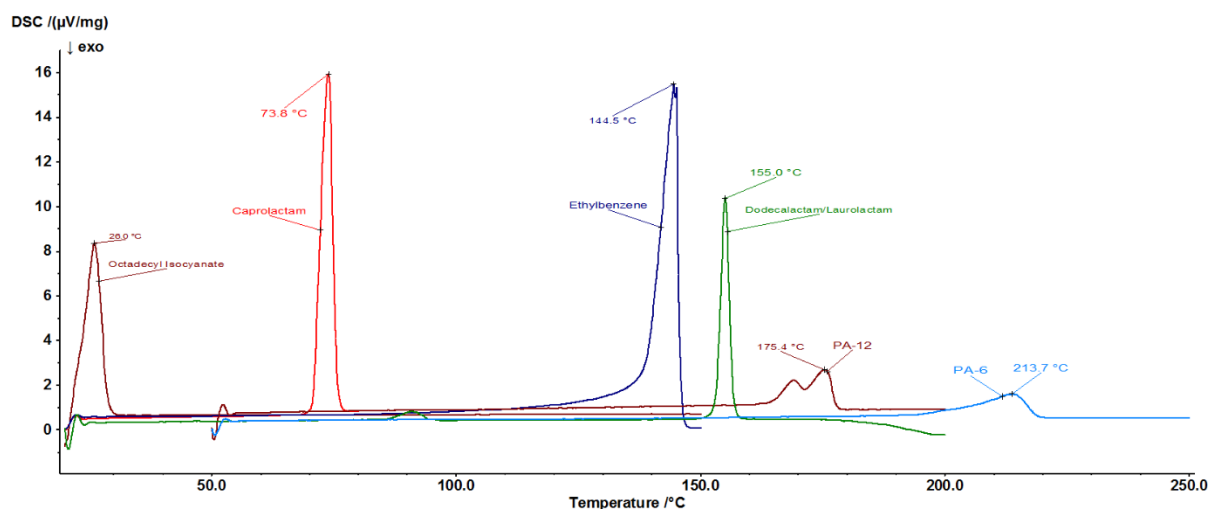


Figure 3.4 DSC spectrum showing melting point of all substances in the reaction mixture

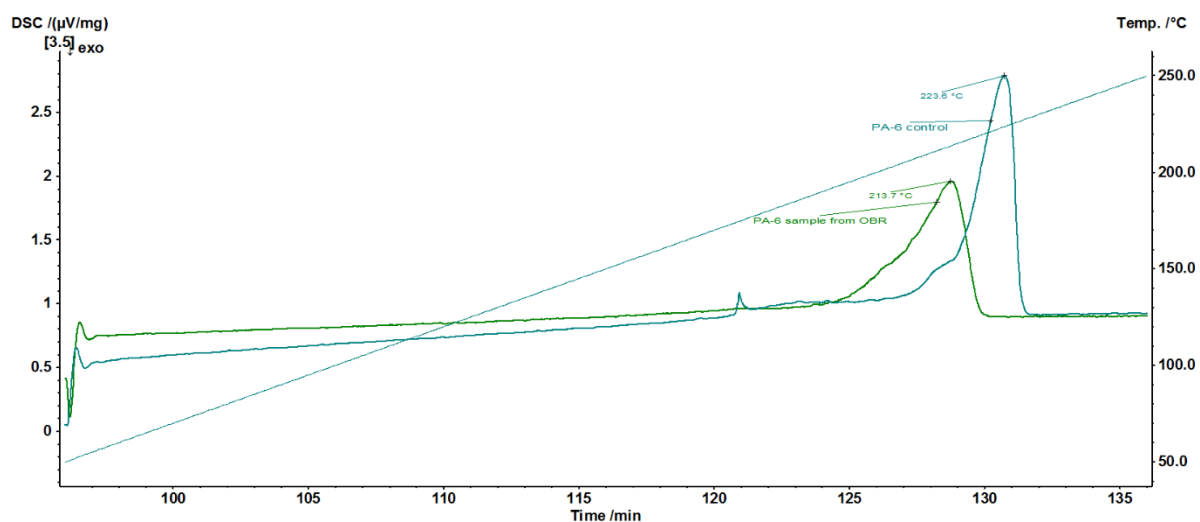


Figure 3.5 DSC spectrum comparing melting point of synthesised PA-6 particles and control PA-6

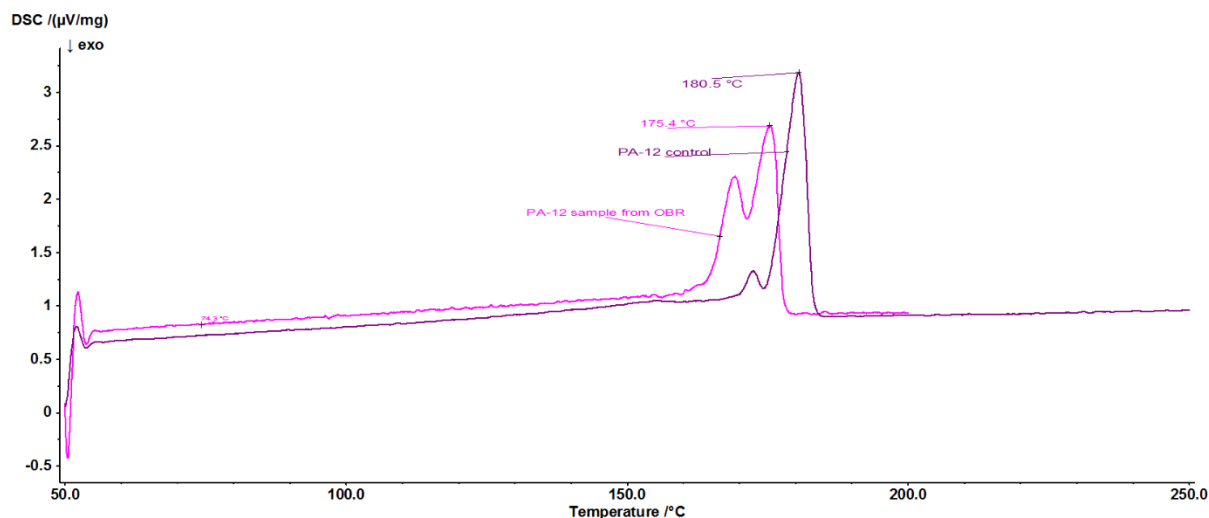


Figure 3.6 DSC spectrum comparing melting point of synthesised PA-12 particles and control PA-12

### 3.4.2-Particle size analysis

The particle size distribution was determined using a Mastersizer (series 3000). The Mastersizer uses laser diffraction to measure the size of particles. Particle sizes are measured by passing a laser beam through the dispersed particulate sample. The angular variation in intensity of the scattered light is measured. Larger particles scatter the light in small angles relative to the laser beam while small particles scatter the light in larger angles. The angular scattering intensity data is then examined using the Mie theory of light scattering. Laser diffraction offers multiple advantages over fractionation sieving techniques. Firstly, analysis is much quicker and easily reproducible. Secondly, if desired, laser diffraction can be used to make real-time measurements. However, laser diffraction techniques require substantial calibration when compared to sieving techniques

Data acquisition and analysis were carried out using the Mastersizer 3000 software v3.40. For each sample, 0.5g of nylon particles were dispersed in approximately 5mL of propan-2-ol. Samples were placed in a Sonicator for 5 minutes and vigorously mixed by hand. Each sample was stirred at 2000 rpm and each sample was measured 5 times. Fresh dispersant was used for each sample. For PA-6 and PA-12, the refractive index was 1.53 and 1.525

respectively. No information on the absorption index could be found for either PA-6 or PA-12 so an index of 0.5 was used for both. Both sets of particles were considered to be none spherical. Figure 3.7 and Table 3.7 shows the typical particle size distribution from the Mastersizer.

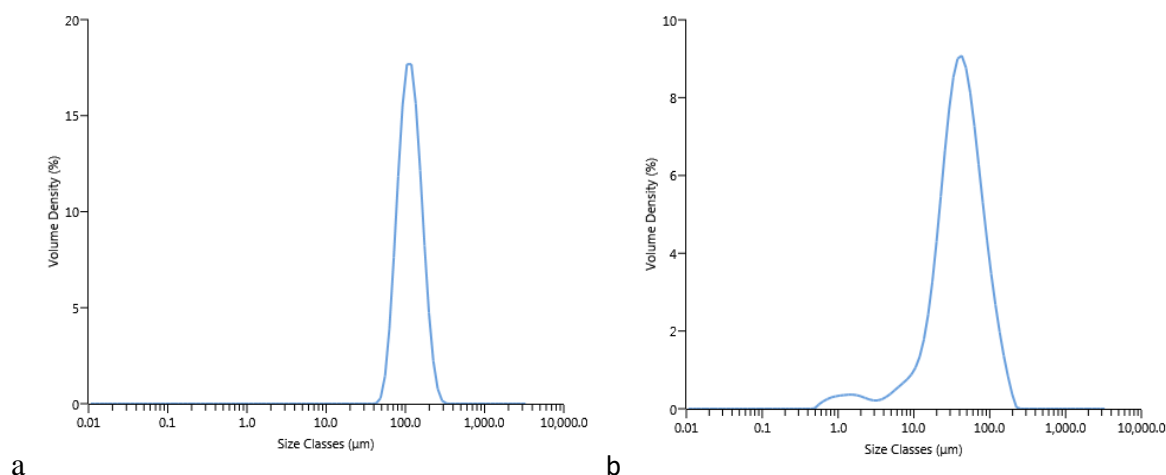


Figure 3.7 a) Particle size distribution of PA-12 synthesised particles b) Particle size distribution of PA-6 synthesised particles

Sample Name	Dx(10) (µm)	Dx(50) (µm)	Dx(90) (µm)
PA-12 OBR retry 8	74.8	113	174
Nylon-6 CL Plankett-5 analysis 2	13.8	40.1	94.3

Table 3.7 Particle size distributions of PA-6 and PA-12 samples

### 3.4.3-Molecular weight analysis

Molecular weight was analysed by Smithers Rapra by Gel Permeation Chromatography, the results of which are shown in Figures 3.8, 3.9 and Table 3.8. Gel Permeation Chromatography is a chromatographic method where molecules in solution are separated by their size and molecular weight. The chromatographic column is packed with fine porous beads that are used to measure the dimensions of the sample. The amount of time the mobile phase stays within the column is based on the size of the polymer. Molecules that are larger than the largest pores

in the column will pass through the column directly. Smaller molecules that partially interact with the pores in the column matrix are separated and eluted from the column in order of decreasing size. The biggest drawback to this technique is the cost. PA-12 has very high chemical resistance. Among the few known solvents include the fertiliser m-cresol, 95% sulphuric acid and Hydrofluoroisopropanol (HFIP). HFIP is the most commonly used solvent in nylon analysis. However, this is very expensive solvent and therefore the amount of sample that can be analysed is limited. The other major drawback to Gel Permeation Chromatography is that it does not, by itself, give absolute values for molecular weight. Therefore, it works best if samples are analysed in bulk, using the same calibration. If analytes are being analysed under different calibrations a reference sample would have to be chosen and analysed under both calibrations to allow for comparison between groups.

The instrument used was a Malvern/Viscotek TDA 301 with associated pump and autosampler. The columns were Agilent PL HFIPgel guard plus 2 x PL HFIPgel 300 x 7.5mm, 9 $\mu$ m. The solvent of choice was 1,1,1,3,3,3-hexafluoropropan-2-ol with 25mM NaTFAc. Samples were eluted at a flow rate of 0.8mL/min at 40°C. The GPC system was calibrated using Agilent Easivial polymethylmethacrylate calibrants. Each sample was prepared by adding 10mL of solvent to 20mg of sample. The sample was left overnight to ensure complete dissolution. The solution was mixed and filtered through a 0.45 $\mu$ m membrane into autosampler vials. Vials are placed in an autosampler. Injection of contents of each vial was carried out automatically.

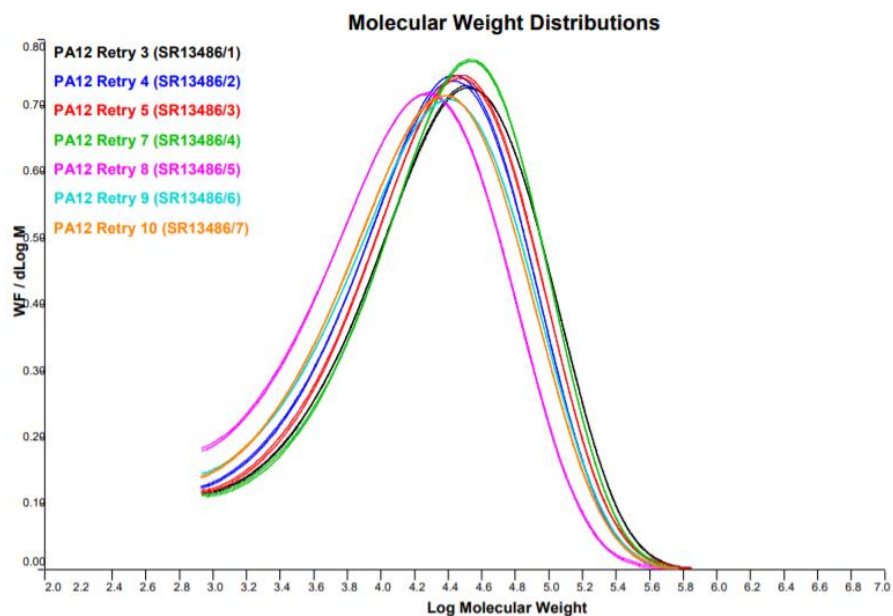


Figure 3.8 Average molecular weight distributions based upon two scans of various synthesised PA-12 polymer particles

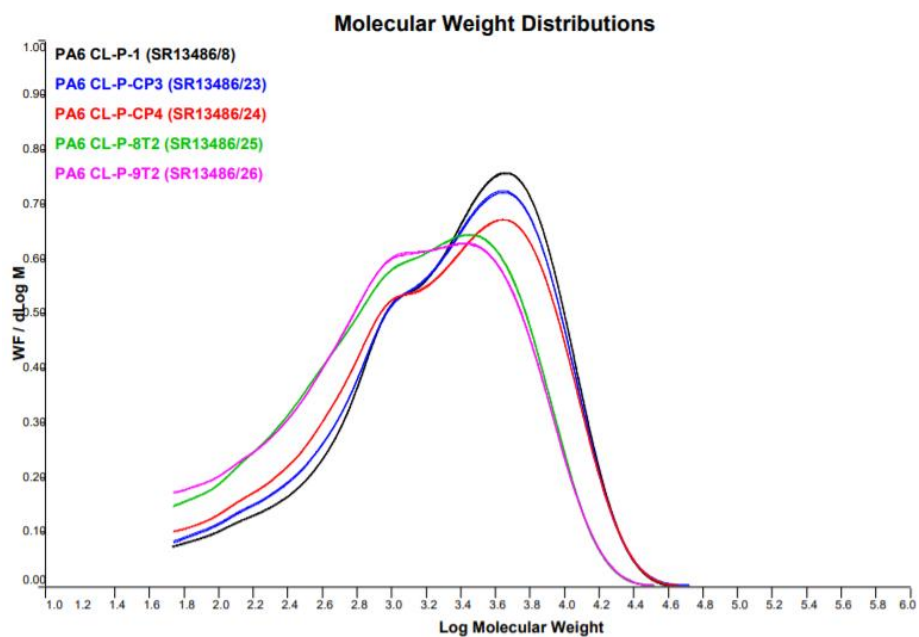


Figure 3.9 Molecular weight distributions of various synthesised PA-6 polymer particles



Nylon-variant	Sample	Molecular Weight
PA-12	Retry 3	45,100
	Retry 4	36,100
	Retry 5	40,100
	Retry 7	42,900
	Retry 8	26,900
	Retry 9	35,300
	Retry 10	
PA-6	PA-6 CL-P-1	4110
	PA-6 CL-CP-1	3990
	PA-6 CL-CP-2	3820
	PA-6 CL-P-8T2	2580
	PA-6 CL-P-9T2	2540

Table 3.8 Molecular weights of PA-6 and PA-12 samples

### 3.4.4 Morphology analysis

Morphology analysis was carried out using an FEI Quanta 3D FEG Dual Beam Scanning Electron Microscope. The electron microscope develops images from samples by scanning the sample with a beam of electrons. The electrons interact with surface of the sample, this produces multiple signals that contain information about the topography and composition of the sample. The electron beam is scanned in a raster scan pattern. The position of the beam is combined with the intensity of the detected signal to produce an image. SEM microscopes have a potential resolution of 0.2nm, allowing for the creation of highly detailed images of organelles within a cell. Something that is not possible to do using light microscopes. However, electrons can be deflected by molecules in the air, therefore the sample must be placed in a vacuum. Additionally, a sample must be electrically conductive. Samples that are nonconductive must be coated with ultrathin layer of a conductive material such as gold. Magnification of PA samples ranged from x100 up to x35,000. An example of which is seen in Figure 3.10.

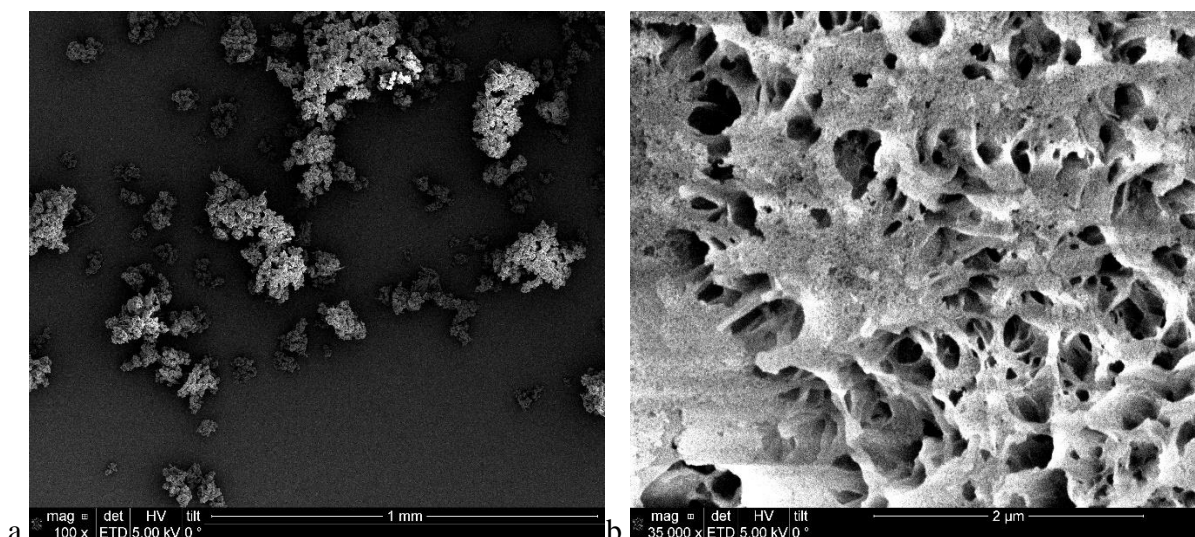


Figure 3.10 Example SEM images of PA-12

### 3.5-Kinetics study

Reaction kinetics were followed via ATR-FTIR by analysing the gradual reduction in the carbonyl peak of the caprolactam as the reaction progresses. This is shown in Figure 3.11. The peak has a very strong signal and is isolated from other large peaks in the spectrum. As nylon particles are formed and precipitate, the intensity of the carbonyl peak decreases. The FTIR instrument sends infrared radiation ranging from  $10,000\text{cm}^{-1}$  to  $100\text{cm}^{-1}$  through the sample. Absorbed energy is converted into rotational and vibrational energy. The detector measures what wavelengths have been absorbed. The resulting signal is presented as a spectrum. Each molecule and chemical structure and functional group has a unique spectrum. Very little analyte is required for successful analysis. Samples can either be in the solid or liquid state and require no preparation. Results are easily reproducible and there are minimal operator-induced variations. However infrared spectroscopy cannot analyse an analyte that does not possess a dipole moment.

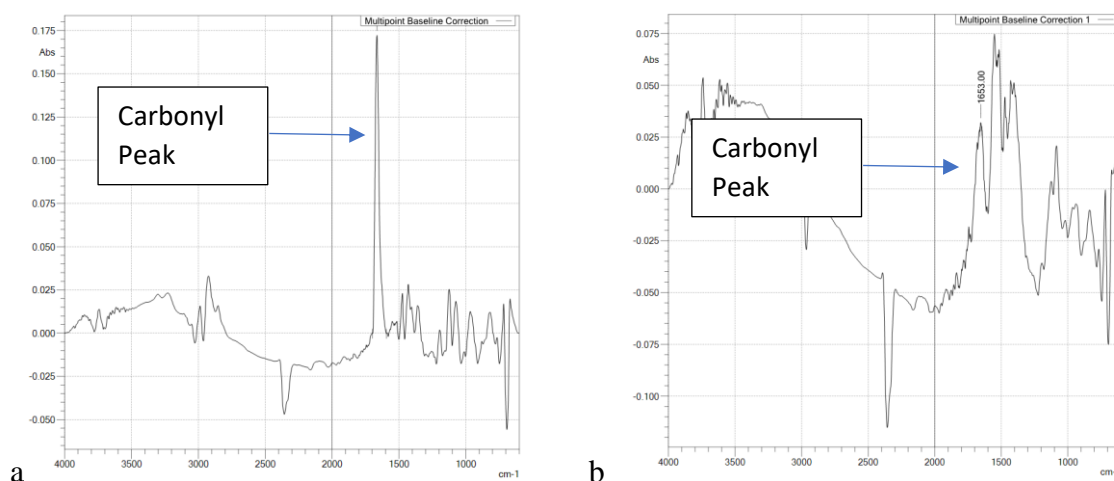


Figure 3.11. a) FTIR spectra of caprolactam dissolved in ethylbenzene at the beginning of the reaction and b) FTIR spectra of caprolactam dissolved in ethylbenzene near the end of the reaction

Kinetic studies were carried out using a Shimadzu IR Prestige-21 Fourier Transform Infrared spectrometer equipped with a Specac® Quest ATR diamond accessory. For each sample, 2-3 drops were placed in the centre of the ATR. Each sample was analysed 5 times. IRsolution software was used for data analysis and acquisition. For each analysis, a Happ-Genzel apodization was employed. The sample was scanned 45 times with a resolution of 4. The resolution indicates the degree of fineness of the data obtained. With a resolution of 4 spectra will be obtained in intervals of  $\sim 2\text{cm}^{-1}$ . The range of each scan was  $600\text{--}4000\text{ cm}^{-1}$ . To account for heavy noise in the spectra from reaction under normal conditions, samples first smoothed by 25 points. This was followed by a two-point baseline correction at points of  $1589.3\text{ cm}^{-1}$  and  $1701.2\text{ cm}^{-1}$ .

For equimolar reactions the isocyanate peak of the CI was followed to measure reaction kinetics instead of the carbonyl peak of the monomer. The isocyanate peak was followed because as nylon wasn't precipitating there would be no change in the carbonyl peak. Upon reacting with caprolactam the isocyanate group on the CI would be transformed to an amide group. Therefore, by monitoring the decrease in the isocyanate peak kinetics can be observed.

To determine how peak heights corresponded to monomer concentration, a calibration curve was created using the quantitation function provided with the IRsolution software. Five samples with known caprolactam concentrations shown in Table 3.9 were used in this

calibration. Each sample was dissolved in 9mL of ethylbenzene. The IRsolution software determined the maximum peak height between the ranges of 1610.56 to 1737.86  $\text{cm}^{-1}$ . Figure 3.12\* is the calibration curve.

Mass of caprolactam (g)	Concentration of caprolactam ( $\text{mol L}^{-1}$ )	Peak height
3	3	0.25
1.5	1.5	0.17
0.75	0.74	0.099
0.375	0.368	0.05
0.1875	0.184	0.025

Table 3.9 Summary of the calibration curve data

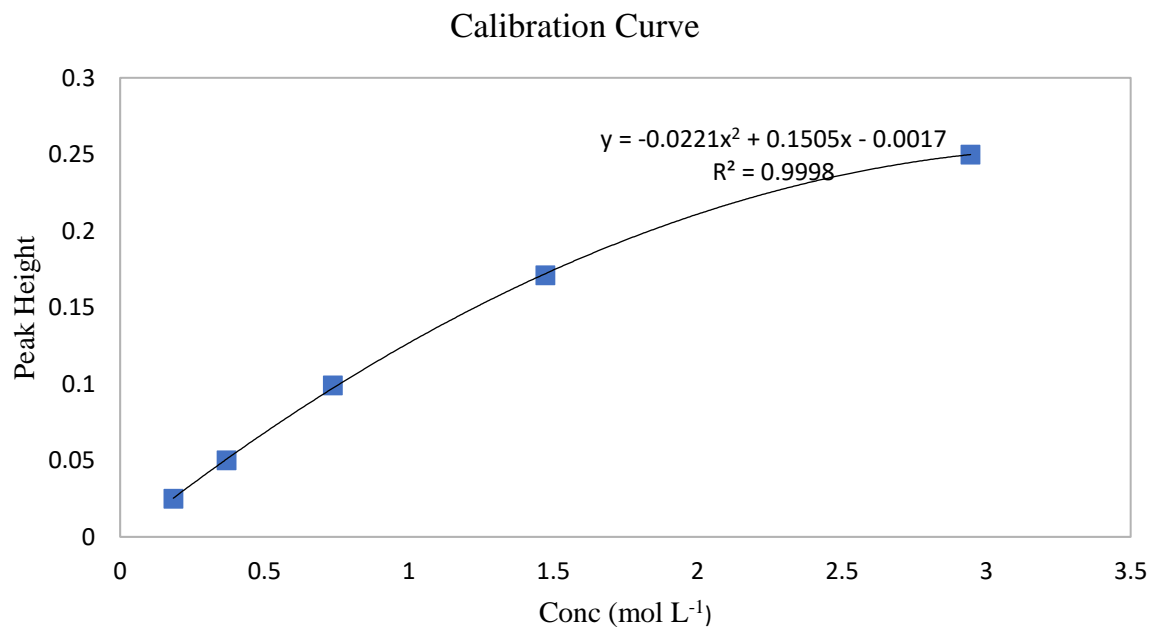


Figure 3.12\* Calibration curve showing how carbonyl peak height is related to monomer concentration

## Chapter 4 - PA-6 synthesis and kinetics

This chapter is split into two sections. The first section presents the results and discussion of the effect of experimental parameters on polymer properties. The second section is focused on the effect of experimental parameters on reaction kinetics.

### 4.1-PA-6 synthesis

#### 4.1.1-Introduction

Nylon particles were first created by the pioneering work of Chrzczonowicz<sup>3, 82</sup> through the anionic precipitation polymerisation of caprolactam. Even with the presence of a catalyst, anionic polymerisation of lactams requires very high temperatures due to the low nucleophilicity of caprolactam. To circumvent this requirement a chain initiator is used. The chain initiator can be added in two different ways, either all at once(‘one-shot’) or through continuous injection over a set time. Published research regarding pure nylon particles is rare, and almost all research was focused on synthesis using the ‘one-shot’ injection method.

There are many different competing variables (or factors) involved in nylon particle synthesis that can affect the resultant polymer’s properties. These variables include but are not limited to temperature, monomer/catalyst ratio, monomer/solvent ratio, catalyst/CI ratio, mixing speed, choice of catalyst, choice of CI etc. The majority of literature has focused on how the choice of CI and catalyst used in the synthesis of nylon particles impacts the polymer properties. Data pertaining to continuous injection of chain initiator is very limited. Patents<sup>47, 49</sup> state what factors affect polymer properties, such as melting point, molecular weight and particle size, but are voided of quantitative data that are crucial to the development of a viable synthesis route and in turn the creation of bespoke particles. Due to the extended reaction time required for synthesis, a factorial design was used to analyse how different variables affected desired responses.

#### 4.1.2-Factorial Design

Factorial design or Design of Experiment (DOE) is a multivariate statistical tool that analyses a system's response to changes in specified variables or process parameters. The impact of each parameter can be quantified and the statistical significance of the process response determined. This allows for the optimal values for a given response to be obtained. A factorial design also has the additional benefit of analysing any potential combination of variables that can affect a chosen response, i.e. a 2-way interaction. For example, both the catalyst concentration and monomer concentration of a system may positively affect the molecular weight of a polymer but at high catalyst concentration the influence the monomer concentration has on molecular weight is reduced. Such observations would be very difficult to make using traditional methods.

This powerful technique can be used to improve control, increase reliability and lower production costs<sup>122</sup>. Factorial designs have previously shown to be an effective method to analyse polymer properties<sup>123-127</sup>. In these factorial designs many different factors were tested by, for example, analysing the impacts temperature, reaction time and oxidant concentration have on the yield of polyaniline particle synthesis. This helped to develop a model that accurately predicted how multiple variables affected drug release from extended-release extrudates<sup>124</sup>.

Once a factorial design goes beyond three factors, it becomes increasingly complex. In the majority of designs, each factor is represented by two levels, 'high' and 'low'. These two levels are the limits of the design. In rare cases, a 3-level design is also used. The number of experiments required by a normal design is  $2^n$ , so 5 factors would require 32 experiments as illustrated in Table 4.1. By this point, it can become advantageous to use either a fractional factorial design (FFD) or a Plackett-Burman screening design. The purpose of design screening is to identify the main variables that have a statistically significant effect on a response. A FFD has a lower or higher resolution to a screening design (see Table 4.2). The resolution of a design describes how the main effects are confounded with 2-level, 3-level interactions and etc. Confounding, or aliasing, is when the estimated effect of one factor includes the influence of another. Like a factorial design, the Plackett-Burman design consists of a series of experiments with high and low values which are then analysed to see their effects<sup>128, 129</sup>.

However, while the screening design has a lower resolution, it can successfully screen up to 11 factors with only 12 experiments (does not include centre points) and can significantly convert any three factors used in the design to a full factorial design without additional experiments. Therefore, assuming you have 11 factors and all responses are only affected by any three (or less) factors, 12 experiments will yield the same amount of information as 2048 experiments required to complete a full factorial design! The fractional factorial design cannot directly be converted into a full design. It was for these reasons that the Plackett-Burman design was chosen over a fractional factorial one.

<b>No. of variables</b>	<b>No. of experiments required</b>
2	4
3	8
4	16
5	32
6	64
11	2048

Table 4.1 List showing how many experiments are required to carry out a full factorial analysis depending on how many variables are present

The six factors of interest in the PA-6 synthesis are temperature, monomer mass, solvent volume, catalyst volume, the rate of CI injection and mixing intensity. These factors were chosen because all have been stated to have an influence over either molecular weight, particle size or melting point, but have not been studied in detail. The effects of different catalysts and CIs combinations have on polymer properties are well documented, so they were not involved in the design.

Design	No. of experiments required
Plackett-Burman screen	12
Fractional (1/8) factorial design	8
Fractional (1/4) factorial design	16
Fractional (1/2) factorial design	32

Table 4.2 List of different factorial designs and required experiments that can be used to analyse 6 factors

### 4.1.3-Experimental design

The Plackett-Burman design uses the following polynomial to correlate the dependant and independent variables:

$$Y = A_0 + A_1Z_1 + A_2Z_2 + A_3Z_3 \pm \dots \mp A_nZ_n \quad (4.1)$$

Where Y is the response,  $Z_1$  to  $Z_n$  are the different factors,  $A_0$  the constant and  $A_1$  to  $A_n$  are the values of the factors. The values of the variables are provided in Table 4.3. A 6 factor 12-run Plackett-Burman was generated via Minitab 17. Within the design, each factor is represented by two levels of ‘high’ and ‘low’. These two levels are the limits of the design.

A parameter is considered significant when it has shown to be not equal to zero. Analysis of variance (ANOVA) calculates a p-value with the null hypothesis that the corresponding parameter value is equal to zero. The p-value, also known as the calculated probability, is the likelihood that under a chosen model the summary of the data would be equal to or greater than it’s observed value<sup>130</sup>. Should the p-value be less than the significance level (alpha,  $\alpha$ ), the null-hypothesis is excluded. A value is considered statistically significant when  $p < 0.05$  and highly significant when  $p < 0.001$ . The magnitude of the factor value determines its influence over the specified response.



The initial regression model has all the factors included in the model. From this point, the values that are not statistically significant are systematically removed with the highest p-value removed first and so on. Values are removed one at a time because the removal of one factor can cause another to become significant. In the cases where there are 3 or less significant factors, the model is then converted into a full factorial design to include any potential interactions so as to further improve the model.

	<b>Code</b>	<b>Low level</b>	<b>High level</b>
Monomer Mass	Z <sub>1</sub>	5g	7g
Solvent volume	Z <sub>2</sub>	16mL	20mL
Catalyst volume	Z <sub>3</sub>	1mL	2mL
Rate of injection	Z <sub>4</sub>	5μ/min	10 μ/min
Temperature	Z <sub>5</sub>	90	110
Stirring speed	Z <sub>6</sub>	250	350
Particle size Dx50	Y <sub>1</sub>		
Molecular weight	Y <sub>2</sub>		
2 <sup>nd</sup> Melting point	Y <sub>3</sub>		
Crystallisation point	Y <sub>4</sub>		

Table 4.3 Table of variables values and desired responses

#### 4.1.4-Interpretion of DOE data

The S-value represents the standard deviation of how far data values diverge from fitted values. Therefore, the lower the S-value, the greater a model's ability to describe the response variable. It must be noted however that a low S-value does not indicate by itself that a model is fit for purpose.

The  $R^2$  value is the percentage of variation in the response variable described by the model. It is calculated by the equation shown below:

$$R^2 = 1 - \frac{\text{First sum of errors}}{\text{Second sum of errors}} \quad (4.2)$$

Where the first sum of errors is the variation not explained by the model and the second sum of errors is all variation within the model. When adding new factors to a model, the  $R^2$  will always be at least as high as its highest value for the previous model. Due to this,  $R^2$  is a tool that is best used to compare models with the same number of factors. The  $R^2$  adjusted is like the  $R^2$  but considers the number of factors included within the model. As such the  $R^2$  adjusted value is useful when comparing different models.  $R^2$  adjusted is calculated using the equation below:

$$R^2(\text{adj}) \left[ \frac{(1 - R^2)(n - 1)}{n - k - 1} \right] = 1 \quad (4.3)$$

Where  $n$  is the number of points within the data sample and  $k$  is the number of variables within the model. The  $R^2$  (pred) is calculated with a formula that is equivalent to systematically removing each observation from the set, estimating the regression equation, then determining how well the model predicts the removed observation. In effect, the  $R^2$  (pred) shows the predictive ability of a model. A model with a substantially lower predicted  $R^2$  than  $R^2$  value can indicate that there are too many predictors in the model.

This thesis uses three different charts to illustrate the results of a model derived from a design. The three charts used were Pareto charts of standardised effect, interaction plots and 3D-cube plots. The Pareto charts show what factors from the highest weight to lowest are involved in the model. Should a factor cross over the red dotted line, they are considered statistically significant. The interaction plot contains two blue and green dots. The blue dots signify the mean value of a factor at its 'low' and 'high' levels and is joined by a single line. The steeper the line, the greater the impact of the variable on the response. The red dot

represents the centre point. The green dots are similar to the blue dots, but they represent the other factor of interest. The 3D cube plot shows various relationships between factors and a response within a model. Each cube can show three factors, and should the model only contain two factors, the cube is reduced to a square.

#### 4.1.5 Results and discussion

RunOrder	PtType	Blocks	Monomer Mass	Solvent Volume	Catalyst Volume	Rate of Injection	Temperature	Stirring speed
1	1	1	7	16	2	5	90	250
2	1	1	7	20	1	10	90	250
3	1	1	5	20	2	5	110	250
4	1	1	7	16	2	10	90	350
5	1	1	7	20	1	10	110	250
6	1	1	7	20	2	5	110	350
7	1	1	5	20	2	10	90	350
8	1	1	5	16	2	10	110	250
9	1	1	5	16	1	10	110	350
10	1	1	7	16	1	5	110	350
11	1	1	5	20	1	5	90	350
12	1	1	5	16	1	5	90	250
13	0	1	6	18	1.5	7.5	100	300
14	0	1	6	18	1.5	7.5	100	300
15	0	1	6	18	1.5	7.5	100	300
16	0	1	6	18	1.5	7.5	100	300

Table 4.4 Plackett-Burman screening design with six variables generated using Minitab software

##### 4.1.5.1-Effect of factors on the molecular weight

The Plackett-Burman (PB) experiments were carried as shown in Table 4.4 (reactions were carried out in a randomised order). The model produced is labelled model 1A (see Figure 4.1 and Table 4.5). The non-significant figures were then removed systematically from the smallest to the largest to produce model 2A. Looking at Table 4.5, model 2A has a poorer fit

than 1A, indicated by the lower  $R^2$  values and larger S value. This may be caused by the confounding of factors that can occur with lower resolution designs. No literature can be found by the author to show that mixing intensity has a significant influence over the molecular weight. Therefore, confounding may have caused the stirring speed to become a significant player. To test this hypothesis, the PB was converted into a full factorial design using the variables temperature, the rate of injection and monomer mass. The subsequent model is labelled model 3A. As can be seen in Table 4.5, the removal of the mixing speed factor in the conversion to full factorial has improved the quality of the model. The S-value has decreased and  $R^2$  (adjusted) value has increased as well. As before the non-significant figures were removed and the final model 4A was produced. For all models in the thesis, the actual p-values can be seen in Table 4.8. All results used to create all DOE models are in Table 4.9.

<b>Plackett-Burman Design</b>		<b>S-value</b>	<b><math>R^2</math></b>	<b><math>R^2</math> (adjusted)</b>	<b><math>R^2</math>(predicted)</b>
	Model 1A	444.3	96.57%	92.57%	80.32%
	Model 2A	466.7	94.96%	91.80%	85.13%
Full Factorial	Model 3A	335.6	98.38%	96.12%	*
	Model 4A	311.5	98.05%	96.66%	94.17%

Table 4.5 Summary of each model studying the influence of various factors over molecular weight

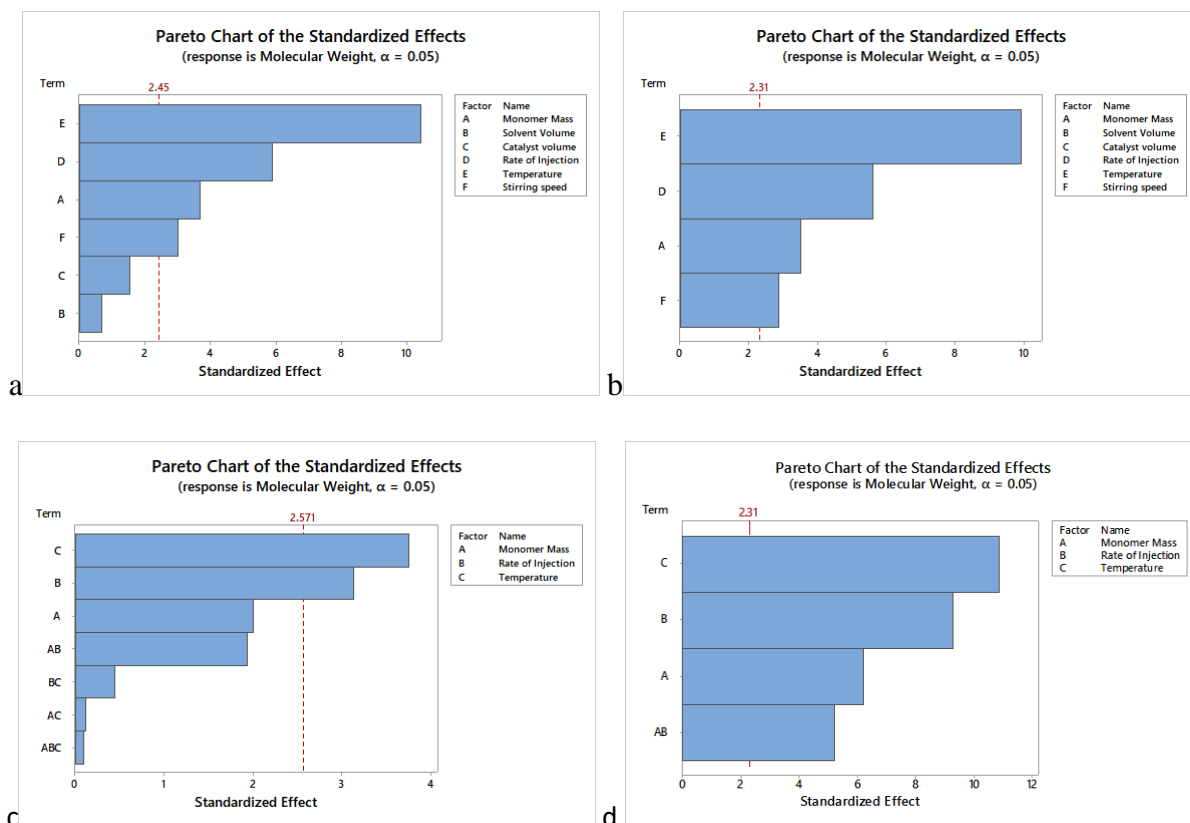


Figure 4.1 Pareto graphs of Models 1A (a) 2A (b), 3A(c) and 4A(d)

In agreement with various patents and literature, increasing the temperature increases the molecular weight of the polymer produced. Of the variables tested, the model found that temperature was the most important factor for controlling molecular weight. The work by Schreiber and Waldman<sup>131</sup> theorised that the temperature dependence of molecular weight was caused by the dissociation of polymer aggregates in the solution that have been made from inter-chain entanglements. Higher reaction temperatures lead to an increase in polymer-solvent interactions. This, in turn, causes gradual disentanglement.

Increasing the rate of injection was found to have a negative impact on molecular weight, as it would lead to more active sites for the monomer to react with, resulting in more, but smaller growing chains. Conversely increasing the monomer concentration leads to an increase in molecular weight. Again, this agrees with various patents and literatures pertaining to the single injection technique as well as other similar chain growth reactions<sup>47, 60, 132-134</sup>.

However, the negative impact the rate of injection has on molecular weight did not agree with the findings of Hilaire and Guerin who observed that reducing CI concentration decreased molecular weight<sup>135</sup>. The possible reason for this contradiction is complex. Using the single injection method it is known that the optimal CI/catalyst ratio is approximately 0.67/1<sup>60</sup>. Any deviation from this ratio would lead to a decrease in molecular weight. Even at the low-level injection rate tested in this work, this ratio may have been exceeded over the duration of the reaction time, with the high-level injection rate causing further deviation. In contrast, the injection rates and times used by Hilaire and Guerin may have never reached the optimum ratio. Furthermore, Udipi et al<sup>74</sup> observed when studying the reaction in bulk that below certain concentrations, decreasing the concentration of the CI further would cause an increase in molecular weight, but above the specific concentration, increasing CI concentration increases the molecular weight.

Interestingly the interaction plot of Figure 4.2 shows that as the rate of injection increases there is a strong negative interaction with monomer mass. At lower rates of injection, increasing monomer mass has a substantial positive effect on the polymer's molecular mass, however, at higher injection rates, this effect becomes negligible. This shows that two dominant factors tested in controlling molecular weight overall are temperature and rate of injection as shown in Figure 4.3, with monomer mass having a smaller, but significant influence.

Where the results differ substantially from literature is the effect the catalyst has on molecular weight. Surprisingly, our results showed that the catalyst concentration had very little influence on molecular weight. This disagrees with other literatures where increasing the catalyst concentration increased the molecular weight until an optimum value is reached, after which further increases in concentration would have a negative effect on molecular weight. This optimum value is dependent on both the monomer and CI concentration. It may be that the continuous injection method limits the influence of the catalyst concentration. Another possible explanation is that the excess of chain initiator masks any impact the catalyst has.

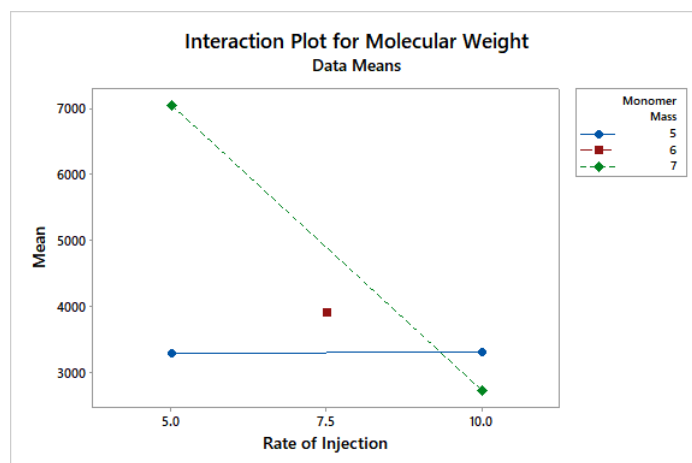


Figure 4.2 Interaction plot between monomer mass and rate of injection

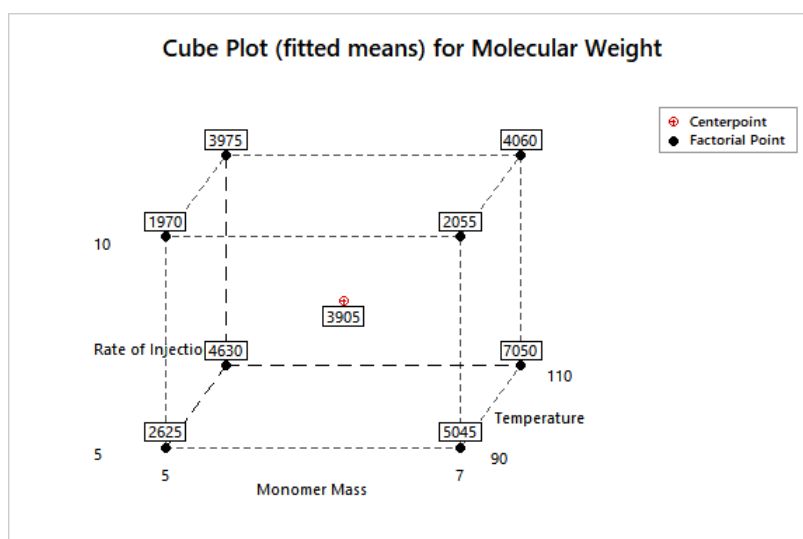


Figure 4.3 Cube plot of temperature, the rate of injection and monomer mass relationship effects on molecular weight

#### 4.1.5.2-Effect of factors on the melting point

The process used to develop the model to describe the melting point is the same as the one used to develop the molecular weight model. Firstly, the initial model 1B is produced and the non-significant figures removed systemically to produce model 2B (see Figure 4.4). The removal of these factors improved the model predictive-ability substantially with  $R^2$  (predicted) going from 17.89% to 68.49% (see Table 4.6), however, improvements to the standard error of the regression analysis were small.



The screening found that the two most important factors were temperature and solvent volume. This is surprising as the relationship between molecular weight and polymer melting point is well known, where as molecular weight increases so does the melting point until it reaches its maximum value. Therefore, it would be expected that the same factors that affect molecular weight would affect the melting point, but this is not the case. The reported melting points for nylon-6 particles vary from 205°C<sup>7, 60</sup> to 215°C<sup>136, 137</sup>. Under optimum conditions, 215°C was reached in this work. It is possible that when the temperature is high, excluding the influence of the solvent volume, the necessary molecular weight is reached regardless of the rate of injection or monomer mass. Work carried out by Florin and Grolier also noted that a higher reaction temperature resulted in particles with a higher melting point. They suggested that this increase was caused by changes in the crystallinity and morphological properties of the particles<sup>7</sup>.

		S-value	R <sup>2</sup>	R <sup>2</sup> (adjusted)	R <sup>2</sup> (predicted)
Plackett-Burman Design	Model 1B	2.28471	89.34%	78.68%	17.89%
	Model 2B	2.25167	83.73%	79.29%	68.49%
Full Factorial	Model 3B	1.33010	96.90%	92.77%	*
	Model 4B	1.33497	95.32%	92.72%	85.77%

Table 4.6 Summary of each model studying the influence of various factors over melting point model

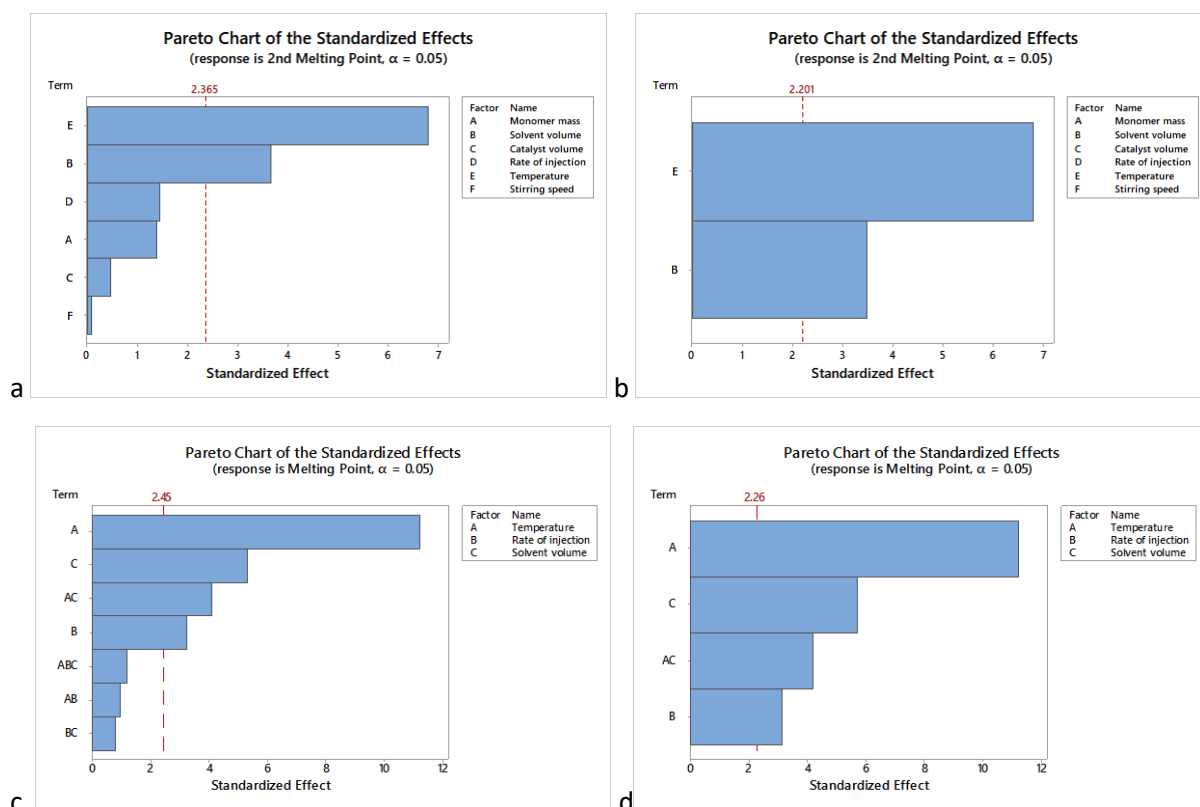


Figure 4.4 Pareto graphs of Models 1B (a) 2B (b), 3B(c) and 4B(d)

The solvent volume having a positive influence was most surprising. This is a direct contradiction to the finding of the molecular weight analysis, which found that the solvent volume had a negative, albeit insignificant impact on molecular weight. One possible explanation is that melting point depression is caused by trapped and unreacted monomer. It is known that one of the issues with precipitation polymerisation is the presence of impurities in the final product. As each experiment was only carried out over a period of two hours, each reaction was not given the required time to reach completion. Because of this, there would still be monomer present in the solution. As the solution volume increases, the corresponding monomer concentration would be lower. Therefore, there will be less unreacted monomer trapped within the polymer particles at higher solvent volumes once the reaction has been quenched and the polymer dried.

Solvent volume and temperature were then involved in the conversion of the PB into an FF design, resulting in model 3B. While it was not considered to be statistically significant, the rate of injection was included within the FF design. Including it did not require any

additional experiments and any impact rate of injection could have may have been masked due to aliasing.

Model 3B saw a substantial improvement in the S-value and smaller increases to the  $R^2$  (adjusted) and  $R^2$  (predicted) values. Again, non-significant factors were removed systematically until model 4B was created. Interestingly the full factorial design showed that the rate of injection had a slight, but a statistically significant negative influence on the melting point, as would be expected due to its impact on the molecular weight. Additionally, the design conversion from PB to FF suggested that there was a minor but statistically significant negative interaction between solvent volume and temperature shown in Figures 4.5 and 4.6. Interestingly, this is despite both the corresponding main factors having a positive influence over the melting point. Further investigations would have to be carried out in order to understand the source of this interaction.

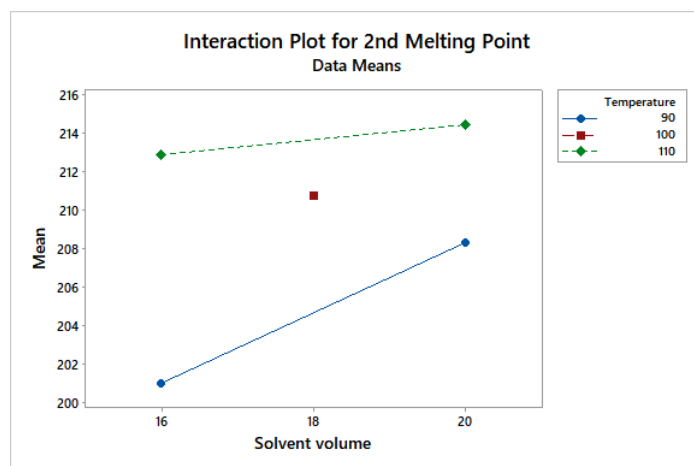


Figure 4.5 Interaction plot between solvent volume and temperature for model 3B

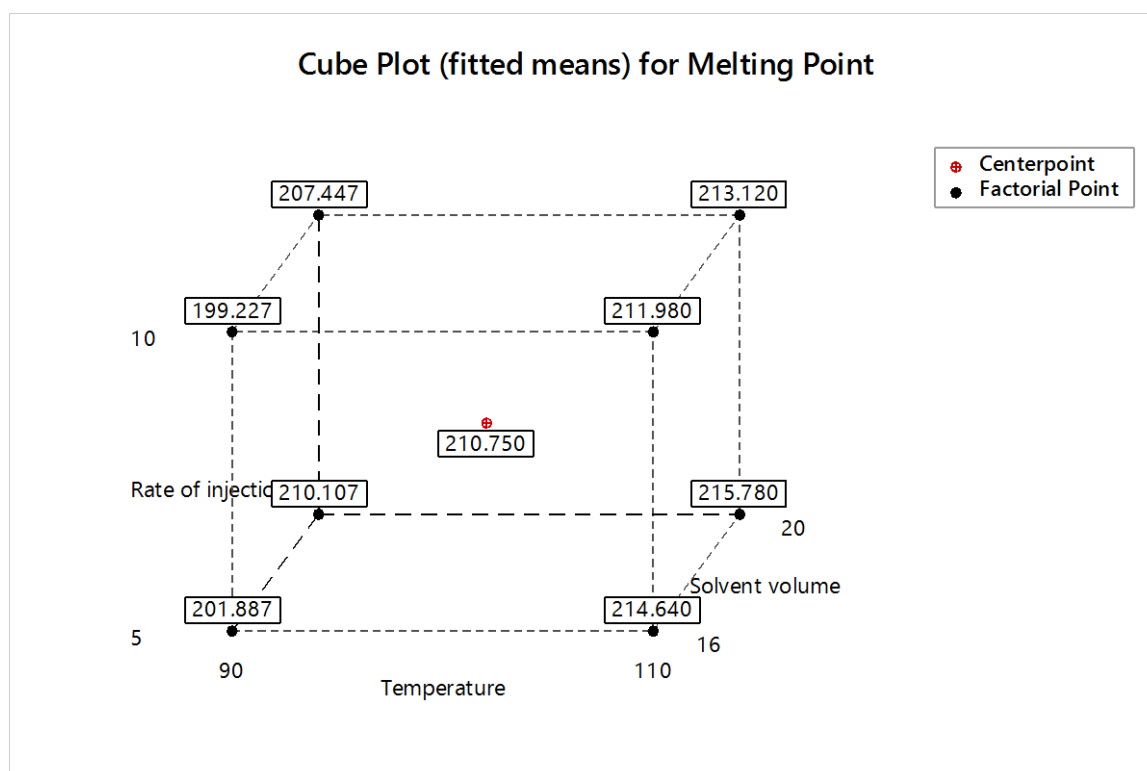


Figure 4.6 Cube plot of temperature and solvent volume effects on 2<sup>nd</sup> melting point

#### 4.1.5.3-Effect of factors on mean particle size

The process used to screen the mean particle size response were the same as the previous two. Model 1C was first produced by the PB screening design. Insignificant variables were then systematically removed, resulting in model 2C. As can be seen from the model summary in Table 4.7, low S-values together with over 90%  $R^2$  values indicate that this is a very good model. The three significant factors were mixing speed, the rate of injection and monomer mass (Figure 4.7).

Research into a range of different polymers formed by precipitation polymerisation have all shown that increasing monomer concentration increases the polymer particle size<sup>.47, 134, 138, 139</sup>. The reasons for this are two-fold: greater monomer concentrations are able to sustain growth of larger particles and; increase in concentration changes the equilibrium distribution between the polymer phase and the rest of the medium, this encourages particle growth.

		S-value	R <sup>2</sup>	R <sup>2</sup> (adjusted)	R <sup>2</sup> (predicted)
Plackett-Burman Design	Model 1C	2.15658	98.21%	95.09%	*
	Model 2C	1.90411	97.56%	96.17%	93.32%
Full Factorial	Model 3A	2.13596	98.05%	95.32%	*
	Model 4C	1.69092	97.80%	97.06%	95.63%

Table 4.7 Model summaries for each mean particle size model

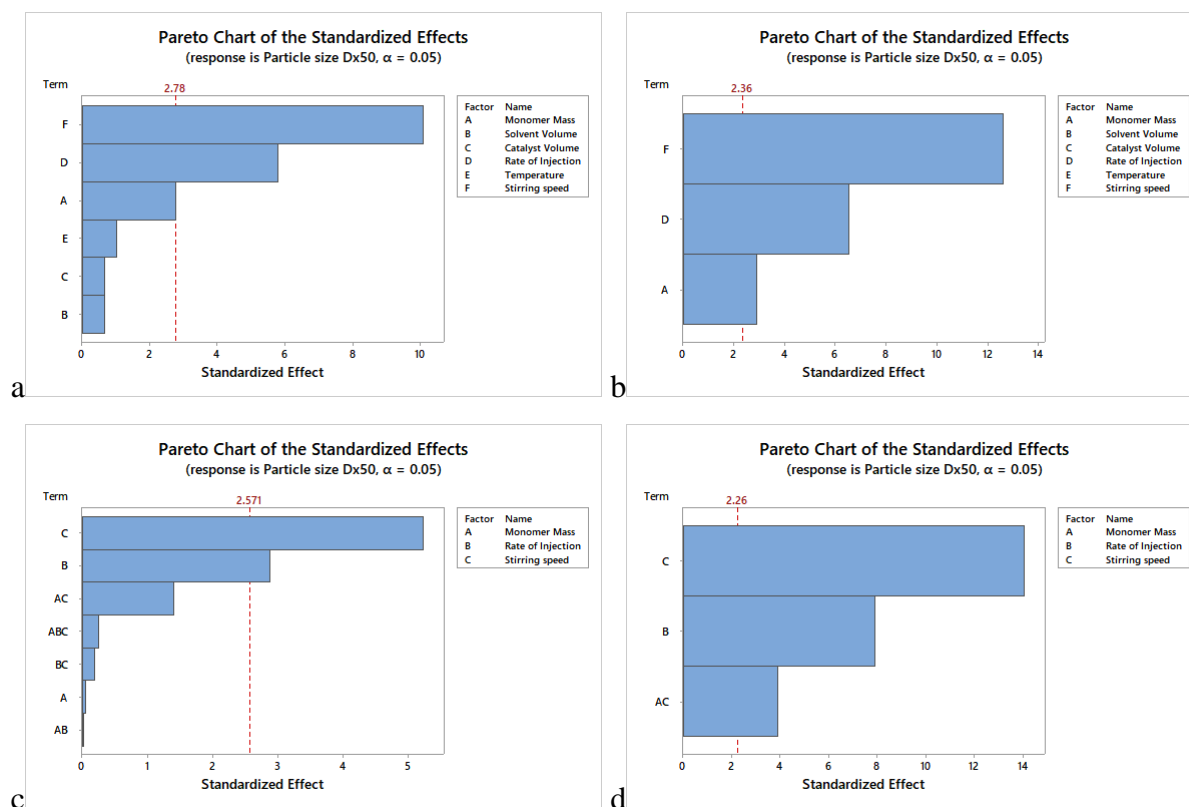


Figure 4.7 Pareto graphs of Models 1C (a) 2C(b), 3C(c) and 4C(d)

By far the most influential variable on the particle size is the stirring speed. It was observed that an increase in stirring speed (agitation) causes the particle size and distribution to decrease, as shown in Figure 4.9. This observation is in agreement by the research by Hilaire et al<sup>47</sup> on PA-6 particle synthesis and a host of other work on polymer particle size control<sup>140, 141</sup>. An explanation for this is that as the shear imposed upon the system increases so does the breakage of agglomerates. This results in finer and narrower particle sizes and distributions.

Again the observation that the rate of injection causing an increase in particle size was in agreement with the work done by Hilaire<sup>47</sup>. A possible explanation for this is that due to increasing injection rate there are more centres for polymer growth at any one time. This, in turn, means that the rate of aggregation of these growing particles will also increase, resulting in greater particles sizes.

The lack of apparent effect caused by temperature is unusual as all work on particle sizes found by the author state that an increase in temperature corresponded to an increase in particle size. Increasing the temperature would increase the rate of collisions between growing particles, leading to a greater rate of agglomeration. On the other hand, higher collisions would lead to more particle breakage, it seems that breakage was dominant over agglomeration. Further investigations should be carried out to see if these results are found at lower stirring speeds.

It should be noted that increasing the catalyst concentration also had little effect on particle size. Based upon previous work investigating nylon particle synthesis it would be expected that increasing the catalyst concentration would cause an increase in particle size as well<sup>47, 60, 142</sup>. As the CI is added continuously over a long period time, there could possibly be an optimum catalyst/CI ratio for particle growth, and even at low injection rates, this ratio may be exceeded. Therefore, again eliminating any influence the catalyst concentration may have at these concentrations.

To determine if the model could be improved upon even further, the PB was converted into a full factorial, resulting in model 3C. Non-significant variables were then systematically removed, result in model 4C (Figures 4.7). As can be seen from Table 4.7, there was a substantial decrease in the S-value but very little change in the  $R^2$  value. The main difference, however, is that the full factorial design did not have monomer mass as a significant factor, instead, it had a two-way interaction between monomer mass and stirring speed as the significant factor. As can be seen from the interaction plot (Figure 4.8) and the cube plot (Figure 4.9), stirring rate becomes more even influential as the monomer mass increases as shown when at higher monomer concentration and at the same stirring speed, the resultant particle size was smaller than particles gained when the lower monomer concentration was used.

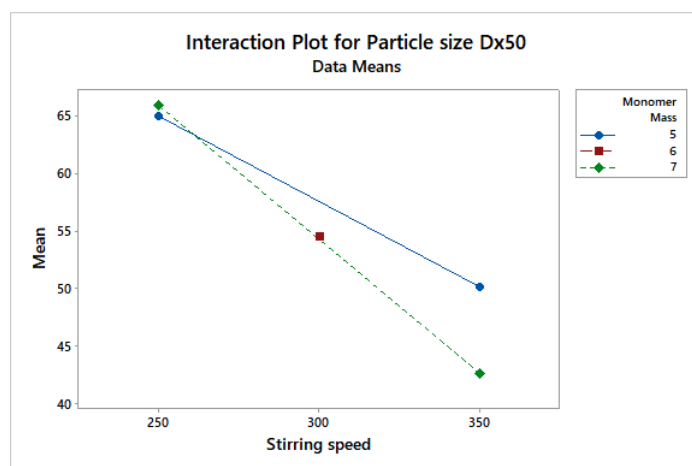


Figure 4.8 Interaction plot between stirring speed and monomer mass for model 4d

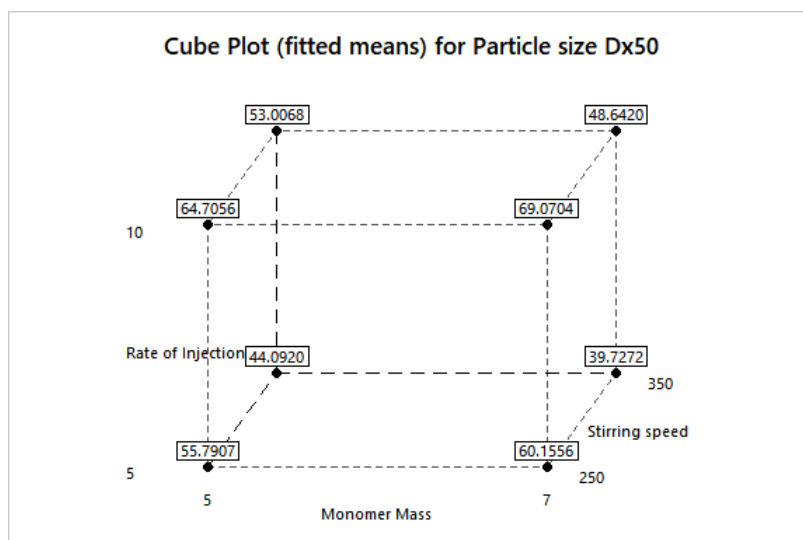


Figure 4.9 Cube plot of monomer mass, the rate of injection and stirring speed relationship effects on molecular weight



Model	Monomer Mass	Solvent Volume	Catalyst Volume	Rate of Injection	Temperature	Stirring speed	Monomer Mass*Rate of Injection	Monomer Mass* Temperature	Monomer Mass*Stirring speed	Monomer Mass*Rate of Injection* Temperature	Monomer Mass*Rate of Injection* Stirring speed	Rate of injection* Solvent volume	Rate of Injection* Temperature	Rate of Injection* Stirring speed	Temperature* Rate of injection	Temperature* Solvent volume	Temperature* Rate of injection* Solvent volume
Model 1A	0.010	0.517	0.176	0.001	0.000	0.024											
Model 2A	0.008			0.001	0.000	0.021											
Model 3A	0.102			0.026	0.013		0.110	0.912		0.932		0.678					
Model 4A	0.000			0.000	0.00		0.001										
Model 1B	0.210	0.008	0.662	0.191	0.000	0.943											
Model 2B		0.005			0.000												
Model 3B		0.002		0.018	0.000						0.464				0.375	0.006	0.277
Model 4B		0.000		0.012	0.000											0.002	
Model 1C	0.051	0.554	0.544	0.004	0.372	0.001											
Model 2C	0.024			0.000	0.000												
Model 3C	0.965			0.035	0.003				0.221		0.820				0.855		
Model 4C				0.000	0.00				0.004								

Table 4.8 Table of all p-values for all models

Variables							Responses		
Run	Monomer Mass (g)	Solvent Volume (mL)	Catalyst volume (mL)	Rate of Injection ( $\mu\text{L}/\text{min}$ )	Temperature ( $^{\circ}\text{C}$ )	Stirring rate (rpm)	Molecular Weight	Melting point ( $^{\circ}\text{C}$ )	Particle size ( $\mu\text{m}$ )
1	7	16	2.0	5.0	90	250	4500	201.9	60.9
2	7	20	1.0	10.0	90	250	1600	207.1	66.3
3	5	20	2.0	5.0	110	250	4840	207.2	57.8
4	7	16	2.0	10.0	90	350	2540	198.6	49.4
5	7	20	1.0	10.0	110	250	4030	212.5	70.6
6	7	20	2.0	5.0	110	350	6900	216.4	40.1
7	5	20	2.0	10.0	90	350	2150	209.4	51.3
8	5	16	2.0	10.0	110	250	4100	213.7	65.0
9	5	16	1.0	10.0	110	350	3670	209.9	54.7
10	7	16	1.0	5.0	110	350	7110	215.0	38.1
11	5	20	1.0	5.0	90	350	2580	208.5	44.4
12	5	16	1.0	5.0	90	250	2460	202.5	53.7
13	6	18	1.5	7.5	100	300	3990	210.4	52.8
14	6	18	1.5	7.5	100	300	3820	210.4	54.6

Table 4.9 Table of raw data from DOE investigations (results are not presented in their initial randomised order)

## 4.2-Reaction Kinetics

### 4.2.1-Introduction

While there has been a substantial amount of literature on the kinetics of anionic polymerisation of nylon in bulk, only two studies were found by the author on the study of the kinetics of nylon particle synthesis though precipitation polymerisation<sup>7, 76</sup>. The investigations by Stratula-Vahnoveanu indicated that the nylon particle synthesis proceeded through pseudo-first-order kinetics.

One other publication investigated nylon variants that stayed in solution after the reaction had finished<sup>75</sup>. Under those conditions, polymerisation exhibited a first-order rate dependence on the monomer and chain initiator and a zero-order rate dependence on the concentration of the catalyst. A somewhat conflicting work revealed how the concentration of

the catalyst and chain initiator increased the rate of polymerisation up to a point<sup>67</sup>, albeit this study was carried out under bulk polymerisation. Work done by Dan et al. stated that similar effects occurred in particle synthesis, however, no quantitative data was provided<sup>60</sup>. These works were primarily interested in the study of reaction kinetics using a one-shot injection method. The work by Dan and Grolier<sup>7</sup> investigated the continuous method but was more interested in how the continuous injection of C controlled heat release more than overall kinetics.

Furthermore, studies using CO<sub>2</sub> and sodium caprolactamate as the chain initiator and the catalyst respectively showed that not only did the CI/catalyst combination influence rate of polymerisation but could potentially change the rate determining step as well. When both the catalyst and CI are considered ‘slow’ acting, the rate determining step is the ‘initiation’ step between the CI and the catalyst<sup>78</sup>. Therefore, the overall rate equation would be of a second order. In contrast when a ‘fast’ acting system is used, the propagation reaction step becomes the rate-determining step leading a first-order reaction mechanism<sup>36, 74</sup>. In most literature, the propagation step is considered the rate-determining step and most kinetic models are based on this. Work done by Ueda et al. stated that even the concentrations of the catalyst and chain initiator can cause the rate equation to change<sup>79</sup>, but it should be noted that these observations were made using a ‘fast’-acting CI/catalyst combination so how valid such observations would be for a slow acting catalyst/CI combination is questionable.

#### **4.2.2-Analytical methods**

Dan et al. and Stratula-Vahnoveanu et al. used isothermal calorimetry and gravimetric analysis, respectively, in studying nylon particle synthesis. Gravimetric analysis is a simple analytical method that requires very little analytical apparatus but is very time-consuming as it requires multiple reactions to investigate a single variable. For example, to study the reaction kinetics at 100°C the reaction would have to be carried out multiple times, with each subsequent reaction being quenched at a later period to analyse how much product had been synthesised in that period. The calorimetric method allows for in situ measurements and is therefore less time-consuming<sup>7</sup>. However kinetic information is gained from a profile of heat-rate against time, not from the more common profile of substrate/product concentration against time. In addition, calorimetry does not differentiate between heat release caused by polymerisation and

heat caused by crystallisation; further analysis would have to be carried out to quantify the heat of crystallisation. When a catalyst is used, either the catalyst or substrate is usually added in either one-shot or multiple injections. Continuous injection is much less common, because should the reaction become inhibited then the quality of the results can become suspect<sup>143</sup>. This could potentially be an issue because it is known that at lower reaction temperatures, polymerisation caprolactam into nylon particles can be ‘physically interrupted’<sup>76</sup>. Calorimetry would not be able to detect this directly.

For these reasons it was decided that a different method would be used to measure polymerisation parameters in order to extract kinetics. The method chosen was Attenuated Total Reflection-Fourier Transform Infrared (ATR-FTIR) spectroscopy. Using this method there is no requirement to dilute samples<sup>144</sup> and spectra can be gained quickly. Since only drops are required for analysis, samples could be analysed multiple times, increasing the reliability of results. The in situ FTIR probes available had a maximum operating temperature of 70°C. At those temperatures the reaction would be prohibitively long therefore in situ measurements were not attempted. Unlike calorimetry, this method follows the rate of the consumption of the reactant directly so there is no need to differentiate between the heat of reaction and the heat of crystallisation. The main disadvantage with this method is that any sample must be analysed immediately once removed from the main reactor. Attempts to quench and store samples for later analysis all failed. More details are provided in section 4.4.2.

To ensure that the correct reaction order is determined, the data of a reactant decreasing with time is fitted to rate equations. Should the data fall on a straight line for a given rate equation, the reaction order is confirmed. Should the plot curve upwards then the actual order of reaction is less than assumed, and vice versa. The first order rate equation and its integrated form are expressed below:

$$-r_A = -\frac{dC_A}{dt} = kC_A \quad (4.4)$$

$$\ln\left(\frac{C_{A0}}{C_A}\right) = kt \quad (4.5)$$

Likewise for a second order:

$$-r_A = -\frac{dC_A}{dt} = kC_A^2 \quad (4.6)$$

$$\frac{1}{C_A} - \frac{1}{C_{A0}} = kt \quad (4.7)$$

For zeroth order

$$-r_A = \frac{dC_A}{dt} = k \quad (4.8)$$

$$C_{A0} - C_A = kt \quad (4.9)$$

Where  $-r_A$  is the reaction rate (units change with reaction order),  $k$  is the rate constant (units change with reaction order),  $t$  is the reaction time (min),  $C_{A0}$  is the initial concentration of material ( $\text{mol L}^{-1}$ ) and  $C_A$  is reactant concentration and any point in time ( $\text{mol L}^{-1}$ ).

#### ***4.2.3-Results and discussion***

Figures 4.10 and 4.11 are the plots of the integrated rate form for both single and continuous injection methods respectively. In both cases, pseudo-first-order reaction kinetics were observed.

A small difference between the single and continuous injection can be visualized at approximately 15 minutes into the reaction. In the single injection (Figure 4.10), there is a sharp drop in monomer concentration from the initial starting point to 15 minutes into the reaction.

This corresponds to the reaction taking place in the homogeneous medium where polymer growth is the fastest<sup>6</sup>. After a certain amount of time dependent on the degree of polymerisation and polymer concentration, a liquid-liquid phase separation occurs, creating a polymer rich phase and a solvent rich phase. This slows down the reaction, which is manifested by a lack of dip as seen past the 15-minute mark in Figure 4.11 when the CI is added continuously. This indicates that the continuous injection method limits the rate of the reaction during the homogeneous phase.

Using a low-efficiency catalyst and chain initiator it was expected, based on the work by Dan and Vasilie-Opera<sup>78</sup> who used a ‘fast-slow’ catalyst/CI combination that the initiation step was the rate-determining step, which would result in second-order reaction kinetics. The first order kinetics observed suggests that propagation is still the rate determining step. One potential reason for this is that the efficiency of the catalyst/CI combination is still high enough to ensure that the propagation step is the slowest step in the reaction. The usage of a slow-acting catalyst, such as Red-Al, helps to suppress the propagation step as well as the initiation step. The combination used by Dan and Vasiliu-Opera would have only suppressed the initiation step but not propagation. One other possibility is that the initiation step is the rate determining step with this catalyst/CI combination, but side reactions are consuming the chain initiator forcing a deviation from a second order.

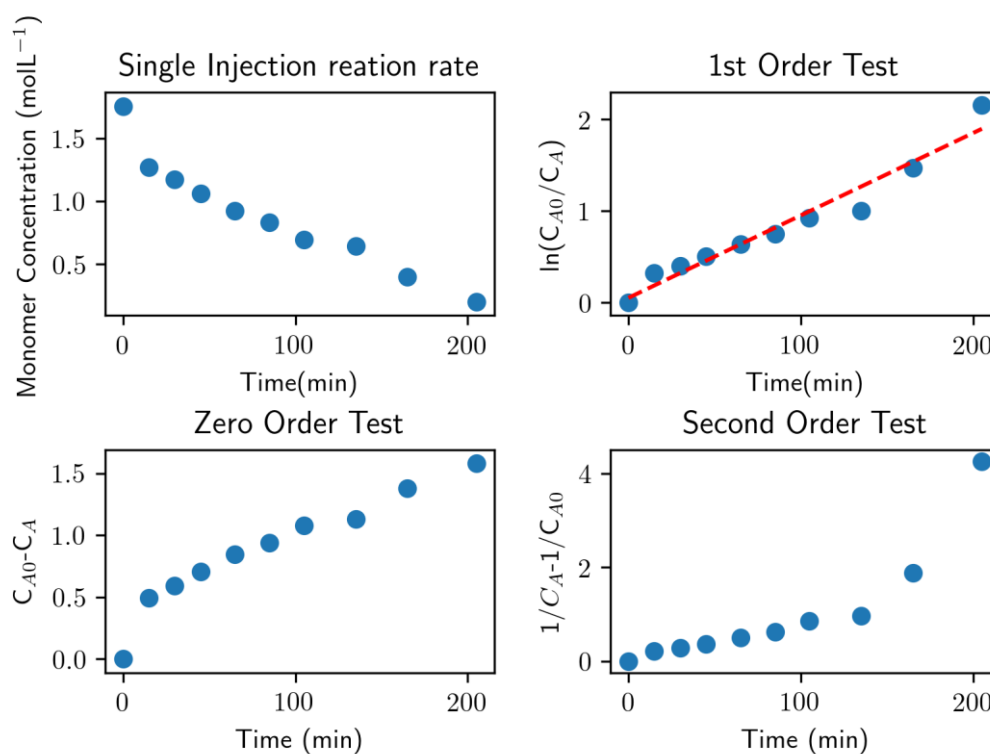


Figure 4.10 Caprolactam consumption with time and the corresponding integrated rate plots for one-shot injection of CI

To investigate if side reactions were causing this deviation further reactions under equimolar conditions without the presence of the catalyst were carried out. The lack of catalyst meant that the chain initiator reacted with the monomer and, in theory, the reaction would progress no further than the ‘initiation’ stage. A potential reaction mechanism for this is shown in Figure 4.12. Under these conditions, both the monomer and the CI would be consumed linearly over time. Therefore, a reaction order of two should be observed regardless of what step determines the overall reaction rate.

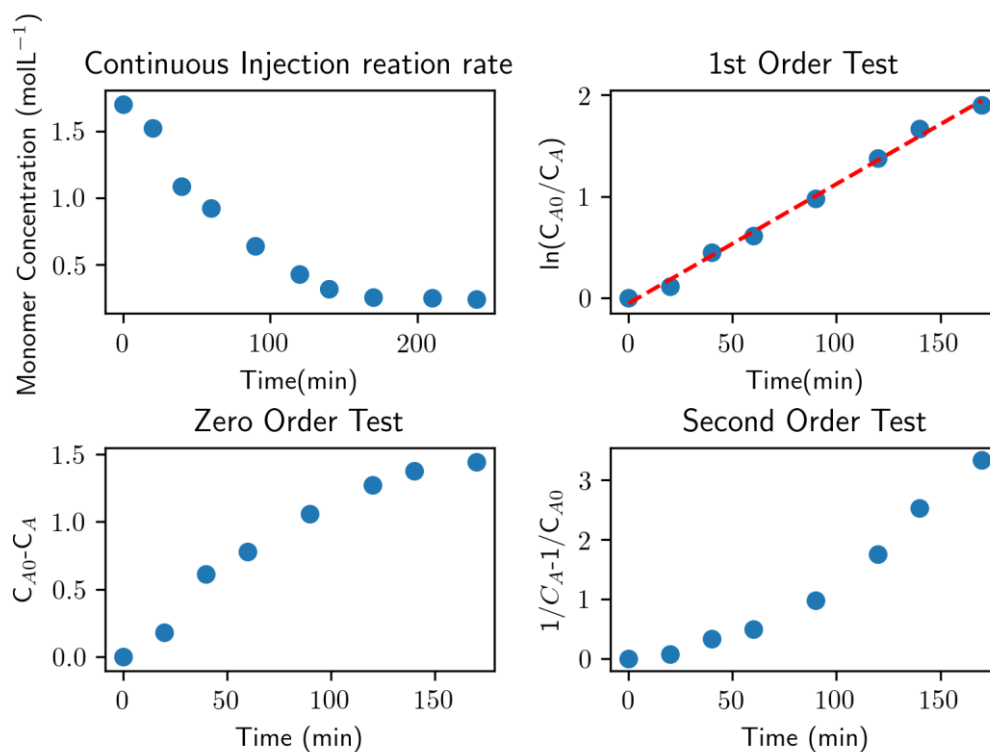


Figure 4.11 Caprolactam consumption with time and the corresponding integrated rate plots for continuous injection of CI at a rate of  $40\mu\text{L/min}$

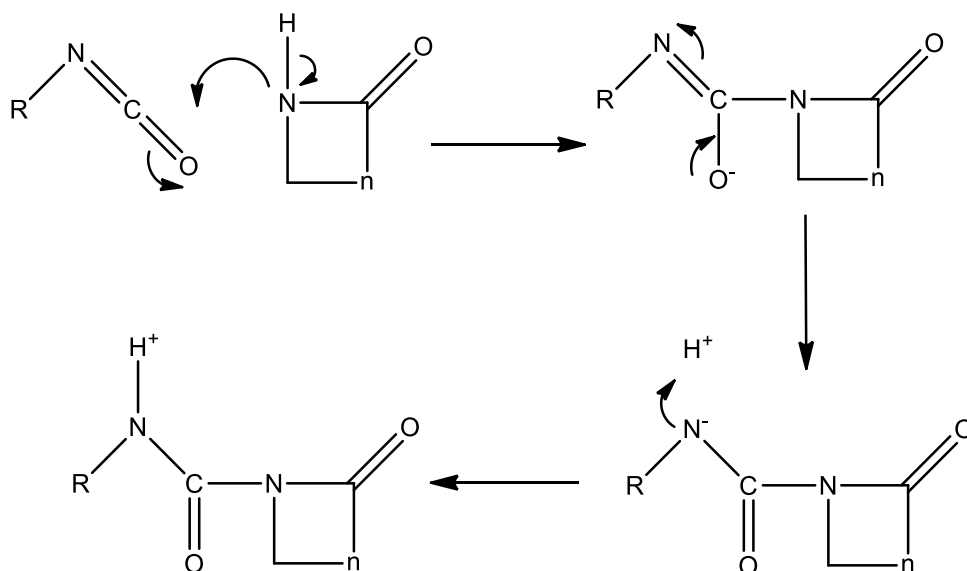


Figure 4.12 Potential reaction mechanism for caprolactam reacting with octadecyl isocyanate



### Section below concerns equimolar reactions only

Under equimolar conditions there is no precipitation of a product, therefore reaction kinetics cannot be followed using the carbonyl group. Thankfully, under equimolar conditions the isocyanate group on the chain initiator becomes visible to FTIR and is consumed during the reaction as shown in Figure 4.12. However, if CI was injected into the mixture it would be very difficult to follow kinetics as the isocyanate group would be consumed as it entered the reactor. Effectively isocyanate signal wouldn't be seen on the FTIR spectrum. To account for this experiments where reaction was carried out under semi-batch conditions the dissolved monomer was injected in the reactor containing the CI and a known volume of ethylbenzene.

Figures 4.13 and 4.14 illustrate that under equimolar conditions both injection methods retain first order kinetics. Therefore, side reactions must be taking place to cause this deviation from second order kinetics. Consequently, the same side reactions may also take place under normal polymerisation conditions.

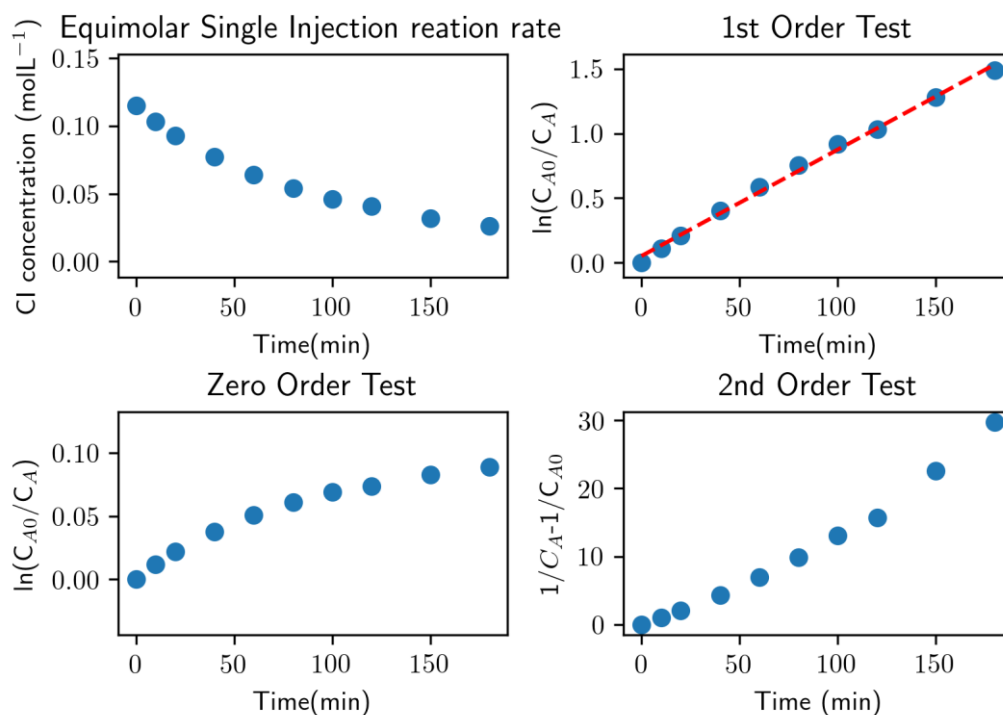


Figure 4.13 a) OI consumption against time for single injection with a reaction temperature of 70°C and corresponding integrated rate order plots

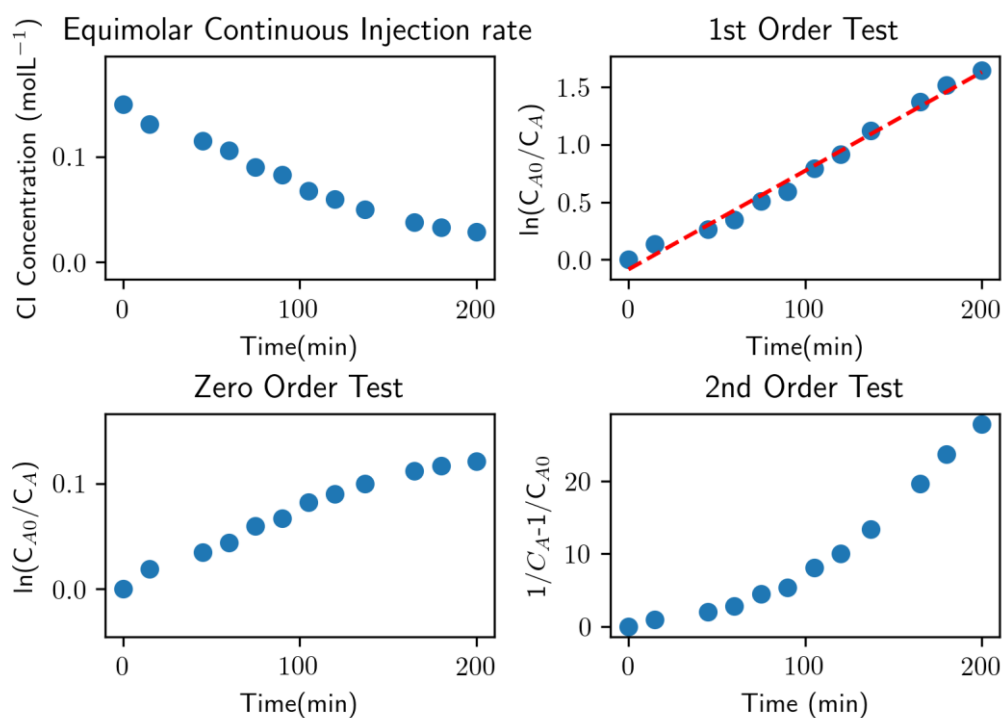


Figure 4.14 OI consumption against time for continuous injection at 70 μL/min and 70°C and corresponding integrated rate plots

The self-polymerisation of caprolactam is known to require temperatures up to 220-250°C<sup>145</sup> but the presence of a chain initiator may allow for some oligomerisation to occur at much lower temperatures. The first order rate dependence on chain initiator concentrations suggests that oligomerisation is occurring. To try to account for these potential side reactions the reaction temperature was lowered from 70°C to 40°C for the single injection run and to 50°C for the continuous injection run (Figures 4.15 and 4.16 respectively).

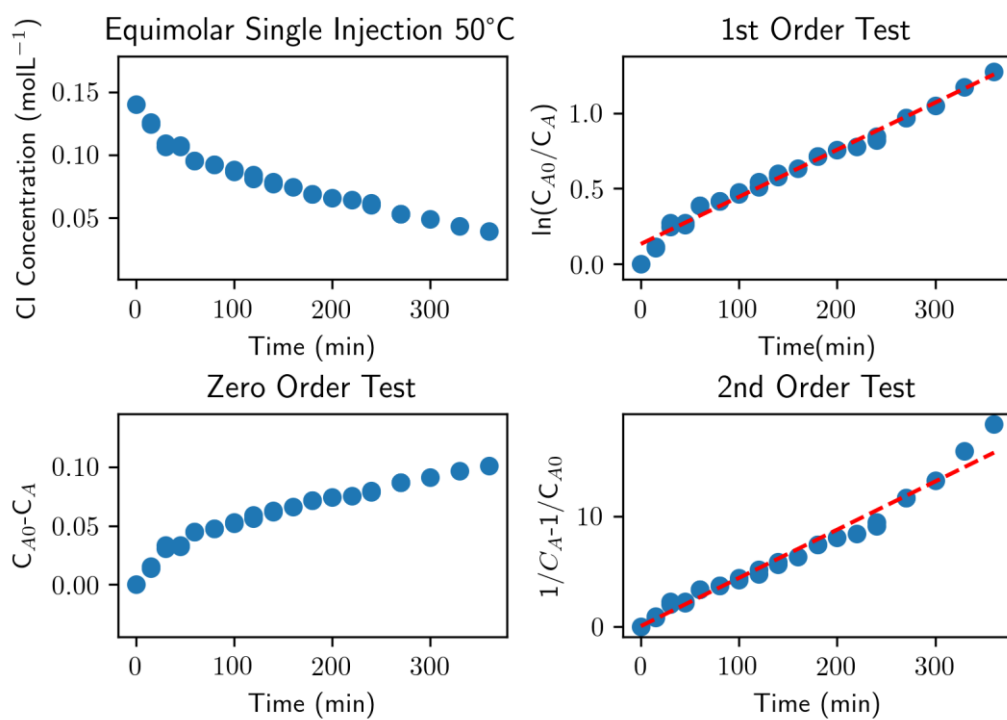


Figure 4.15 OI consumption against time for one-shot injection at 40°C and corresponding integrated rate order plots

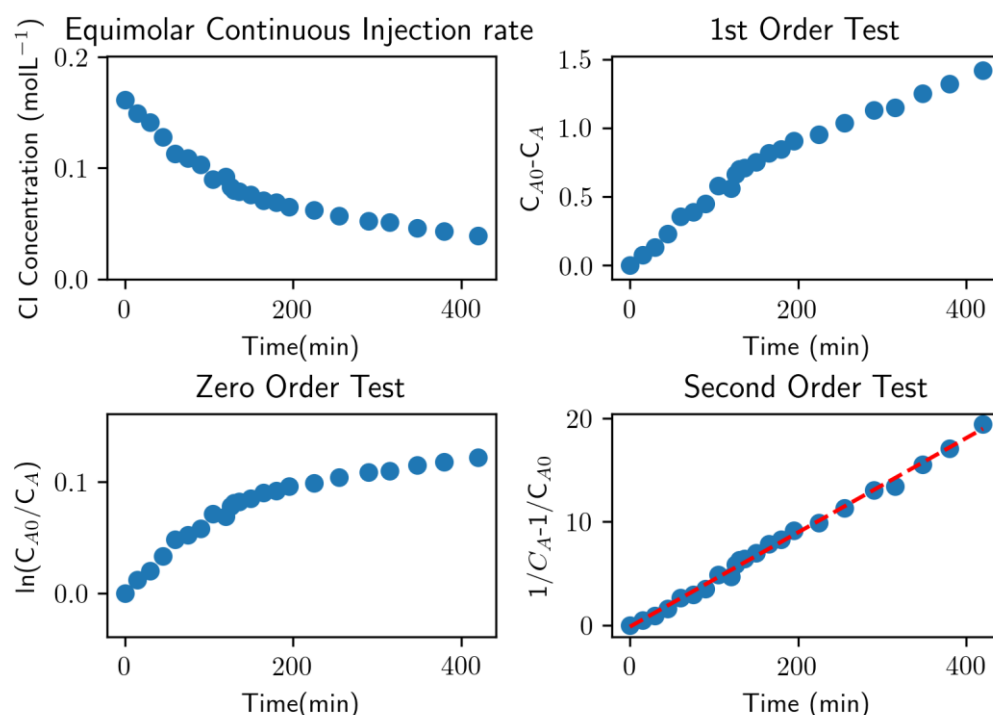


Figure 4.16 a) OI consumption against time for continuous injection at 70  $\mu\text{L}/\text{min}$  and 50°C and corresponding integrated order rate plots

At lower temperatures, the difference in CI injection method had a substantial impact on the reaction order; pseudo-first-order kinetics are seen for the single injection method (see Figure 4.15). Conversely, second order kinetics were achieved using the continuous injection (Figure 4.16). When the monomer mixture is added continuously, the CI is in large excess until the end of the reaction. This suggests that the side reactions, at least at elevated temperatures, are caused by oligomerisation, not by the CI-monomer molecule reacting with the chain initiator. At lower CI concentration levels there may be a deviation from second-order kinetics, but this would require further experimentation to confirm.

Interestingly when the injection rate lowers from 70  $\mu\text{L}/\text{min}$  to 35  $\mu\text{L}/\text{min}$  and the reaction temperature was raised to 80°C, the reaction order changes again from first to zero order as shown in Figure 4.17. Under these conditions, the reaction rates for the initial reaction between OI and the monomer and any potential side reactions are greater than that for the rate of injection of the monomer. This means the kinetics are controlled solely by the rate of

injection. Zero-order kinetics would be favoured with high reaction temperatures and low injection rates. However, this is in a delicate balance. Should the rate of injection increase or the temperature be below a certain point then the reaction would revert to first order. This reversion is caused by the rates of injection exceeding the rate of formation, allowing the monomer to accumulate within the reaction mixture and to take part in side reactions that were not possible at lower injection rates.

It is impossible to tell from these results if polymerisation, specifically is of 1<sup>st</sup> or 2<sup>nd</sup> order using the OI/Red-Al combination. However, in practice even if polymerisation has second-order kinetics it would be very difficult to achieve the required reaction conditions to observe it and synthesise nylon particles in a reasonable time frame. In practice, overall reaction kinetics is either first or zero order depending on reaction temperature and injection rate

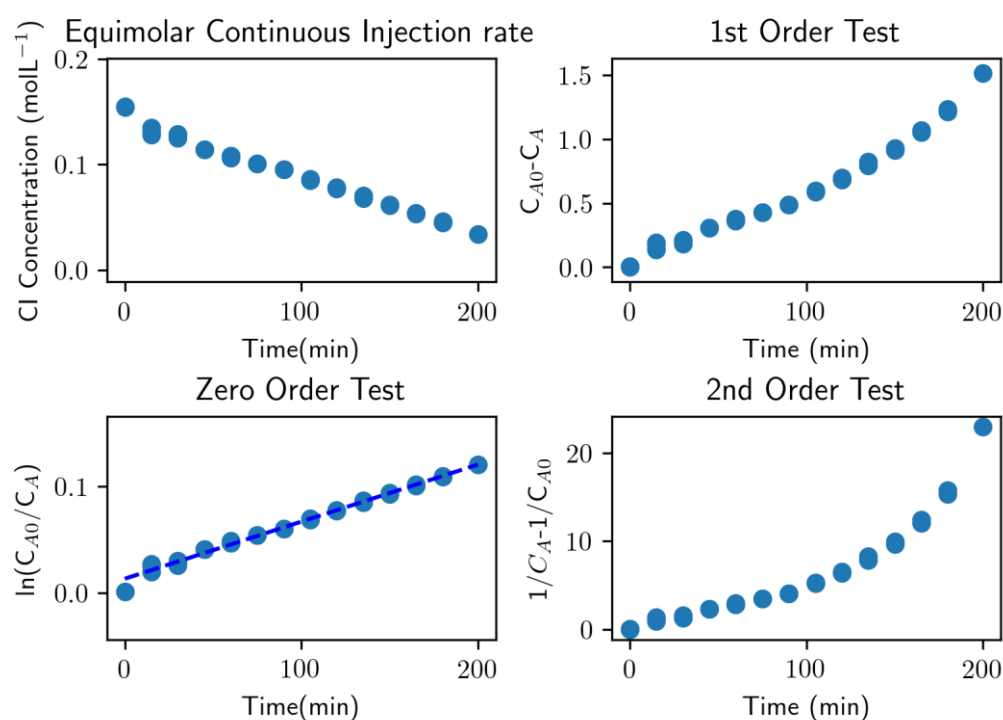


Figure 4.17 a) OI consumption against time for continuous injection (35 $\mu$ L/min) at 80 C, b)  
Zero-order integrated rate plot

**End of equimolar section**

#### **4.2.3.1-Effect of Chain initiator and catalyst concentration**

As shown previously in Figure 4.11 under continuous injection conditions a first order reaction was achieved, assuming that the rate of production of particles is less than the rate of injection of the CI, resulting in the accumulation of CI in the reaction mixture.

In both cases, the reaction stops before the caprolactam is completely consumed. This premature cessation of the polymerisation has been noted before in the work carried out by Stratula-Vahnoveanu and Vasiliu-Opera<sup>76</sup>. Davé et al. found something similar when studying the reaction in bulk, albeit the reaction didn't stop, only slowed down significantly. Two relevant reasons were proposed. Firstly, because the reaction temperature is below crystallisation temperature, there is a competition between polymerisation and crystallisation. Therefore, if the polymerisation rate is slow, then growing crystals may entangle with the growing chains, encumbering the mobility of active sites. Secondly, the gel-like structure may force a shift from a kinetic-controlled mechanism to diffusion based one<sup>67</sup>. In the case of precipitation polymerisation, Dan and Vasiliu-Oprea stated<sup>60</sup> that if the reaction temperature was sufficiently low, crystallisation could occur, hindering the various phase separations that continue within each droplet and hampering the transport of monomer within the solution phase to the active sites in the polymer-rich phase. As crystallisation progresses, polymerisation would eventually cease.

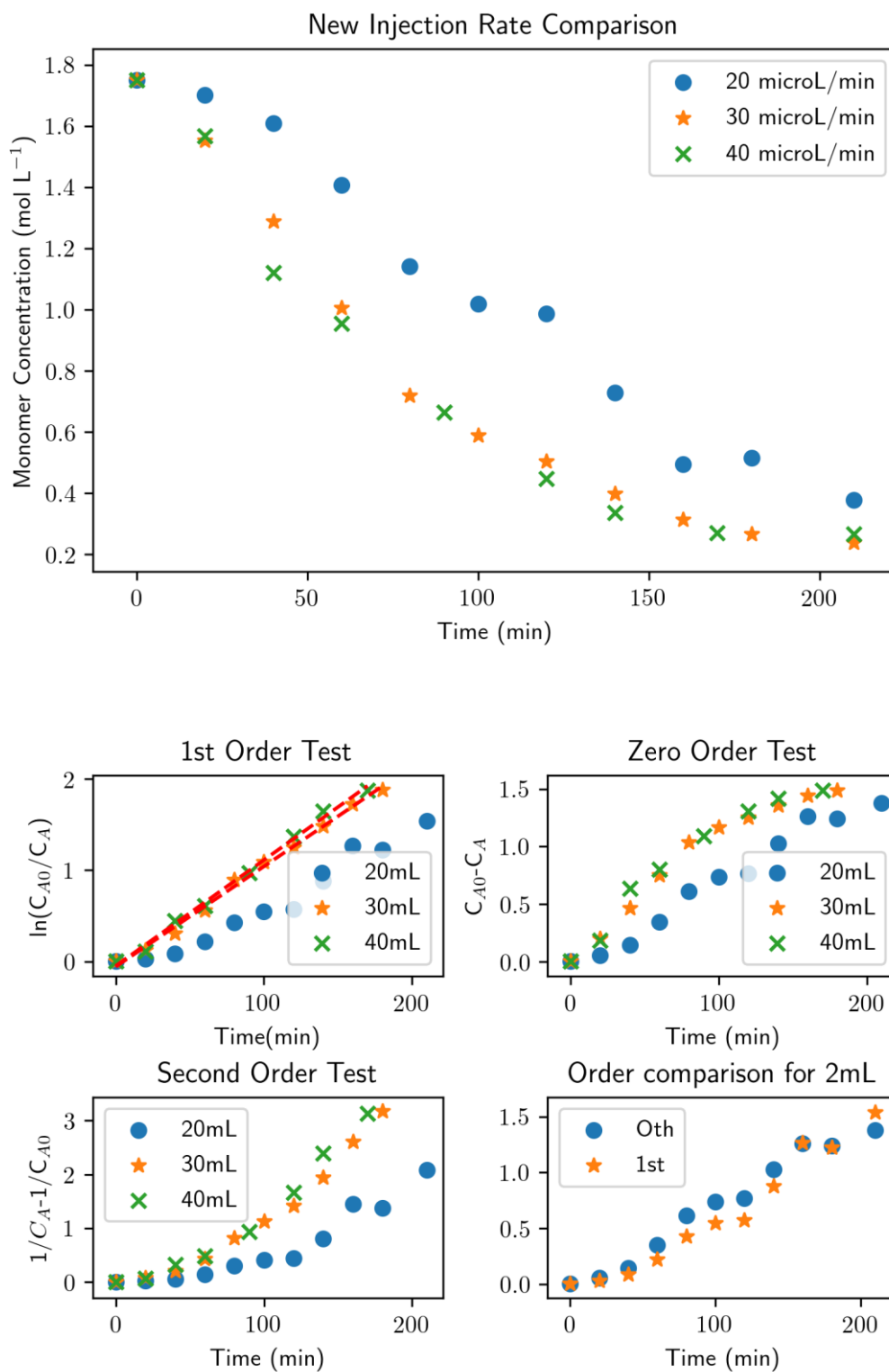


Figure 4.18 Caprolactam consumption at injection rates of 40 $\mu$ L/min, 30 $\mu$ L/min and 20 $\mu$ L/min and corresponding integrated rate order plots for all injection rates

Injection rate ( $\mu\text{L}/\text{min}$ )	Order of reaction	Rate constant ( $\text{s}^{-1}$ )
20	1 <sup>st</sup> *	0.0078
30	1 <sup>st</sup>	0.0102
40	1 <sup>st</sup>	0.0104

Table 4.10 Table of CI injection rates with corresponding reaction orders and rate constants

\* Reaction could be either 1<sup>st</sup> or 0<sup>th</sup> order based upon results. First order was chosen to determine approximate reaction rate

As shown in Figure 4.18 when an injection rate of 20  $\mu\text{L}/\text{min}$  is used it is impossible to determine if the reaction is either 1<sup>st</sup> or 0<sup>th</sup> order, however it can be determined that the reaction is not 2<sup>nd</sup> order. This difficulty in determining reaction order may indicate that at low injection rates a diffusion-based mechanism is competing with a chemical based one over the control over reaction kinetics. Due to subsequent injection rates having clear first order kinetics the first order rate law was used to determine reaction rate for the reaction at 20  $\mu\text{L}/\text{min}$ . Figure 4.18 and Table 4.10 show that increasing the injection rate from 20  $\mu\text{L}/\text{min}$  to 30  $\mu\text{L}/\text{min}$  led to an increase in the rate constant from 0.0078  $\text{s}^{-1}$  to 0.0102  $\text{s}^{-1}$  but increasing the injection rate further had no impact on reaction rate. As mentioned previously crystallisation due to low reaction temperature would cause the premature cancellation of polymerisation, but that should not stop the newly added CI reacting with the monomer in the solution phase. Clearly, something else is stopping the reaction. It has already been shown that oligomerisation can occur without the monomer being anionically active. This oligomerisation leads to an increase in viscosity. As viscosity increases, it gets increasingly difficult for the active monomer to reach the active site of a growing chain. Furthermore, as more oligomer is synthesised, the solvent becomes poorer, leading the oligomer itself to crystallise hampering the reaction further. At higher injection rates, this oligomerisation becomes more pronounced, at a critical point oligomerisation and crystallisation will inhibit the maturation of polymer particles. This places an upper limit on the impact injection rate has on the reaction rate.



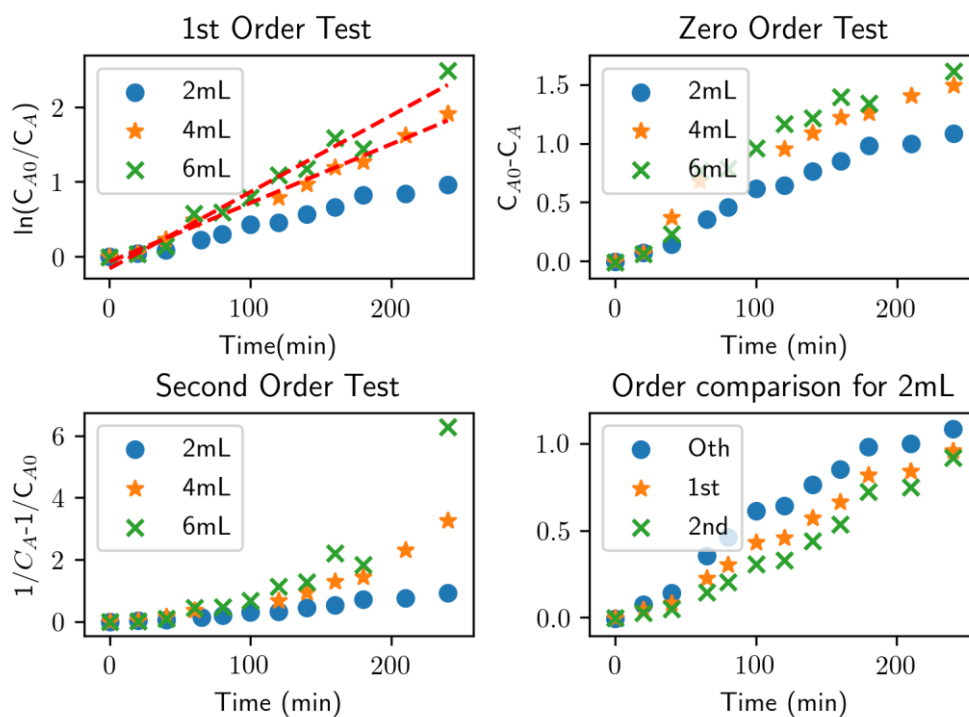
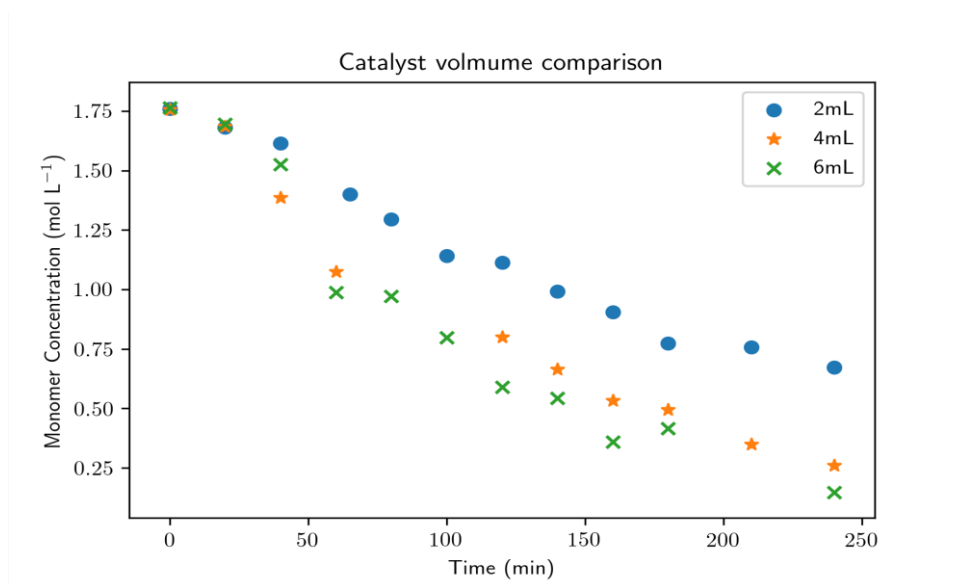


Figure 4.19 Caprolactam consumption with catalyst volumes of 2mL, 4mL and 6mL and corresponding integrated rate order plots for all catalyst volumes

As can be seen in Figure 4.19 similar observations were made in respect to catalyst concentration. At low catalyst volumes it becomes very difficult to determine the reaction order. In the case of catalyst volume, it appears that the reaction is either 1<sup>st</sup> or 2<sup>nd</sup> order. As

higher catalyst volumes clearly had a reaction order of 1 the first order rate law was used to determine the approximate reaction rate. Again, it appears that there is a competition between diffusion and chemical-based mechanisms over control of the reaction rate. Table 4.11 shows that as the catalyst volume increases from 2mL to 4mL, the reaction rate constant increases from  $0.0043\text{s}^{-1}$  to  $0.00792\text{s}^{-1}$ , however the increases in the rate constant from 4mL to 6mL were somewhat smaller. As the catalyst will always be in vast excess of the CI at any given point, increasing or decreasing catalyst concentration should have no real effect on reaction kinetics. However, the oligomerisation and subsequent crystallisation would be hindering the access of active monomer to an active site. With more anionically active monomer, the probability that active monomer would be able to find a growing chain would increase. As the rate constant when using 6mL of catalyst was identical to the ones gained using higher injection rates it appears that oligomerisation becomes the dominating factor with respect to the reaction rate.

These results are similar to those gained by Davé et al<sup>67</sup>. studying bulk polymerisation. They found that increasing the concentration of the chain initiator increased the reaction rate until an optimum point was reached. In the study carried out by Zhang et al. looking at the solution polymerisation of variously substituted  $\beta$ -lactams, they reported that polymerisation had a first order-rate dependence on the concentration of the CI but no mention of any limitation placed upon it. This difference is likely caused by the polymers of these  $\beta$ -lactams remaining in solution. Therefore, no early crystallisation can take place to cause premature cessation to polymerisation. Zhang et al<sup>43</sup>. found that the reaction was of zero order with respect to the catalyst. Davé et al., like Zhang et al., reported that the concentration of the catalyst had no impact on reaction rate. But it should be noted that in the study carried out by Davé the catalyst was always in excess of the chain initiator. Consequently, as the catalyst cannot begin polymerisation on its own, such a change in catalyst concentration would have shown no effect on the reaction rate.

Catalyst volume (mL)	Order of reaction	Rate constant (s <sup>-1</sup> )
2	1 <sup>st</sup> *	0.0043
4	1 <sup>st</sup>	0.0079
6	1 <sup>st</sup>	0.0102

Table 4.11 Table of catalyst volumes with corresponding reaction orders and rate constants

#### 4.2.3.2-Effect of temperature on reaction kinetics

As shown in Figure 4.20 and Table 4.12 the temperature had a dramatic effect on the kinetics of the reaction. Below 90°C the reaction rate and monomer consumption decrease substantially. There is a smaller but noticeable increase in the reaction rate and monomer consumption between 90°C and 100°C. However as shown by the two final samples in Figure 4.20, polymerisation has effectively ended before all caprolactam has been reacted. The reaction temperature is closer to the melting point of the polymer, therefore, it takes longer for both the polymer-rich phase within each individual droplet and oligomer made from excess CI to crystallise.

Temperature	Order of reaction	Rate constant
80	1 <sup>st</sup>	0.0058 s <sup>-1</sup>
90	1 <sup>st</sup>	0.008 s <sup>-1</sup>
100	0	0.0083 mol s <sup>-1</sup>

Table 4.12 Table of reaction temperatures with corresponding reaction orders and rate constants

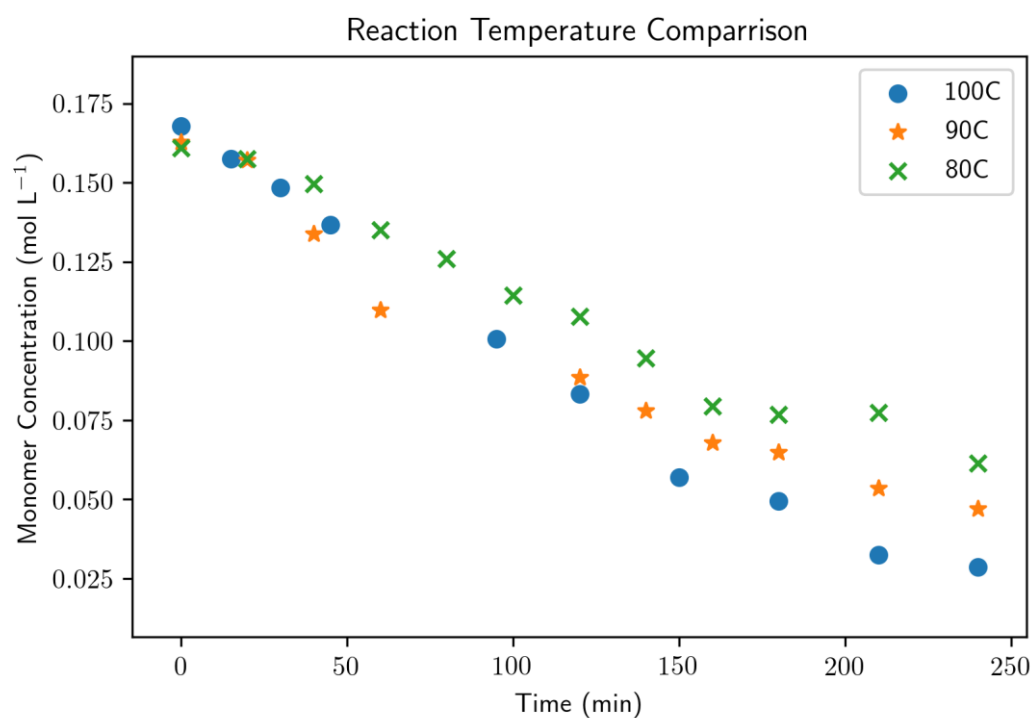


Figure 4.20 Caprolactam consumption at temperatures 80°C, 90°C and 100°C. All three experiments were carried out with an injection rate of 20 $\mu\text{L}/\text{min}$

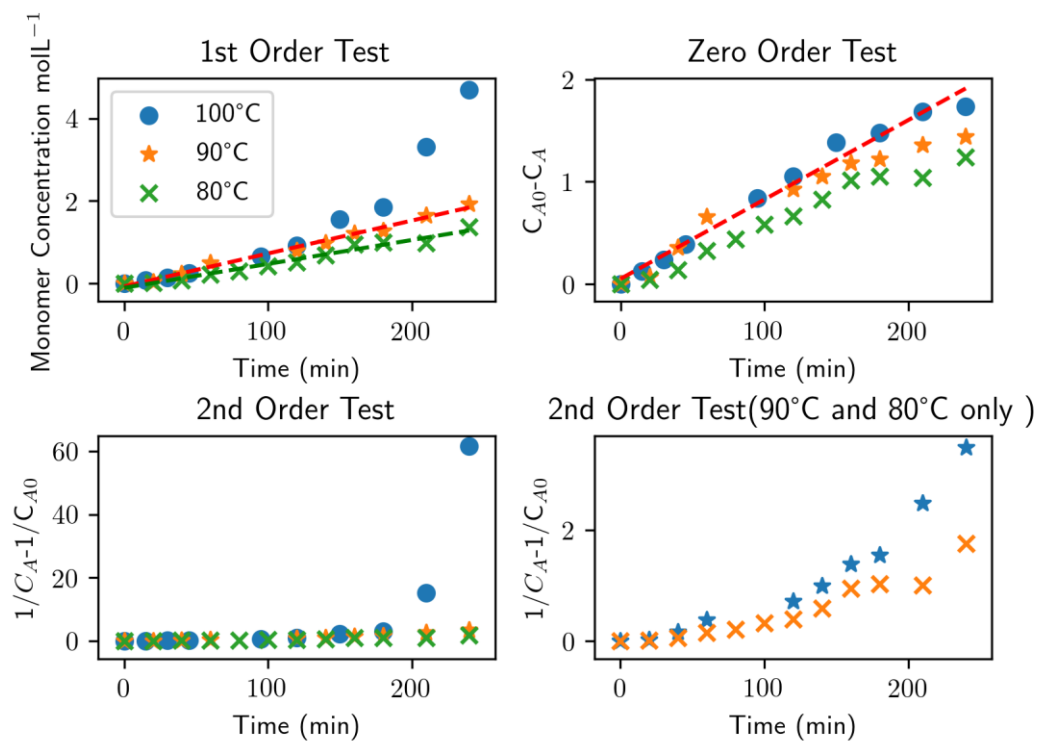


Figure 4.21 a) Order tests for reaction temperatures of 80°C, 90°C and 100°C

The calorimetric studies carried out by Dan and Grolier<sup>7</sup> showed that temperature has very little influence on the initiation step but has a huge impact on the propagation step.<sup>7</sup> If initiation was the rate-determining step there is a possibility that temperature would have a limited impact on the reaction rate.

As proven in Figure 4.21 increasing the reaction temperature from 90°C to 100°C causes the reaction to shift from an overall first-order to a zero-order reaction as shown in Table 4.12. For these conditions to occur, the rate of polymer maturation, from inception to solidification, must be slower than the rate of injection. Therefore, as the polymerisation cannot take place without the presence of a chain initiator, the reaction rate is controlled by mechanical injection of the chain initiator. Under these conditions at any instant in time, the number of available anionically active monomer molecules will vastly exceed the number of chain initiator molecules. These reaction conditions are similar to those found in a reaction catalysed by enzymes<sup>146</sup>. Reaction conditions that favour zero order kinetics are high temperatures and low injections rates that ensure that initiation and subsequent particle maturation happen quickly, limits the amount excess oligomer formed and hinders the crystallisation of said oligomer. Low reaction temperatures and high injections rate will favour a return to first order reaction kinetics.

#### 4.2.3.3-Effect of mixing on kinetics

This section concerns single injection only.

The importance that mixing intensity has on the kinetics of a chemical reaction has been known since the 1950's<sup>147</sup>. As mentioned previously the synthesis of polyamide particles is a highly complex process involving multiple phase changes where the non-polar solvent transports both monomer and catalyst to the growing chains. Additionally due to the substantial difference in densities between the solvent used and fully formed polyamide particles ( $866 \text{ g/cm}^3$  and  $1150 \text{ g/cm}^3$  respectively), the minimal mixing intensity would have to ensure that particles are kept in suspension<sup>76</sup>. Investigations carried out by Stratula-Vahnoveanu and Vasiliu-Oprea determined that at higher mixing intensities (1000 and 2000rpm), altering mixing speed had no effect on reaction rate. These results were corroborated by Dan and Grolier who found that increasing mixing speeds rapidly increased reaction rate until the optimal point was reached, after which further increases of mixing intensity had no effect. Similar results were observed when the reaction was carried within an OBR at oscillation frequencies 1.5, 1.0 and 0.5Hz as shown below in Figure 4.22.

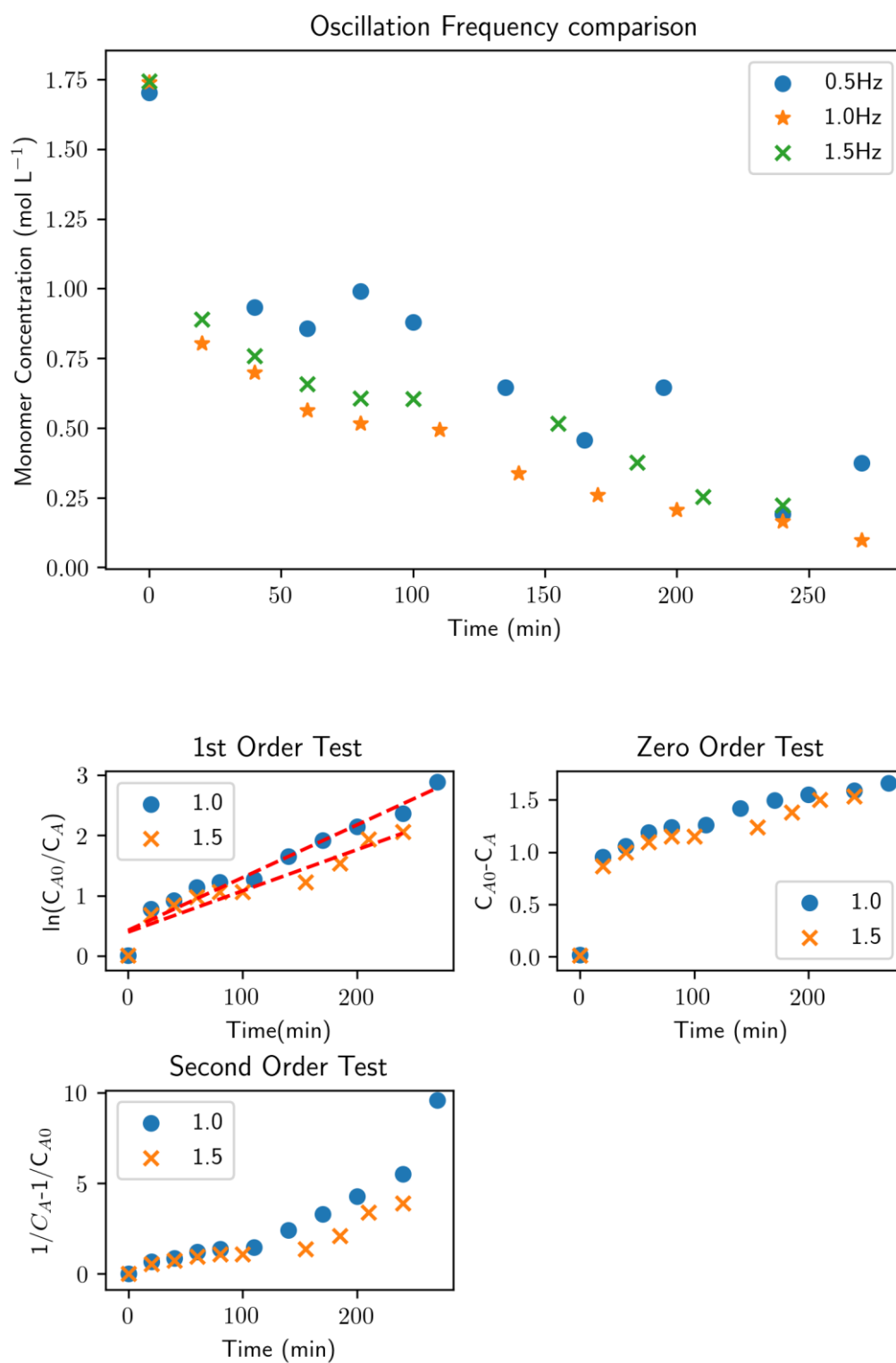


Figure 4.22 Concentration profiles at different oscillation frequencies and corresponding integrated rate order plots

As shown in Figure 4.22 at all three frequencies, concentration profiles remain broadly the same. It should be noted however that there is greater variance in the results for the experiment carried out at 0.5Hz, the reasons for this are unknown. The investigations carried out by Stratula-Vahnoveanu and Vasiliu-Oprea discovered something interesting. At lower mixing speeds, the order of reaction deviated from a pseudo-first to a pseudo-zeroth. Initially, it was theorised that fluid motion, characterised by the Reynolds number,  $N_{Re}$ , was responsible for this change. Stratula-Vahnoveanu and Vasiliu-Oprea then examined the effect of changing the Reynolds number (initial starting values ranged from 5000 to 16,000) throughout the reaction and postulated that below a certain  $N_{Re}$ , specifically at the edge between laminar and intermediate flow regimes, the reaction progressed via pseudo-zero order kinetics. In most cases, the border between these flow regimes occurs around Reynolds numbers of 2000-5000. The OBR allows good mixing to be achieved at substantially lower Reynolds numbers than STRs. This makes them very suitable to investigate this hypothesis. The Oscillatory Reynolds number can be determined using the equation below

$$Re_o = \omega x_o D / \nu \quad (4.10)$$

Where  $\omega$  is the oscillation frequency,  $x_o$  is the centre-to-peak amplitude, the  $D$  is the diameter of the tube and  $\nu$  is the dynamic viscosity. Table 4.13 gives the range of  $Re_o$ .

Oscillation frequency (Hz)	Order of reaction	Oscillatory Reynolds number
0.5	Undetermined	1678
1.0	1 <sup>st</sup>	3356
1.5	1 <sup>st</sup>	5035

Table 4.13 Oscillatory Reynolds numbers for the corresponding oscillation frequency

Using oscillation frequencies of 1.0Hz and 1.5Hz, first-order kinetics were retained, indicating that the flow regime did not influence reaction order. The results from 0.5Hz were



messy and too inconsistent to be used to determine the reaction order. In addition, the dip between first and second measurement was severe in all cases. Large dips in monomer concentration early in the reaction have been seen before but never to this degree. The reason for this abnormally large dip is not known. In the work carried out by Stratula-Vahnoveanu and Vasiliu-Oprea, the shift in reaction order from zero to one was not accompanied by a substantial decrease in reaction rate. As shown in Figure 4.23 under equimolar conditions, lowering the mixing intensity did not lead to a decrease in reaction rate or a change in reaction order. Therefore, any change must occur at later stages of the reaction. One possible explanation is that the lower mixing speeds the reaction shifts from a chemical control mechanism to diffusion one and under these conditions, the reaction rate becomes independent of the monomer concentration. In the work carried out by Stratula-Vahnoveanu and Vasiliu-Oprea, there was not a large decrease in reaction rate following the change in the reaction order, indicating that poor mixing was not responsible for this change. It has been proven that shear rate has a strong influence on the size of polymer phase droplets. The weaker the agitation, the larger the liquid-like droplets and the lower the corresponding surface area to volume ratio. This hinders diffusion of active and normal monomer into the polymer droplets. Past a certain size of droplet, diffusion would become independent from monomer concentration and pseudo-zero order kinetics would be observed.

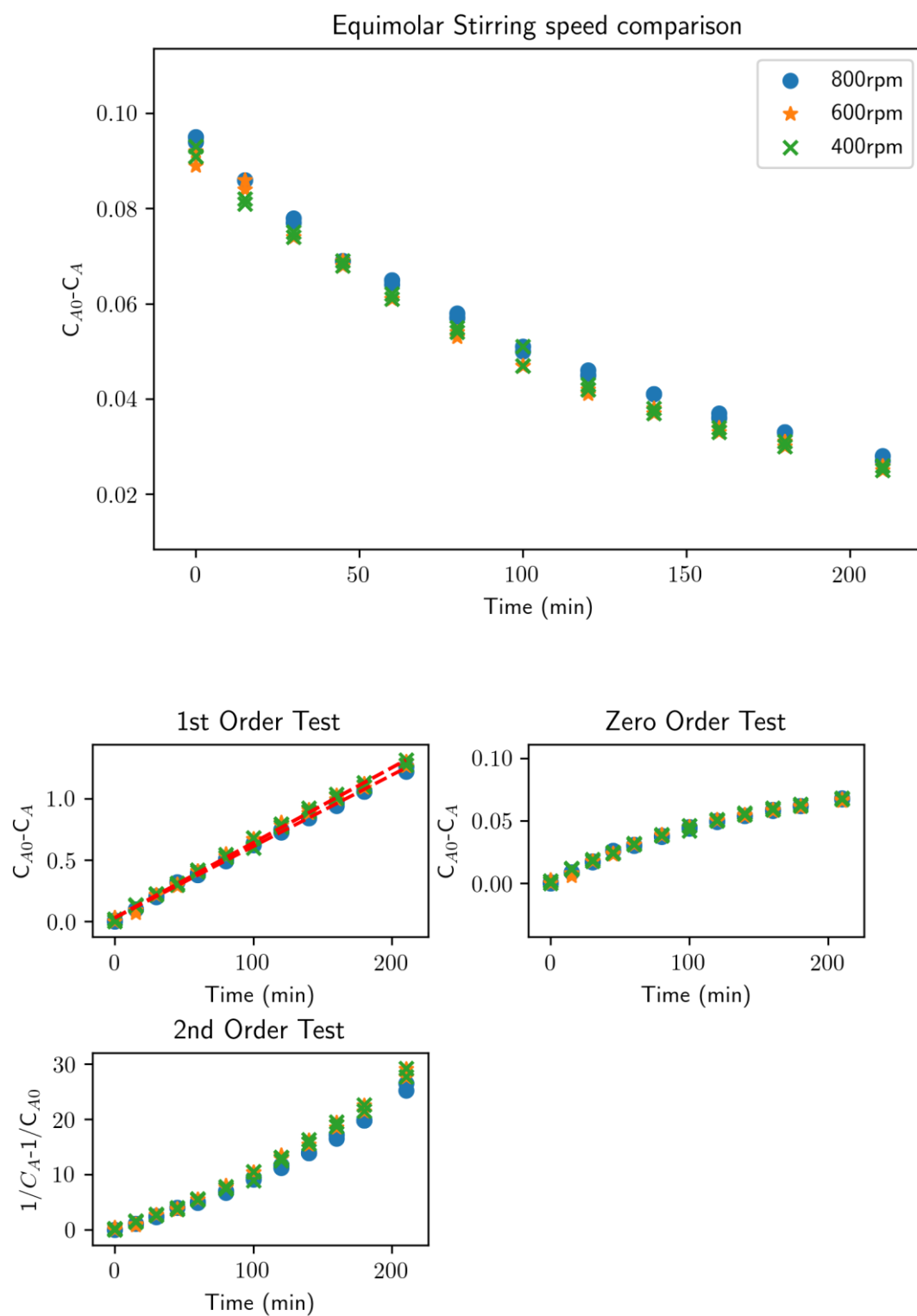


Figure 4.23 OI consumption under equimolar at stirring speeds 400, 600, and 800rpm and corresponding integrated rate order plots

## **4.3-Conclusions**

### **4.3.1-Plackett-Burman design conclusions**

In this chapter, using the Plackett-Burman factorial design, the factors that affect molecular weight, particle size distribution and the melting point of nylon-6 particles were determined and analysed in detail when the chain initiator was injected continuously. The most important factors affecting molecular weight were temperature, the rate of injection and monomer concentration.

Similar to molecular weight, the injection rate and temperature had a significant impact on the melting point. Conversely to molecular weight, increasing the monomer/solvent ratio in favour of the solvent actually increased the melting point. It is theorised that small amounts of unreacted monomer are trapped within the polymer particles and the greater solvent volume minimalizes the amount of monomer trapped.

For particle size, the most important factors were mixing speed followed by the injection rate. Oddly while monomer mass was not found to be a significant factor, a 2-way interaction between monomer mass and mixing speed was.

The biggest deviation from the single injection method was the apparent lack of influence that the catalyst concentration had on either particle size or molecular weight. When the chain initiator is added in a single injection, the catalyst/monomer/chain initiator ratio has influence over both. Adding the chain initiator continuously it appears that the CI/catalyst stoichiometry becomes irrelevant.

### **4.3.2-Kinetic measurement conclusions**

A new method to analyse the kinetics of nylon-6 particle synthesis using ATR-FTIR was successfully developed. In theory, using the ‘slow-slow’ catalyst combination, the rate determining step would be the initiation reaction between the CI and active monomer. Under these conditions, the reaction would have second order kinetics. In practice, first-order kinetics

were observed in most cases. This deviation is caused by the CI reacting with the non-activated monomer to form small oligomer chains. At no point was second order kinetics achieved.

The three factors of interest were the catalyst concentration, CI injection rate and reaction temperature. All three factors were shown to influence reaction kinetics. Both catalyst and CI injection rate affected the reaction rate, however no further increase in reaction rate was observed past an optimum concentration. Additionally, in all cases, there was a cessation of polymerisation before the complete consumption of the monomer. This cessation occurred at the same point in the reaction. It is thought that the excess oligomerisation and crystallisation due to low reaction temperatures are the cause of these limitations. Only with increasing the reaction temperature was this premature stoppage of polymerisation delayed. The reaction order was found to change depending on the rate of injection and reaction temperature. If the reaction was carried out using a low injection rate under high temperatures, polymerisation proceeded via zero order kinetics. However, at lower reaction temperatures and higher injection rates, overall reaction kinetics reverted back to first order.

Previous research carried out in an STR found that the reaction proceeded through pseudo-first order kinetics under a turbulent flow regime and via a zero-order mechanism under a flow regime in the intermediate-laminar boundary region. From these results, it was suggested that the flow regime can influence reaction kinetics. When polymerisation was carried out in an OBR, a first order reaction kinetics was maintained. From these observations, it was hypothesised that large particles with poor surface-area to volume ratios were the cause of the change in order.

#### **4.4.-Problems**

##### **4.4.1-PA-6 synthesis**

Two substantial problems arose when attempting to synthesise PA-6, both were related to the continuous injection of the CI. Originally Isophorone Diisocyanate (IDI) was chosen as it is a liquid at room temperature. However, particles made using this CI were of poor quality. It may

have been possible to improve upon these results using IDI however it was recommended that the CI should be changed to OI.

The use of OI presented a second problem, OI is a solid at room temperature. The experimental apparatus had to be adjusted to take this into account. The simplest solution required two stages. The first was to keep the exposure of Teflon tubing connecting the chamber of the syringe pump to the reaction vessel the cool air as minimal as possible. The second step was to heat the syringe pump chamber and Teflon connecting tube with a hair dryer placed above them. Once these steps had been implemented, PA-6 particles of high quality were synthesised consistently.

#### **4.4.2 Kinetics measurements**

Initially, samples were not analysed immediately but were quenched using a specified aliquot of methanol, sealed immediately to ensure that the solvent and methanol did not evaporate and stored for later analysis. However, as samples cooled they solidified due to the previously growing chains coming out of solution. This makes High Performance Liquid Chromatography (HPLC) and Gas Chromatography (GC) impossible. Initial attempts to use GC were ineffective. Methanol is a good solvent for caprolactam and subsequent oligomers so in theory increasing methanol concentration would ensure dissolution at room temperature. Even so, the high boiling point of caprolactam and oligomers would require the usage of the expensive High Temperature Gas Chromatography technique (HT-GC). The HPLC technique also suffers from difficulties as there have been no pre-existing methods to analyse caprolactam. The development of a new method is a complex and time-consuming process.

Instead of trying to keep samples in solution, Thermal-Gravimetric Analysis-Mass Spectroscopy (TGA-MS) was proposed. Using this technique, the state of the sample would be irrelevant and both the consumption of caprolactam and the formation of products, in theory, could be followed. However, it was impossible to find these two pieces of equipment equipped with a connector that could withstand the temperatures ( $>510^{\circ}\text{C}$ ) required. A different thermal analytical technique, Thermal Volatilisation Analysis (TVA), was also attempted, however, the boiling point of caprolactam was too high for this technique to be valid.

FTIR analysis was also attempted using additional methanol to keep the samples in solution, however the results were very poor and inconsistent. It was decided that samples would be analysed immediately to circumvent the necessity of using methanol altogether.

## Chapter 5 - PA-12 synthesis

This chapter presents the development of a synthesis route to synthesise PA-12 within an OBR.

### 5.1-Introduction

The majority of literature concerning nylon particle synthesis focuses on PA-6 particles, there is very little available concerning the synthesis of PA-12 particles. Most of what was found by the author were in the form of patents or books. Like with the PA-6 variant, when synthesised in bulk, the main method used is hydrolytic polymerisation or anionic. Due to the poor quality of polymers formed using cationic polymerisation, this method has not been reported to have been used in industry<sup>148</sup>. In terms of properties, PA-12 has characteristics that are between aliphatic nylons with shorter chains (such as Nylon-6) and polyolefins<sup>149</sup>. PA-12 has similar mechanical properties to PA-6 and PA-6,6 but has a substantially lower melting point (178°C-180°C)<sup>150</sup> than either of them and its low water absorbance characteristics and density are closer to polyolefins<sup>151</sup>. It crystallises in a pseudo-hexagonal modification. Thanks to its relatively long hydrocarbon chain length, PA-12 possess dimensional stability and paraffin-like structure. PA-12 has numerous applications ranging from laser sintering (or UV curing)<sup>49</sup>, use as an additive in polyethylene films<sup>152</sup>, electrostatic coating<sup>153, 154</sup> and cosmetics<sup>154</sup>.

There are two known ways to form PA-12 particles, both involve anionic polymerisation. Attempts to replicate synthesis of PA-12 particles via precipitation polymerisation using methods provided in patents were not successful. The other involves polymerising styrene to form polystyrene and then polymerising the lauro lactam trapped within it. This requires two polymerisation steps and styrene polymerisation may damage the motor used for oscillation. For these reasons the method chosen was precipitation polymerisation.

### 5.2-Results and discussions

#### 5.2.1-Development of synthesis route

At first glance, the main issue with PA-12 synthesis seems to be the overall speed of the reaction. It appears that the dodecalactam is much more reactive than caprolactam. Using conditions that would successfully produce PA-6 particles instead results in a tough rubbery

like substance precipitating from solution quickly and beginning to coat the baffles as shown in Figure 5.1. This substance is most likely a mixture of the oligomer, small polymer chains and monomer. However, the work by Frunze et al.<sup>155</sup> studying the formation of nylon-6/12 copolymers in bulk polymerisation found that caprolactam was more reactive than dodecalactam. Therefore, the problems must arise from either the rate of agglomeration of growing particles, poor solvency of the monomer and subsequent oligomer or a combination of the two.

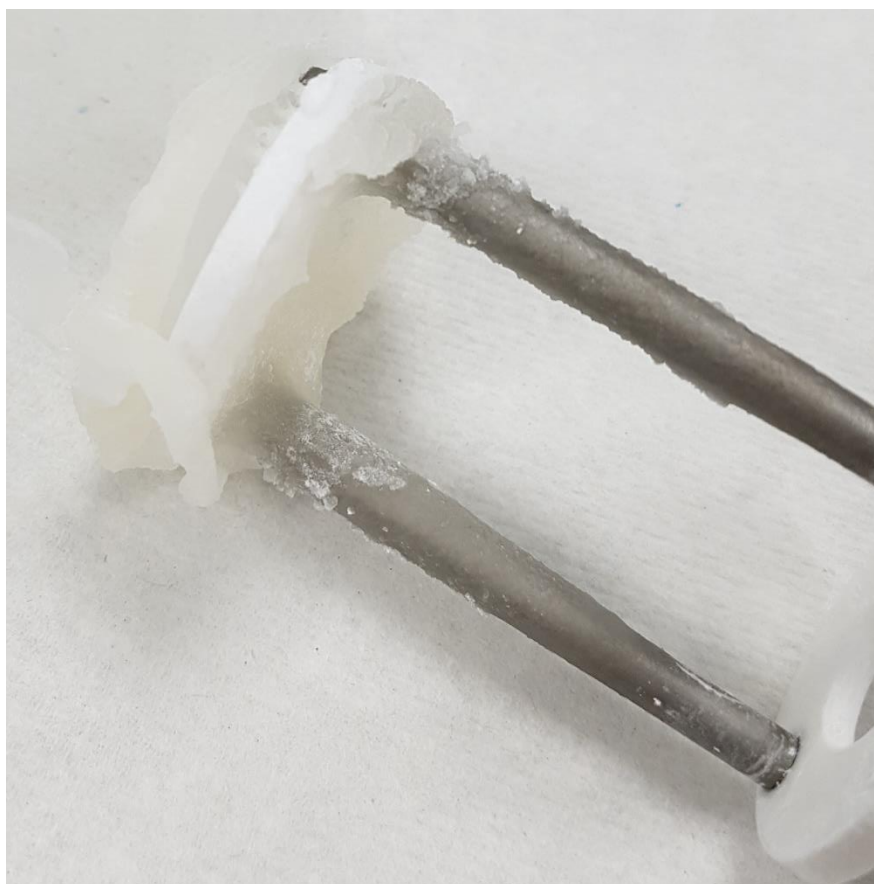


Figure 5.1 The build-up of oligomer on the baffle

If the CI is being added quickly, the precipitation of the rubbery oligomer occurs very fast, almost immediately in some cases. Slowing the injection rate lowers the rate of formation of this coating by 15-30 minutes but does not stop it. In theory, it may be possible to avoid altogether by making the injection rate very low, on the scale of nl/min. However, in practice, this would make the reaction time prohibitively long.



If the issue was purely down to agglomeration, the easiest solution to counteract this would be to lower the temperature. Unfortunately, dodecalactam comes out of solution at ~70°C and the reaction remains uncontrollable at this temperature. If solvency was the only issue, then lowering temperature will have made the problem even worse.

The work by Florin and Vasiliu-Opera went into substantial detail of the multiple phase separations that occur during polymer synthesis<sup>6</sup>. While all these phases somewhat over-lap, they noted that polymerisation was the quickest when the reaction mixture was in the homogeneous phase. Initial phase separation occurred due to the solvent becoming ‘poorer’ as polymerisation progressed, which led to liquid-liquid demixing resulting in the two phases. Depending on the solvent quality, this can lead to rapid precipitation and solidification. The phase separation results in a polymer rich phase and solvent rich one. It was theorised that the polymer phase is in the shape of liquid like droplets. The polymerisation is slower in this phase, as would be agglomeration of polymer chains and particles. In the majority of cases, it was noticed that the formation of the rubbery oligomer began before the initial phase separation. As this is where polymerisation is fast, rapid polymerisation will be making the solvent ‘poorer’, very quickly leading to precipitation and solidification seen on the baffles.

By adding a small amount of caprolactam to the system, the polymer will begin to grow as a PA-6 oligomer chain. Due to the greater acidity of the hydrogen on the caprolactam amide group, the catalyst would react to with caprolactam first and not the dodecalactam, therefore caprolactam would have to be consumed before reaction could continue with the dodecalactam. The greater solubility granted to the growing chains due to the incorporation of the caprolactam, monomer would help the reaction pass through the homogeneous phase and allow phase separation to occur without issue. Care has to be taken to ensure that the PA-12 properties are not affected by this incorporation of caprolactam.

In a patent published by Arkema<sup>49</sup>, the inorganic additive N,N-Ethylene bis(stearamide) (EBS) was added to help the control of the particle size of synthesised PA-12. The additive interacts at the polymer-solvent interface, coats the surface of individual particles resulting in

long-range repulsion between them. This helps to prevent the agglomeration of particles<sup>156</sup>. Unfortunately, any attempt to replicate the conditions used in the patent failed. However, the addition of the additive to the reaction mixture aids in the prevention of agglomeration at all stages of the reaction.

A secondary problem that was encountered was clogged Teflon tubing. In some cases, particularly with fast injection rates, oligomer would form at the end and sometimes inside the tubing. This clogging was caused by the OI immediately reacting with the monomer and the resultant oligomer coming out of solution. To circumvent this, the OI was ‘capped’ with caprolactam. The capped OI takes longer to react with activated anion due to lower nucleophilicity of the carbonyl carbon on the caprolactam, therefore, enabling the CI blend to mix within the reactor. To keep the CI blend in a liquid form, it must be dissolved in ethylbenzene and be constantly heated. Furthermore, the addition of the solvent will also dilute the OI, further slowing the reaction, aiding in the prevention of uncontrolled agglomeration.

To cap the CI, an equimolar amount of caprolactam was dissolved in ethylbenzene and mixed with the OI. The mixture was then heated to 55°C for 20 minutes to ensure that all the caprolactam had reacted with the OI. By combining all three additions, consistent PA-12 synthesis was achieved. EBS, in particular, had a significant effect on polymerisation as shown in Table 5.1.

Mass of EBS	Mass of caprolactam	Percentage Yield
0.5	0.6	0
0.25	0.6	5.2%
0.15	0.6	55%
0.15	0	Reaction failed
0	0.6	Reaction failed

Table 5.1 Percentage yield of PA-12 after 2 hours using different masses of EBS and caprolactam contents. Reaction considered a failure if uncontrollable agglomeration occurred.

When 0.5g of EBS was used, the reaction was slowed so significantly that even after 2 hours phase separation had not even begun. Halving the EBS concentration allowed for the formation of only a small amount of product but, crucially, PA-12 was successfully synthesised. Lowering the EBS further to 0.15g substantially increased the percentage yield. Attempts to remove the small amount of caprolactam while using 0.15g of EBS were not successful. This indicates that the problems with rapid solidification of the oligomer from agglomeration occurred mainly in the homogeneous phase.

Removing EBS from the system also resulted in rapid solidification of the growing oligomer. EBS helps to prevent agglomeration in the homogeneous phase so it may be possible that increasing the amount of caprolactam in the mixture would enable the reaction to proceed smoothly without the EBS, this however may compromise the quality of the particles. In addition, it is possible that the rapid precipitation of particles may be induced/ continue to proceed after phase separation because of the absence of EBS.

### **5.2.2-Effect of experimental parameters on molecular weight**

The most immediate difference between PA-12 and PA-6 is that the PA-12 molecular weights are significantly larger than the PA-6 particles formed in section 4.1. This most likely arises from the difference in CI/monomer molar ratio. When synthesising PA-6 the ratio was more in favour of the chain initiator, resulting in lower molecular weights. As the results show in Table 5.2 and in section 4.1.5.1, decreasing the injection rate caused an growth in the molecular weight. By decreasing the concentration of CI, there will be fewer active sites leading to longer polymer chains. This observation is in agreement with Udipi et al.<sup>74</sup> in their work on bulk polymerisation where below a certain CI concentration, decreasing the CI concentration resulted in an increase in molecular weight. However, Udipi et al. found that passed a certain point increasing the molecular weight lead to an increase in molecular weight. Alternatively, the patent by Hilaire et al. made no mention of the positive impact decreasing the CI concentration can have on the molecular weight. Alternatively, the patent by Hilaire et al. only states that increasing the CI concentration increases molecular weight. Ultimately, however,

the changing of injection rate had a noticeable but minor impact when compared to the reaction temperature.

Variable	Variable value	Molecular weight (g mol <sup>-1</sup> )
Injection Rate	30μL/min	33700
	22.5μL/min	35300
	15μL/min	36100
Temperature	90°C	42900
	80°C	36100
	70°C	26900
EBS	0.35g	36100
	0.25g	45100
	0.15g	40100

Table 5.2. Table displaying the influence of CI injection rate, temperature and mass of EBS on the molecular weight

The temperature of the reaction had the most powerful influence over the molecular weight. Increasing the reaction temperature by 20°C nearly doubled the molecular weight of the particles. This observation agrees with multiple patents and articles<sup>47, 60, 74</sup>. The work by Dan and Grolier<sup>7</sup> found that temperature had little influence over the initiation step but greatly affected the rate of the propagation step. Noticeably, the impact temperature has on molecular weight of PA-12 is much more substantial than it had on PA-6, this could be attributed to the fact that molecular weight's temperature dependence becomes more pronounced at greater molecular weights<sup>131</sup>.

The impact EBS has on molecular weight is slightly harder to assess. The middle mass value, 0.25g, corresponded to the highest molecular weight recorded, substantially higher than

the value gained with a higher reaction temperature. While the mixture with the lowest mass of EBS resulted in the particles with the second highest molecular weight. Neither Hilaire and Guerin<sup>47</sup> nor Vasiliu et al.<sup>156</sup> mentioned that an additive such as EBS had any effect on the molecular weight.

As previously noted, soon after the reaction has initiated, the homogeneous mixture demixes into a polymer rich phase and solvent rich one. The polymer rich phase is theorised to be in the form of liquid-like droplets. It is within these droplets that the majority of polymerisation takes place. The EBS only covers these droplets. Therefore, the additive has no influence over potential chain entanglements within the droplets. The solvent phase transports the monomer to the droplets. The EBS layer covering the droplets could be hindering the access of the monomer to these droplets, resulting in lower molecular weights. Unfortunately, there were no articles found by the author detailing how an additive may affect the molecular weight of a polymer to compare with this hypothesis.

### **5.2.3-Effect of experimental parameters on mean particle size**

As shown in Table 5.3, as temperature increases so does the mean particle size. This observation is in agreement with other patents and articles<sup>47, 60</sup> focused on particle size control of PA-6 particles. Increasing the reaction temperature would lead to greater collisions between the growing particles, resulting in particle amalgamation. Likewise, increasing the EBS concentration resulted in a decrease in particle size. This is expected as increasing the coating of the polymer droplets would lead to greater repulsion between them, leading to fewer particle collisions.

Variable	Variable value	Mean Particle size
Injection Rate	30 $\mu$ L/min	145
	22.5 $\mu$ L/min	162
	15 $\mu$ L/min	175
Temperature	90°C	284
	80°C	175
	70°C	113
EBS	0.35g	157
	0.25g	141
	0.15g	175

Table 5.3 Table displaying the influence of CI injection rate, reaction temperature and mass of EBS on the PA-12 particle size

The most surprising set of results were those concerning the injection rate. The results were the opposite of what was expected. Both the observations by Hilaire and Guerin<sup>47</sup> studying PA-12 synthesis and those in Chapter 4 investigating PA-6 particle size control showed that increasing the injection rate led to larger particles, not smaller ones. However, similar observations have been found when polystyrene was formed via suspension polymerisation using a semi-batch process<sup>157</sup>.

With the EBS acting as a coating for the ‘liquid-like’ polymer phase droplets to help the prevention of coalescence, the reaction in some respects could be considered to be carried out in a pseudo-suspension. Nogueira et al. studied the effect of injecting additional styrene monomer into an already polymerising system<sup>157</sup> and reported that at lower feeding rates particles became larger. The reasons for which are not completely understood but it was theorised that at low feeding rates there was more uniform interaction between old and new

droplets, because of this interaction, existing particles swell. Such interactions may be the cause of the patterns observed in PA-12 particle synthesis.

#### 5.2.4 Effect of experimental parameters on melting point

Both the reaction temperature and the injection rate had no real impact on the melting point of PA-12 particles. The melting point of polymers is controlled by various factors including but not limited to, main chain structure, intermolecular forces, molecular weight, crystallinity and the absence or presence of certain additives such as plasticizers. When the molecular weight of a polymer is below a certain point, further reductions in molecular weight will have a negative effect on the melting point. Both temperature and injection rate adjust the molecular weight of the particles but as shown in Table 5.4, not to the degree where the melting point is affected.

Variable	Variable value	Melting Point (C	Degree of Crystallinity
Injection Rate	30 $\mu$ L/min	178.7	37.68
	22.5 $\mu$ L/min	178.4	39.14
	15 $\mu$ L/min	179.7	38.93
Temperature	90°C	177.3	38.10
	80°C	179.7	39.15
	70°C	178.2	38.68
EBS	0.35g	174.3	38.54
	0.25g	173.7	38.09
	0.15g	179.7	39.71

Table 5.4 Influence of variables on the PA-12 melting point and degree of crystallinity

At low concentrations, EBS did not affect the melting point, however, at higher concentrations, EBS lowered the melting point by approximately 5°C. EBS has been shown to be a capable nucleating agent in the synthesis of polylactic acid<sup>158</sup>. While unlikely, it may

be possible that in the context of polyamide synthesis EBS was acting as a nucleation inhibitor. To determine if this was the case, the degree of crystallinity was determined using the equation below:

$$X_c = \frac{(\Delta H_m - \Delta H_c)}{\Delta H_{c(100\%)}} \times 100 (\%) \quad (5.1)$$

Where  $X_c$  is the degree of crystallinity,  $\Delta H_m$  (J/g) is the enthalpy of melting of the sample,  $\Delta H_c$  (J/g) is the enthalpy of crystallisation and  $\Delta H_{c(100\%)}$  (J/g) is the heat of fusion for 100% crystalline polymer. The value for the heat of fusion for 100% crystalline polymer was taken to be 209.3 J/g determined by Gogolewski<sup>159</sup>.

As seen in Table 5.4, while the crystallinity of each sample varies slightly, overall there was no real difference in the degree of crystallinity between samples. This indicates that the EBS was not acting as nucleation inhibitor. An alternate explanation for the reduction in melting point is that EBS is being trapped within the polymer particles but only at higher concentrations is there enough EBS present to have a negative impact over the melting point.

### 5.2.5 Morphology

Investigations by Dan et al.<sup>6</sup> showed that the morphology of PA-6 particles was controlled by a complex process involving phase separation and crystallisation. Both of which are strongly influenced by the catalyst/CI combination used, e.g. ‘slow’ acting and ‘fast’ acting. The efficiency of a catalyst is dependent on its nucleophilicity. Therefore, caprolactamates of alkali metals are considered ‘fast’ acting, while alkali metal aluminium alcolates are ‘slow’ acting<sup>6</sup> for the purposes of PA-6 synthesis. The efficiency of the chain initiator is dependent on the electron deficiency of the carbonyl carbon. The more electron deficient the carbon atom is, the more efficient the CI.



Dan and Vasiliu-Oprea reported that when using a ‘slow-slow’ or a ‘slow-quick’ CI/catalyst combination, the resultant particles were irregularly shaped and roughly textured. The polymer particles had a continuous structure giving cohesion to the particle, consequently, the particles were highly porous as shown in Figure 5.2.

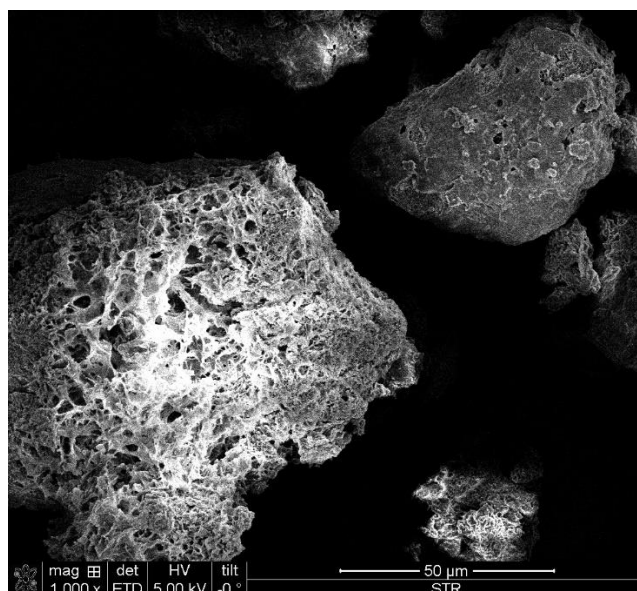


Figure 5.2 Micrograph of PA-6 particles formed using a ‘slow-slow’ CI/catalyst system

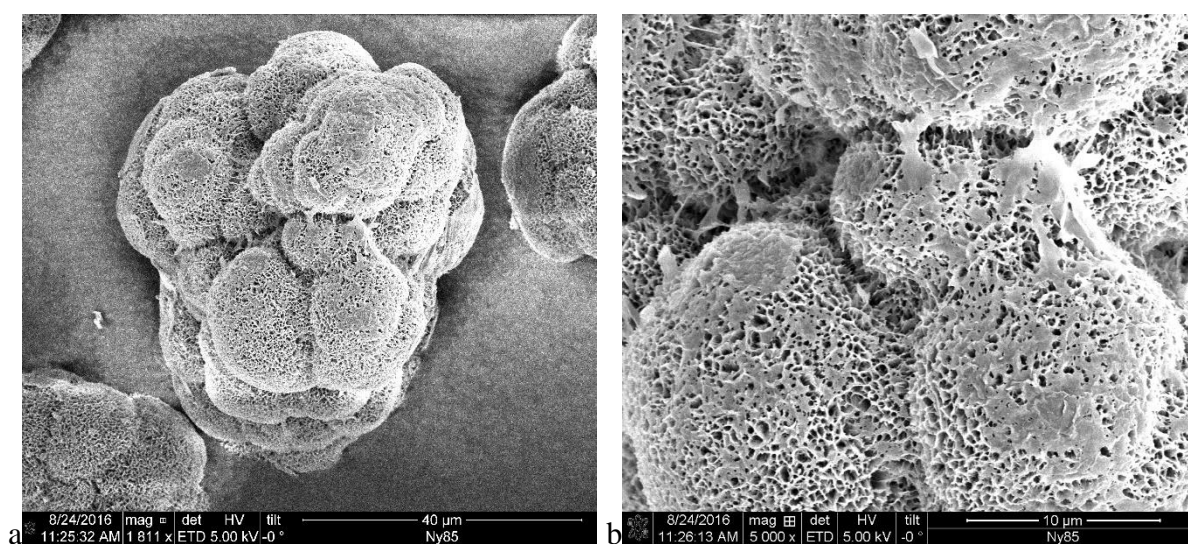


Figure 5.3 Micrographs of Nylon-12 particles formed using a slow/slow CI/catalyst combination at a magnification of a)x1811 and b) x5000

However, the morphology of PA-12 resulting from the usage of a ‘slow-slow’ CI/catalyst system was substantially different as shown in Figure 5.3. There are no individual particles, instead, there are fused agglomerates from individual globules. In this case, the globules have a porous, spherulitic structure that is commonly seen in PA-6 particles made from highly efficient CIs.

Particle morphology is highly influenced by the initial phase separation that occurs once the concentration of growing chains and the degree of polymerisation reaches a certain level. This liquid-liquid phase separation results in a polymer rich phase and a solvent rich phase. The former is made from liquid-like droplets and polymerisation continues within these spheres. When phase separation is reached quickly, shear forces caused by mixing allow polymer phase droplets to collide before solidification, resulting in agglomeration. Additionally, chain growth also has a strong influence on the morphology, when all the chain initiator reacts immediately, demixing domains are more uniform.

Less efficient (‘slow-acting’) CIs react slowly, therefore the viscosity of the homogeneous medium increases slowly. When enough active sites are generated, chain growth begins. As with more efficient CIs, a polymer phase and solvent rich phase are formed with the polymer phase in the shape of liquid-like droplets. However, in this case, the droplets do not collide, instead, phase separation continues to occur within each droplet. A small increase in polymer concentration can then induce spinodal demixing, leading to the creation of continuous structures seen in Figure 5.2.

### **5.3 Conclusions**

A method to synthesise PA-12 particles was successfully created. The main issue to overcome was the rapid agglomeration of oligomer in the initial phase of the reaction. This was achieved by three alterations to a method that is used to synthesise PA-6. Firstly, small amounts of caprolactam was added to help smooth the reaction during the initial homogeneous phase. Secondly, the additive EBS was added. EBS coats the ‘liquid’-like droplets of the polymer phase and causes steric repulsion between these droplets, lowering the agglomeration rate.

Lastly, the CI was capped with caprolactam and dissolved in ethylbenzene. All three alterations were required for successful synthesis.

Using this method, the influences of reaction temperature, EBS concentration and injection rate on the molecular weight, the particle size and the melting point were investigated. Expectedly, the reaction temperature had a substantial influence over the molecular weight and particle size, but no impact on melting point. Increasing the injection rate led to a small decrease in both molecular weight and particle size. This decrease in particle size was the opposite of what was expected. It is theorised that the presence of EBS is responsible for this unexpected result. Again, the injection rate had no impact on the melting point. Only the concentration of EBS had any effect on the melting point. At higher concentrations, EBS noticeably lowered the melting point. Furthermore, particle size was lowered with increasing EBS concentration. Increasing the EBS would lead to a greater repulsive coating, hindering agglomeration and subsequently lowering particle size. Theoretically, EBS should have no impact on the molecular weight but in practice the EBS coating may be hindering the monomer from entering the polymer phase droplets.

#### **5.4 Problems, observations and solutions**

To ensure that CI is added continuously, it is preferred that the tip of the tubing is submerged within the reaction mixture. However, backwards fluid oscillations can force the CI mixture back into the Teflon tubing, leading to blockage. Unfortunately, the only means to resolve this issue was to remove the tubing from the reaction mixture and suspend the tubing over it. It was attempted to ensure that the tubing exit was in contact with the reactor wall so as to avoid the formation of droplets, but this was not always successful.

Capping the CI with caprolactam resulted in the eventual solidification of the CI at room temperature. The addition of ethylbenzene to the mixture helped to keep the CI mixture in a liquid state for longer, however eventually the capped CI would come out of solution within either the syringe or the Teflon tubing. To account for this, the syringe and Teflon tubing had to be constantly heated.

It must be noted that, initially, Nylon-12 particles were formed without the aid of EBS. It was later discovered that the catalyst used in these had been poisoned/contaminated. From this, it can be assumed that if a catalyst is sufficiently weak, the EBS is then not required for synthesis.

## Chapter 6-Conclusions and future work

The final chapter presents the major conclusions reached in this work. In addition, some suggestions for future research are also put forward.

### 6.1 Conclusions

The factorial design was successful in determining which factors control polymer properties of interest when the chain initiator was added continuously over a set time. The most important factors influencing molecular weight were reaction temperature, the rate of injection and monomer concentration and two-way interaction between the monomer mass and the CI injection rate. Increasing the temperature lead to a substantial increase to the molecular weight. Conversely, increasing the injection rate of the CI lead to a decrease in the molecular weight. Additionally, increasing the monomer mass also increased the molecular weight. However, due to the two-way interaction between the monomer mass and the CI injection rate the influence monomer mass has molecular weight decreases greatly as the CI injection rate increases.

For particle size, the significant factors were stirring speed, the CI injection rate and a two-way interaction between monomer mass and the stirring speed. The stirring speed was the dominating factor controlling the particle size. It was found that increasing the stirring speed resulted in a marked decrease in the particle size. And due to the two-way interaction between monomer mass the stirring rate becomes even more influential at greater monomer masses. Lastly, increasing the CI lead to an increase in particle size.

The melting point was affected by the reaction temperature, a two-way interaction solvent volume and temperature and the solvent volume. As expected, increasing the reaction temperature lead to an increase in the melting point, however so did increasing the solvent volume. This is surprising as the solvent volume had no influence over molecular weight and if it had it would be expected that increasing the solvent volume would decrease the molecular weight and therefore melting point. It is thought that the concentration of un-reacted monomer trapped within the particles was minimised due to increased solvent volume.

The most surprising results from the design was the apparent lack of influence the catalyst concentration had on the polymer properties. For the reaction under batch conditions it was reported that both the monomer/catalyst ratio and the monomer/CI ratio had influence over molecular weight and particle size. Under semi-batch conditions neither ratio appeared to have any influence over polymer properties.

The kinetics of PA-6 synthesis under semi-batch conditions were studied in substantial detail. In theory, with the combination of slow acting catalyst and CI used, the reaction kinetics would be second order due to the initiation step becoming the rate determining step. In practice, however, second order kinetics were never observed under full reaction conditions. Reactions under equimolar conditions without the presence of the catalyst were undertaken to investigate the initiation stage of the reaction. It was found that side reactions may be taking place forcing a deviation from second order kinetics. Under equimolar conditions the single injection method always resulted in first order kinetics but under continuous injection conditions 1<sup>st</sup>, 2<sup>nd</sup> and 0<sup>th</sup> order kinetics were observed. Under continuous conditions 1<sup>st</sup> order kinetics were observed when both the CI injection rate and reaction temperature were high, 0<sup>th</sup> order kinetics were observed when the reaction temperature was high, and the injection rate was low. 2<sup>nd</sup> order kinetics were observed when the reaction temperature was low, and the injection rate was high. Three different stirring rates were tested to determine if mixing had any influence over chemical kinetics. None of the three stirring rates tested had any influence over the reaction rate.

The four factors of interest under normal reaction conditions were reaction temperature, CI injection rate, catalyst concentration and mixing intensity. In all cases there was a premature cessation of the reaction. It was theorised that this cessation was caused by the pre-mature crystallisation of nylon particles and oligomer due to undercooling. This pre-mature crystallisation first hinders then completely inhibits the reaction. By increasing the reaction temperature crystallisation can be hindered allowing the reaction to progress further than it would at lower temperatures. However, other than reaction temperature, no other variable had any influence over this stoppage. Increasing both the catalyst and CI concentration increased reaction rate, but beyond a certain point, increasing concentration further had no further impact on kinetics. At low catalyst and... concentrations the order of reaction was undefinable, indicating that reaction kinetics were controlled via a diffusion mechanism and

not a chemical one. The upper limits of influence for both catalyst concentration and CI injection was the same, with the reaction rate being near identical when either the CI injection rate or the catalyst concentration was at its maximum value. Again, the stirring rate was not found to have any impact over the reaction kinetics.

In practice, the order observed was either first or zero for the reaction under normal conditions. At no point were 2<sup>nd</sup> order kinetics observed. The order was depended on the reaction temperature and rate of injection. With slow injection rates and high temperatures, zero order kinetics were favoured, while first order kinetics were favoured with fast injection rates and low reaction temperatures. With slow injection rates and high reaction temperatures it was theorised that the rate of polymer maturation, from inception to precipitation was greater than the rate of injection. Under these conditions the reaction rate would be independent of monomer concentration. With higher injection rates and lower temperatures the CI would be able to accumulate within the reactor making it more single injection-like in character, resulting in first order kinetics.

A method to synthesise PA-12 particles was successfully developed. This was achieved by capping the CI with caprolactam and by adding small amounts of caprolactam and EBS to the reaction mixture. All three were required for successful synthesis. Using this method, the effects of temperature, CI injection rate and EBS concentration on molecular weight, particle size and melting point were studied. Increasing the reaction temperature led to an increase in particle size and molecular weight but had no impact on the melting point. Conversely, increasing the CI injection rate led to a decrease in both molecular weight and particle size; however, again, there was no change in melting point. Only by increasing EBS concentration, was the melting point negatively affected. The reasons for this was not determined. Like with injection rate, increasing EBS concentration resulted in a small decrease in and particle size. The influence EBS had over molecular weight could not be determined. Results were erratic with the median value for the EBS concentration giving by far the largest reported molecular weight. Investigations would have to repeated to determine the effect of EBS has on the molecular weight of PA-12.

Currently it is not recommended to attempt the synthesis of PA-12 under continuous conditions. There are two major related issues that would need to be resolved. The first issue is that there is still substantial build-up of a mixture of product and oligomer forming between the columns of the baffles. In addition, a thin layer of oligomer can form on the surface of the reactor. This build-up, while not ideal does not interfere with oscillation of the baffle under batch conditions. However, under continuous conditions these two problems would be heightened and eventually either of these issues may interfere with the oscillatory motion of the baffle/fluid. The second major issue is that cleaning the reactor is difficult. Even provided that the reaction recipe in its current state could be used in a continuous reactor for a limited time it would be very difficult to clean the reactor. Under batch conditions the build-up of product and oligomer is relatively easy to clean by hand. Under continuous conditions were there could be many baffle cells the reactor would have to be cleaned using solvents. The only chemicals found by the author that are known to fully dissolve PA-12 are m-cresol, 90%+ sulphuric acid and HFIP. All of which are dangerous and in the case of HFIP, expensive. Additionally, the polymer would act as a thickening agent. To counteract this excessive solvent would have to be used. To solve both these major issues the reaction recipe and conditions would have to be optimised to make it as 'smooth' as possible to circumvent this build-up. If this can be achieved, then further studies in a continuous reactor can be recommended.

## 6.2 Future research

Due to the time constraints, some aspects of the research work cannot be investigated, the following is a list of potential future work in this area:

- The factorial design was successful in analysing a host of experimental properties that influence PA-6 particle synthesis. However, there is room for improvement. Further study of the various two-way interactions that influence polymer properties may substantially improve the model. Udipi et al.<sup>74</sup> showed that the mechanisms controlling polymer properties such as molecular weight can change dramatically depending on the concentration of the reactants. Expanding the model to study greater variations in reactant concentrations would give a greater understanding of these mechanistic changes. Additionally, new factorial designs to investigate different combinations of



catalysts, CIs and solvents would give a better insight into the most efficient ways to manipulate polymer properties;

- It is advisable to repeat previous kinetic measurements using In-situ methods. It was observed that due to the reaction mixture shifting from the homogeneous to heterogeneous phase the reaction rate could change substantially during the first 15 minutes. The In-situ methods would provide greater detail to what is happening during this phase change as well as the whole reaction. In addition, it would give clarity to measurements gained when a 0.5Hz oscillation frequency was used. There are other variables that potentially impact polymerisation kinetics that have not been studied. Of interest would be to investigate how solvent properties and monomer concentration affect reaction kinetics.
- It was theorised that a physical interruption of the polymerisation process occurs at low reaction temperatures due to premature crystallisation caused by undercooling. It was theorised that this could be overcome by a simultaneous increase in catalyst and chain initiator concentration. Further reactions would have to be carried out to determine if this is the case;
- There is substantial room for improvement to the method developed to synthesise PA-12. Currently, there is still considerable build-up of material in the baffle pillars and a thin layer of sticky oligomer formed on the surface of the reactor. Reaction conditions would have to be optimised to avoid these issues;
- It was theorised that the oscillation of the reaction mixture was forcing the mixture into the Teflon tubing used to inject the CI mixture, leading to blockages in the tubing during PA-12 synthesis. To circumvent this the Teflon tubing was not submerged within the reaction mixture. However, now it cannot be guaranteed that the injection rate of the CI into the reaction mixture is consistent. Therefore, it is important to develop a method that would allow Teflon tubing to be submerged in the mixture. One possibility would be to lower the concentration of CI in the CI mixture and increase the volume of ethylbenzene. This would allow the injection rates of the CI to be increased without causing the reaction to fail and the greater pressure in the Teflon tubing would stop the backflow of the reaction mixture into the tubing.

- Despite synthesis of PA-6 being carried in both a STR and OBR there was no direct comparisons made. Changing from STR and OBR should have no effect over the melting point and molecular weight, but particle size would be influenced strongly by the change in reactor. Studies would have carried to determine if an OBR can control particle size more effectively than an STR. Additionally, it would have to be determined if the OBR was a more efficient reactor overall through the study of the power density of both reactors. Normally OBR's are much more efficient than STR's but under conditions required to synthesise desired particle sizes this may not be the case.
- The investigation as to how experimental parameters effect PA-12 properties was limited, particularly, the influence of EBS over molecular weight could not be determined. Factorial designs could provide further/in-depth analyses of how various parameters affect PA-12 properties. Using factorial designs multiple factors can be investigated thoroughly, quickly and with an efficient use of resources. The result from this design could also be easily compared to those gained through the study of PA-6 formation. Such designs and comparisons may lead to greater insight as to why PA-12 synthesis is so difficult to control;

## References

1. Seymour, R. B.; Kirshenbaum, G. S.; Meeting, A. C. S., *High performance polymers, their origin and development: proceedings of the Symposium on the History of High Performance Polymers at the American Chemical Society Meeting held in New York, April 15-18, 1986*. Elsevier: 1986.
2. Paul, S. Manufacture of artificial silk. US2142007A, 1938/12/27/, 1938.
3. Chrzczonowicz, S., Zesz. Nauk. Polit. Lbdkiej, Chemia, 1955; Vol. 3, p 94.
4. Blackmore, C. E., Nylon Powders and their Application as Surface Coatings Using Flame Spraying. *Surface Engineering* **1987**, 3 (1), 29-34.
5. Kiefer, S. L.; Hart, S.; Creech, R. G. Method of electrostatic powder spray coating. US4774102A, 1988/09/27/, 1988.
6. Dan, F.; Vasiliu-Oprea, C., Anionic polymerization of caprolactam in organic media. Morphological aspects. *Colloid and Polymer Science* **1998**, 276 (6), 483-495.
7. Dan, F.; Grolier, J.-P. E., Spectrocalorimetric screening for complex process optimization. In *Chemical Thermodynamics for Industry*, The Royal Society of Chemistry: 2004; pp 88-103.
8. Ni, X.; Gao, S., Mass transfer characteristics of a pilot pulsed baffled reactor. *Journal of Chemical Technology & Biotechnology* **1996**, 65 (1), 65-71.
9. Mackley, M. R.; Stonestreet, P., Heat transfer and associated energy dissipation for oscillatory flow in baffled tubes. *Chemical Engineering Science* **1995**, 50 (14), 2211-2224.
10. Ni, X.; Gao, S., Scale-up correlation for mass transfer coefficients in pulsed baffled reactors. *The Chemical Engineering Journal and the Biochemical Engineering Journal* **1996**, 63 (3), 157-166.
11. An, W. K.; Han, M. Y.; Wang, C. A.; Yu, S. M.; Zhang, Y.; Bai, S.; Wang, W., Insights into the Asymmetric Heterogeneous Catalysis in Porous Organic Polymers: Constructing A TADDOL-Embedded Chiral Catalyst for Studying the Structure-Activity Relationship. *Chemistry-a European Journal* **2014**, 20 (35), 11019-11028.
12. Jiang, D. L.; Xu, F., Porous organic materials for electric energy storage and power supply. *Abstracts of Papers of the American Chemical Society* **2014**, 248, 2.
13. Zhang, Y. W.; A, S. G.; Zou, Y. C.; Luo, X. L.; Li, Z. P.; Xia, H.; Liu, X. M.; Mu, Y., Gas uptake, molecular sensing and organocatalytic performances of a multifunctional carbazole-based conjugated microporous polymer. *Journal of Materials Chemistry A* **2014**, 2 (33), 13422-13430.
14. Zhang, C.; Yang, X.; Zhao, Y.; Wang, X. Y.; Yu, M.; Jiang, J. X., Bifunctionalized conjugated microporous polymers for carbon dioxide capture. *Polymer* **2015**, 61, 36-41.
15. Cowie, J. M. G.; Arrighi, V., *Polymers : chemistry and physics of modern materials*. 3rd ed.; CRC Press: Florida, 2007; p 499 p.
16. Misra, G. S., *Introductory Polymer Chemistry*. J. Wiley & Sons: 1993.
17. Nicholson, J. W.; Chemistry, R. S. o., *The Chemistry of Polymers*. Royal Society of Chemistry: 2006.
18. Seymour, R., *Applications of Polymers*. Springer US: 2012.
19. Sharma, B. K., *Industrial Chemistry*. GOEL Publishing House: 1991.
20. VivaldoLima, E.; Wood, P. E.; Hamielec, A. E.; Penlidis, A., An updated review on suspension polymerization. *Industrial & Engineering Chemistry Research* **1997**, 36 (4), 939-965.
21. Jensen, A. T.; Neto, W. S.; Ferreira, G. R.; Glenn, A. F.; Gambetta, R.; Gonçalves, S. B.; Valadares, L. F.; Machado, F., 8 - Synthesis of polymer/inorganic hybrids through heterophase polymerizations. In *Recent Developments in Polymer Macro, Micro and Nano Blends*, Visakh, P. M.; Markovic, G.; Pasquini, D., Eds. Woodhead Publishing: 2017; pp 207-235.
22. Odian, G., *Principles of Polymerization*. Wiley: 2004.
23. Anderson, C. D.; Daniels, E. S., *Emulsion Polymerisation and Latex Applications*. Rapra Technology Limited: 2003.

24. Thickett, S. C.; Gilbert, R. G., Emulsion polymerization: State of the art in kinetics and mechanisms. *Polymer* **2007**, *48* (24), 6965-6991.
25. Chern, C. S., Emulsion polymerization mechanisms and kinetics. *Progress in Polymer Science* **2006**, *31* (5), 443-486.
26. El-hoshoudy, A. N. M. B., Emulsion Polymerization Mechanism. In *Recent Research in Polymerization*, InTech: 2018.
27. Kohan, M. I.; Kohan, M. I., *Nylon Plastics Handbook*. Hanser Publishers: 1995.
28. Seymour, R. B., *Polymers for engineering applications*. ASM International: 1987.
29. Seymour, R. B.; Porter, R. S., *Manmade Fibres: Their origin and development*. Springer Netherlands: 1993.
30. Doubravsky Von, S.; Geleji, F., Über probleme der kationischen polymerisation des caprolactams. II. Die polymerisation mit caprolactam-hydrochlorid. *Die Makromolekulare Chemie* **1967**, *110* (1), 246-256.
31. Mizerovskii, L. N.; Silant'eva, V. G., Cationic polymerization of caprolactam in the presence of HPO<sub>3</sub>. *Polymer Science U.S.S.R.* **1978**, *20* (9), 2280-2289.
32. Van der Want, G. M.; Kruissink Ch, A., A non-hydrolytic polymerization of  $\epsilon$ -caprolactam. The polymerization initiated by hydrogen chloride. *Journal of Polymer Science* **1959**, *35* (128), 119-138.
33. Majury, T. G., Amines and carboxylic acids as initiators of polymerization in caprolactam. *Journal of Polymer Science* **1958**, *31* (123), 383-397.
34. Frost, J. W., *Synthesis of caprolactam from lysine*. 2005.
35. Giori, C.; Hayes, B. T., Hydrolytic polymerization of caprolactam. I. Hydrolysis—polycondensation kinetics. *Journal of Polymer Science Part A-1: Polymer Chemistry* **1970**, *8* (2), 335-349.
36. Šebenda, J., Chapter 6 Lactams. In *Comprehensive Chemical Kinetics*, Bamford, C. H.; Tipper, C. F. H., Eds. Elsevier: 1976; Vol. 15, pp 379-471.
37. Puffr, R.; Kubanek, V., *Lactam-based Polyamides Volume II Modification, Technology, and application*. CRC Press: 1991; p 368.
38. Brydson, J. A., 18 - Polyamides and Polyimides. In *Plastics Materials (Seventh Edition)*, Brydson, J. A., Ed. Butterworth-Heinemann: Oxford, 1999; pp 478-530.
39. Puffr, R.; Kubanek, V., *Lactam-based Polyamides: Polymerization Structure*. CRC Press: 1991; Vol. 1.
40. Kang, K.-S.; Hong, Y.-K.; Kim, Y. J.; Kim, J. H., Synthesis and properties of Nylon 4/5 copolymers for hydrophilic fibers. *Fibers and Polymers* **2014**, *15* (7), 1343-1348.
41. Rusu, G.; Rusu, E., Caprolactam-Laurolactam (Nylon 6/12) Copolymers: Synthesis and Characterization. *High Performance Polymers* **2004**, *16* (4), 569-584.
42. Kim, N. C.; Kim, J.-H.; Kim, J. H.; Nam, S. W.; Jeon, B. S.; Kim, Y. J., Preparation of Nylon 4 microspheres via heterogeneous polymerization of 2-pyrrolidone in a paraffin oil continuous phase. *Journal of Industrial and Engineering Chemistry* **2015**, *28*, 236-240.
43. Zhang, J.; Kissounko, D. A.; Lee, S. E.; Gellman, S. H.; Stahl, S. S., Access to Poly- $\beta$ -Peptides with Functionalized Side Chains and End Groups via Controlled Ring-Opening Polymerization of  $\beta$ -Lactams. *Journal of the American Chemical Society* **2009**, *131* (4), 1589-1597.
44. Rahman, M. A.; Renna, L.; Venkataraman, D.; Desbois, P.; J. Lesser, A., *High crystalline, porous polyamide 6 by anionic polymerization*. 2018; Vol. 138.
45. Telen, L.; Van Puyvelde, P.; Goderis, B., Random Copolymers from Polyamide 11 and Polyamide 12 by Reactive Extrusion: Synthesis, Eutectic Phase Behavior, and Polymorphism. *Macromolecules* **2016**, *49* (3), 876-890.
46. Stavila, E.; Loos, K., Synthesis of lactams using enzyme-catalyzed aminolysis. *Tetrahedron Letters* **2013**, *54* (5), 370-372.
47. Hilaire, J. C.; Guerin, R., Anhydrous process for the manufacture of polyamide powder from lactam in the presence of N,N'-alkylene bis amide. Google Patents: 1987.

48. Nuyken, O.; Pask, S. D., Ring-Opening Polymerization-An Introductory Review. *Polymers* **2013**, 5 (2), 361-403.
49. Luyen, K.; Senff, H.; Pauly, F. X., Process for the manufacture of polyamide-12 powder with a high melting point. Google Patents: 2012.
50. Marchildon, K., Polyamides – Still Strong After Seventy Years. *Macromolecular Reaction Engineering* **2010**, 5 (1), 22-54.
51. Yamazaki, N.; Matsumoto, M.; Higashi, F., Studies on reactions of the N-phosphonium salts of pyridines. XIV. Wholly aromatic polyamides by the direct polycondensation reaction by using phosphites in the presence of metal salts. *Journal of Polymer Science: Polymer Chemistry Edition* **1975**, 13 (6), 1373-1380.
52. Yamazaki, N.; Niwano, M.; Kawabata, J.; Higashi, F., Preparation of peptides and active esters by a hydrolysis-dehydration reaction with phosphonites, and the application of the reaction to polymer synthesis. *Tetrahedron* **1975**, 31 (7), 665-670.
53. Preston, J.; Hofferbert, W. L., Preparation of poly amides via the phosphorylation reaction. I. Wholly aromatic polyamides and polyamide-hydrazides. *Journal of Polymer Science: Polymer Symposia* **1978**, 65 (1), 13-27.
54. Higashi, F.; Goto, M.; Nakano, Y.; Kakinoki, H., Wholly aromatic polyamides by the direct polycondensation reaction using triphenyl phosphite in the presence of poly(4-vinylpyridine). *Journal of Polymer Science: Polymer Chemistry Edition* **1980**, 18 (3), 851-856.
55. Higashi, F.; Nakano, Y.; Goto, M.; Kakinoki, H., High-molecular-weight polyterephthalamide by direct polycondensation reaction in the presence of poly(ethylene oxide). *Journal of Polymer Science: Polymer Chemistry Edition* **1980**, 18 (3), 1099-1104.
56. Higashi, F.; Taguchi, Y., Aromatic polyamides by phosphorylation reaction with triphenylphosphite and LiCl in the presence of polymer matrix. *Journal of Polymer Science: Polymer Chemistry Edition* **1980**, 18 (9), 2875-2877.
57. Yokoyama, A.; Yokozawa, T., Converting Step-Growth to Chain-Growth Condensation Polymerization. *Macromolecules* **2007**, 40 (12), 4093-4101.
58. Kawanobe, W.; Yamaguchi, K.; Rokicki, G.; Mei Sha, K.; Yamazaki, N.; Nakahama, S., Direct synthesis of polyamides by N-acyl phosphoramidites. *Journal of Polymer Science: Polymer Chemistry Edition* **1984**, 22 (10), 2371-2380.
59. Burch, R. R.; Manring, L. E., N-Alkylation and Hofmann elimination from thermal decomposition of R<sub>4</sub>N<sup>+</sup> salts of aromatic polyamide polyanions: synthesis and stereochemistry of N-alkylated aromatic polyamides. *Macromolecules* **1991**, 24 (8), 1731-1735.
60. Vasiliu-Oprea, C.; Dan, F., On the relation between synthesis parameters and morphology of anionic polycaprolactam obtained in organic media. I. Influence of the Na [O (CH<sub>2</sub>)<sub>2</sub> OCH<sub>3</sub>]<sub>2</sub> AlH<sub>2</sub>/isophorone diisocyanate catalytic system. *Journal of applied polymer science* **1996**, 62 (10), 1517-1527.
61. Park, Y.; Curtis, C. W.; Roberts, C. B., Formation of Nylon Particles and Fibers Using Precipitation with a Compressed Antisolvent. *Industrial & Engineering Chemistry Research* **2002**, 41 (6), 1504-1510.
62. Pei, A.; Liu, A.; Xie, T.; Yang, G., A new strategy for the preparation of polyamide-6 microspheres with designed morphology. *Macromolecules* **2006**, 39 (23), 7801-7804.
63. Pei, A.; Liu, A.; Xie, T.; Yang, G., Effect of in situ synthesized macroactivator on morphology of PA6/PS blends via successive polymerization. *Journal of Applied Polymer Science* **2007**, 105 (4), 1757-1765.
64. Wu, B.; Xie, T.; Yang, G., Investigation on particular phase morphology of immiscible polyamide 12 and polystyrene blends prepared via anionic ring-opening polymerization. *Polymer Engineering & Science* **2012**, 52 (9), 1831-1838.
65. Ricco, L.; Monticelli, O.; Russo, S.; Paglianti, A.; Mariani, A., Fast-activated anionic polymerization of epsilon-caprolactam in suspension, 1 - Role of the continuous phase on

- characteristics and properties of powdered PA6. *Macromolecular Chemistry and Physics* **2002**, *203* (10-11), 1436-1444.
66. Crespy, D.; Landfester, K., Anionic polymerization of epsilon-caprolactam in miniemulsion: Synthesis and characterization of polyamide-6 nanoparticles. *Macromolecules* **2005**, *38* (16), 6882-6887.
  67. Davé, R. S.; Kruse, R. L.; Stebbins, L. R.; Udipi, K., Polyamides from lactams via anionic ring-opening polymerization: 2. Kinetics. *Polymer* **1997**, *38* (4), 939-947.
  68. Greenley, R. Z.; Stauffer, J. C.; Kurz, J. E., The Kinetic Equation for the Initiated, Anionic Polymerization of  $\eta$ -Caprolactam. *Macromolecules* **1969**, *2* (6), 561-567.
  69. Šittler, E.; Šebenda, J., Alkaline polymerization of 6-caprolactam. XXXII. The kinetics of polymerization activated by N,N,N',N'-tetraacetylhexamethylenediamine. *Collection of Czechoslovak Chemical Communications* **1968**, *33* (1), 270-277.
  70. Rigo, A.; Fabbri, G.; Talamini, G., Kinetic study of anionic polymerization of 6-caprolactam by differential calorimetry. *Journal of Polymer Science: Polymer Letters Edition* **1975**, *13* (8), 469-477.
  71. Malkin, A. Y.; Frolov, V. G.; Ivanova, A. N.; Andrianova, Z. S., The nonisothermal anionic polymerization of caprolactam. *Polymer Science U.S.S.R.* **1979**, *21* (3), 691-700.
  72. Malkin, A. Y.; Ivanova, S.; Frolov, V.; Ivanova, A.; Andrianova, Z., Kinetics of anionic polymerization of lactams. (Solution of non-isothermal kinetic problems by the inverse method). *Polymer* **1982**, *23* (12), 1791-1800.
  73. Bolgov, S. A.; Begishev, V. P.; Malkin, A. Y.; Frolov, V. G., Role of the functionality of activators during isothermal crystallization accompanying the activated anionic polymerization of  $\epsilon$ -caprolactam. *Polymer Science U.S.S.R.* **1981**, *23* (6), 1485-1492.
  74. Udipi, K.; Davé, R. S.; Kruse, R. L.; Stebbins, L. R., Polyamides from lactams via anionic ring-opening polymerization: 1. Chemistry and some recent findings. *Polymer* **1997**, *38* (4), 927-938.
  75. Zhang, J.; Gellman, S. H.; Stahl, S. S., Kinetics of Anionic Ring-Opening Polymerization of Various Substituted  $\beta$ -Lactams: Homopolymerization and Copolymerization. *Macromolecules* **2010**, *43* (13), 5618-5626.
  76. Stratula-Vahnoveanu, B.; Vasiliu-Oprea, C., Anionic Polymerization of Lactams in Microdispersion. I. Kinetic Aspects of the Process of Caprolactam Polymerization. *Polymer-Plastics Technology and Engineering* **2002**, *41* (5), 981-995.
  77. Photoelectric methods of measuring the velocity of rapid reactions I-General principles and controls. *Proceedings of the Royal Society of London. Series A - Mathematical and Physical Sciences* **1936**, *155* (885), 258.
  78. Dan, F.; Vasiliu-Oprea, C., On the relationship between synthesis parameters and morphology of the anionic polycaproatamide obtained in organic media. III. Macroporous powders obtained using CO<sub>2</sub> and carbodiimides as activating compounds. *Journal of Applied Polymer Science* **1998**, *67* (2), 231-243.
  79. Ueda, K.; Nakai, M.; Hosoda, M.; Tai, K., Synthesis of High Molecular Weight Nylon 6 by Anionic Polymerization of  $\epsilon$ -Caprolactam. Mechanism and Kinetics. *Polymer Journal* **1997**, *29*, 568.
  80. Chrzczonowicz, S.; Włodarczyk, M.; Ostaszewski, B., Polymerization of  $\epsilon$ -caprolactam and  $\zeta$ -enantholactam in non-polar solvents. *Die Makromolekulare Chemie* **1960**, *38* (1), 159-167.
  81. Chrzczonowicz, S.; Włodarczyk, M., Polymerization of  $\epsilon$ -caprolactam in solvent. II. The infrared study of the mechanism of polymerization. *Die Makromolekulare Chemie* **1961**, *48* (1), 135-143.
  82. Chrzczonowicz, S., Zesz nauk Politech Lodz: Chemia, 1957; Vol. 5, p 65.
  83. Biernacki, P.; Włodarczyk, M., A study of molecular weight of polycaproatamide obtained by anionic polymerization of caprolactam in solvent. *European Polymer Journal* **1975**, *11* (1), 107-109.
  84. Biernacki, P.; Chrzczonowicz, S.; Włodarczyk, M., Molecular weight distribution of polycaproatamide obtained by anionic polymerization of caprolactam in solvent. *European Polymer Journal* **1971**, *7* (6), 739-747.

85. US Patent Application for NOVEL POWDER POLYMER, METHOD FOR THE PREPARATION THEREOF, AND USE AS A THICKENER Patent Application (Application #20160167040 issued June 16, 2016) - Justia Patents Search.
86. Vasiliu-Oprea, C.; Dan, F., On the relation between synthesis parameters and morphology of anionic polycaproatamide obtained in organic media. I. Influence of the Na [O (CH<sub>2</sub>)<sub>2</sub>OCH<sub>3</sub>] 2AlH<sub>2</sub>/isophorone diisocyanate catalytic system. *Journal of applied polymer science* **1996**, 62 (10), 1517-1527.
87. Stehlíček, J.; Šebenda, J., Anionic polymerization of  $\epsilon$ -caprolactam-lix effect of the ratio of reacting components, of the medium and of the ring size on the initial stage of the anionic polymerization of lactams. *European Polymer Journal* **1986**, 22 (10), 769-773.
88. Dijck, W. J. D., Process and apparatus for intimately contacting fluids. Google Patents: 1935.
89. Sergeev, S., Fluid oscillations in pipes at moderate Reynolds numbers. *Fluid Dynamics* **1966**, 1 (1), 121-122.
90. Karr Andrew, E., Performance of a reciprocating-plate extraction column. *AIChE Journal* **1959**, 5 (4), 446-452.
91. Bellhouse, B. J.; Bellhouse, F. H.; Curl, C. M.; MacMillan, T. I.; Gunning, A. J.; Spratt, E. H.; MacMurray, S. B.; Nelems, J. M., A HIGH EFFICIENCY MEMBRANE OXYGENATOR AND PULSATILE PUMPING SYSTEM, AND ITS APPLICATION TO ANIMAL TRIALS. *ASAIO Journal* **1973**, 19 (1), 72-79.
92. Sobey, I. J., On flow through furrowed channels. Part 1. Calculated flow patterns. *Journal of Fluid Mechanics* **1980**, 96 (1), 1-26.
93. Stephanoff, K. D.; Sobey, I. J.; Bellhouse, B. J., On flow through furrowed channels. Part 2. Observed flow patterns. *Journal of Fluid Mechanics* **1980**, 96 (1), 27-32.
94. Mackley, M., Usingocillatory flow to improve performance. *Chemical engineer* **1987**, (433), 18-21.
95. Ni, X.; Zhang, Y.; Mustafa, I., An investigation of droplet size and size distribution in methylmethacrylate suspensions in a batch oscillatory-baffled reactor. *Chemical Engineering Science* **1998**, 53 (16), 2903-2919.
96. Knott, G.; Mackley, M., On eddy motions near plates and ducts, induced by water waves and periodic flows. *Phil. Trans. R. Soc. Lond. A* **1980**, 294 (1412), 599-623.
97. Brunold, C. R.; Hunns, J. C. B.; Mackley, M. R.; Thompson, J. W., Experimental observations on flow patterns and energy losses for oscillatory flow in ducts containing sharp edges. *Chemical Engineering Science* **1989**, 44 (5), 1227-1244.
98. Dickens, A.; Mackley, M.; Williams, H., Experimental residence time distribution measurements for unsteady flow in baffled tubes. *Chemical Engineering Science* **1989**, 44 (7), 1471-1479.
99. Mackley, M. R.; Ni, X., Mixing and dispersion in a baffled tube for steady laminar and pulsatile flow. *Chemical Engineering Science* **1991**, 46 (12), 3139-3151.
100. Fitch, A. W.; Jian, H.; Ni, X., An investigation of the effect of viscosity on mixing in an oscillatory baffled column using digital particle image velocimetry and computational fluid dynamics simulation. *Chemical Engineering Journal* **2005**, 112 (1), 197-210.
101. Ni, X.; Gough, P., On the discussion of the dimensionless groups governing oscillatory flow in a baffled tube. *Chemical Engineering Science* **1997**, 52 (18), 3209-3212.
102. Sarpkaya, T., Experimental Determination of the Critical Reynolds Number for Pulsating Poiseuille Flow. *Journal of Basic Engineering* **1966**, 88 (3), 589-598.
103. Sobey, I. J., Observation of waves during oscillatory channel flow. *Journal of Fluid Mechanics* **1985**, 151, 395-426.
104. Jones, J. E. H.; Bajura, R. A., A Numerical Analysis of Pulsating Laminar Flow Through a Pipe Orifice. *Journal of Fluids Engineering* **1991**, 113 (2), 199-205.
105. Ni, X.; Zhang, Y.; Mustafa, I., Correlation of polymer particle size with droplet size in suspension polymerisation of methylmethacrylate in a batch oscillatory-baffled reactor. *Chemical Engineering Science* **1999**, 54 (6), 841-850.

106. Hopff Von, H.; Lüssi, H.; Gerspacher, P., Zur kenntnis der perlpolymerisation. 2. Mitt. praktische anwendung der dimensionsanalyse auf das system MMA – mowiol 70/88. *Die Makromolekulare Chemie* **1964**, 78 (1), 37-46.
107. Erbay, E.; Blgç, T.; Karali, M.; Savaşçi, Ö. T., Polystyrene Suspension Polymerization: The Effect of Polymerization Parameters on Particle Size and Distribution. *Polymer-Plastics Technology and Engineering* **1992**, 31 (7-8), 589-605.
108. Langner, F.; Moritz, H.; Reichert, K., On particle size of suspension polymers, II. Polymerising two-phase systems. . *Ger. Chem., Engng*, **1979**, 2, 329-336.
109. Schroder, R.; Piotrowski, P., On particle formation during suspension polymerisation of styrene. *Ger. Chem. Engng* **1982**, 5, 139-146.
110. Oldshue James, Y., Mixing—principles and applications, by Shinji Nagata, Published by Halsted Press, 458 pages, \$32.50. *AIChE Journal* **1976**, 22 (2), 412-413.
111. Chew, C. M.; Ristic, R. I., Crystallization by oscillatory and conventional mixing at constant power density. *AIChE Journal* **2005**, 51 (5), 1576-1579.
112. Jealous, A. C.; Johnson, H. F., Power Requirements for Pulse Generation in Pulse Columns. *Industrial & Engineering Chemistry* **1955**, 47 (6), 1159-1166.
113. Mackley, M. R., *Process innovation using oscillatory flow within baffled tubes*. *Trans. IChemE* **1991**, 69(A), 197-199.
114. Baird, M. H. I.; Stonestreet, P., Energy dissipation in oscillatory flow within a baffled tube. *Trans. IChemE* **1995**, 73 (5), 503-511.
115. Ni, X.; Liao, A., Effects of Cooling Rate and Solution Concentration on Solution Crystallization of L-Glutamic Acid in an Oscillatory Baffled Crystallizer. *Crystal Growth & Design* **2008**, 8 (8), 2875-2881.
116. Ni, X.; Cosgrove, J. A.; Arnott, A. D.; Greated, C. A.; Cumming, R. H., On the measurement of strain rate in an oscillatory baffled column using particle image velocimetry. *Chemical Engineering Science* **2000**, 55 (16), 3195-3208.
117. Abbott, M. S. R.; Harvey, A. P.; Perez, G. V.; Theodorou, M. K., Biological processing in oscillatory baffled reactors: operation, advantages and potential. *Interface Focus* **2013**, 3 (1).
118. Baird, M. H. I.; Rao, N. V. R., Power dissipation and flow patterns in reciprocating baffle-plate columns. *The Canadian Journal of Chemical Engineering* **1995**, 73 (4), 417-425.
119. Ni, X.; Nelson, G.; Mustafa, I., Flow patterns and oil—water dispersion in a 0.38 m diameter oscillatory baffled column. *The Canadian Journal of Chemical Engineering* **2009**, 78 (1), 211-220.
120. Ni, X.; Mackley, M. R., Chemical reaction in batch pulsatile flow and stirred tank reactors. *The Chemical Engineering Journal* **1993**, 52 (3), 107-114.
121. Mazlan, H. W. Y. a. S. S. B. a. N. A., Evaluation of power density on the bioethanol production using mesoscale oscillatory baffled reactor and stirred tank reactor. *IOP Conference Series: Materials Science and Engineering* **2018**, 334 (1), 012070.
122. Montgomery, D., Design Analysis of Experiments 5ed.
123. Li Pi Shan, C.; Soares João, B. P.; Penlidis, A., Ethylene/1-octene copolymerization studies with in situ supported metallocene catalysts: Effect of polymerization parameters on the catalyst activity and polymer microstructure. *Journal of Polymer Science Part A: Polymer Chemistry* **2002**, 40 (24), 4426-4451.
124. Chen, C.-H., Application of factorial experimental design to study the influence of polymerization conditions on the yield of polyaniline powder. *Journal of Applied Polymer Science* **2002**, 85 (7), 1571-1580.
125. De Wet-Roos, D.; Knoetze, J. H.; Cooray, B.; Sanderson, R. D., Emulsion polymerization of an epoxy-acrylate emulsion stabilized with polyacrylate. II. Using the results of statistically designed experiments to deduce a possible polymerization mechanism. *Journal of Applied Polymer Science* **2000**, 76 (3), 368-381.
126. Vivaldo-Lima, E.; Wood Philip, E.; Hamielec Archie, E.; Penlidis, A., Kinetic model-based experimental design of the polymerization conditions in suspension copolymerization of



- styrene/divinylbenzene. *Journal of Polymer Science Part A: Polymer Chemistry* **2000**, 36 (12), 2081-2094.
127. Jain, S. P.; Singh, P. P.; Javeer, S.; Amin, P. D., Use of Plackett–Burman Statistical Design to Study Effect of Formulation Variables on the Release of Drug from Hot Melt Sustained Release Extrudates. *AAPS PharmSciTech* **2010**, 11 (2), 936-944.
  128. Haaland, P. D., *Experimental design in biotechnology*. CRC press: 1989; Vol. 105.
  129. Stanbury, P. F.; Whitaker, A.; Hall, S. J., *Principles of fermentation technology*. Elsevier: 2013.
  130. Wasserstein, R. L.; Lazar, N. A., The ASA's Statement on p-Values: Context, Process, and Purpose. *The American Statistician* **2016**, 70 (2), 129-133.
  131. Schreiber, H. P.; Waldman, M. H., Effect of temperature on molecular weight measurements in polyethylene. *Journal of Polymer Science Part A: General Papers* **1964**, 2 (4), 1655-1668.
  132. Giz, A.; Çatalgil-Giz, H.; Alb, A.; Brousseau, J.-L.; Reed, W. F., Kinetics and Mechanisms of Acrylamide Polymerization from Absolute, Online Monitoring of Polymerization Reaction. *Macromolecules* **2001**, 34 (5), 1180-1191.
  133. Haraguchi, K.; Xu, Y.; Li, G., Poly(N-isopropylacrylamide) Prepared by Free-Radical Polymerization in Aqueous Solutions and in Nanocomposite Hydrogels. *Macromolecular Symposia* **2011**, 306-307 (1), 33-48.
  134. Nigmatullin, R.; Bencsik, M.; Gao, F., Influence of polymerisation conditions on the properties of polymer/clay nanocomposite hydrogels. *Soft Matter* **2014**, 10 (12), 2035-2046.
  135. Hilaire, J.-C.; Guerin, R. Anhydrous process for the manufacture of polyamide powder from lactam in the presence of N,N'-alkylene bis amide. US4694063A, 1987/09/15/, 1987.
  136. Chakraborty, J. N., 23 - Dyeing of nylon. In *Fundamentals and Practices in Colouration of Textiles*, Chakraborty, J. N., Ed. Woodhead Publishing India: 2014; pp 286-300.
  137. Rahman, M. A.; Renna, L. A.; Venkataraman, D.; Desbois, P.; Lesser, A. J., High crystalline, porous polyamide 6 by anionic polymerization. *Polymer* **2018**, 138, 8-16.
  138. Lok, K. P.; Ober, C. K., Particle size control in dispersion polymerization of polystyrene. *Canadian Journal of Chemistry* **1985**, 63 (1), 209-216.
  139. Walbridge, D. J., Polymerization in Non-aqueous Dispersions. In *Comprehensive Polymer Science and Supplements*, Elsevier: 1989; pp 243-260.
  140. Baudonnet, L.; Grossiord, J. L.; Rodriguez, F., Effect of Dispersion Stirring Speed on the Particle Size Distribution and Rheological Properties of Three Carbomers. *Journal of Dispersion Science and Technology* **2004**, 25 (2), 183-192.
  141. Gupta, B. S.; Afshari, M., 14 - Tensile failure of polyacrylonitrile fibers. In *Handbook of Tensile Properties of Textile and Technical Fibres*, Bunsell, A. R., Ed. Woodhead Publishing: 2009; pp 486-528.
  142. Vasiliu-Oprea, C.; Dan, F., On the Relation Between Synthesis Parameters and Morphology of Anionic Polycapromide Obtained in Organic Media. II. Influence of the Na [O (CH<sub>2</sub>)<sub>2</sub>~ 2OCH<sub>2</sub>~ 3]~ 2AlH~ 2/Aliphatic Diisocyanates Catalytic Systems. *Journal of applied polymer science* **1997**, 64 (13), 2575-2583.
  143. Vacca, A.; Sabatini, A.; Bologni, L., A procedure for the calculation of enthalpy changes from continuoustitration calorimetric experiments. *Journal of the Chemical Society, Dalton Transactions* **1981**, (6), 1246-1250.
  144. Schuttlefield, J. D.; Grassian, V. H., ATR–FTIR Spectroscopy in the Undergraduate Chemistry Laboratory. Part I: Fundamentals and Examples. *Journal of Chemical Education* **2008**, 85 (2), 279.
  145. Hanford, W. E.; Joyce, R. M., Polymeric amides from epsilon-caprolactam. *Journal of Polymer Science* **1948**, 3 (2), 167-172.
  146. Cornish-Bowden, A., Chapter 2 - Introduction to enzyme kinetics. In *Fundamentals of Enzyme Kinetics*, Cornish-Bowden, A., Ed. Butterworth-Heinemann: 1979; pp 16-38.
  147. Rushton, J. H., Power characteristics of mixing impellers Part 1. *Chem. Eng. Prog.* **1950**, 46, 395-404.
  148. Pepper, D. C., Cationic ring-opening polymerization, Part 2: Synthetic applications (Advances in Polymer Science, Volumes 68/69). By S. Penczek, P. Kubisa and K. Matyjaszewski, Springer- Verlag,

- Berlin Heidelberg, 1985. pp. 300, price DM 188.00. ISBN 3-540-13781-5. *British Polymer Journal* **1986**, 18 (6), 399-400.
149. Mark, J. E., *Polymer Data Handbook*. Oxford University Press: 2009.
150. Yan, C.; Shi, Y.; Yang, J.; Liu, J., Preparation and selective laser sintering of nylon-12 coated metal powders and post processing. *Journal of Materials Processing Technology* **2009**, 209 (17), 5785-5792.
151. Griehl, W.; Ruestem, D., Nylon-12-Preparation, Properties, and Applications. *Industrial & Engineering Chemistry* **1970**, 62 (3), 16-22.
152. Du, L.; Yang, G., Reactive extrusion for the synthesis of nylon 12 and maleated low-density polyethylene blends via the anionic ring-opening polymerization of lauryllactam. *Journal of Applied Polymer Science* **2009**, 114 (5), 2662-2672.
153. F. Hughes, J., *Electrostatic Powder Coating*. 1984.
154. Macchio, R. A.; Russ, J. G.; Slobody, B.; Tietjen, M. Microfine cosmetic powder comprising polymers, silicone, and lecithin. US5023075A, 1991/06/11/, 1991.
155. Frunze, T. M.; Kotel'nikov, V. A.; Kurashev, V. V.; Ivanova, S. L.; Komarova, L. I.; Korshak, V. V., The relative reactivities of  $\epsilon$ -caprolactam and  $\omega$ -dodecalactam in activated anionic copolymerization. *Polymer Science U.S.S.R.* **1976**, 18 (2), 348-353.
156. Vasiliu-Opera, C.; Dan, F.; Stratula-Vahnoveanu, B., Ultrafine Polycapraamide particles synthesis and characterisation. *Buletinul Institutului Politehnic din Iasi* **2000**, XLVI, 81-92.
157. Nogueira, A. L.; Quadri, M. B.; Araújo, P. H. H.; Machado, R. A. F., Influence of Semi-Batch Operations on Morphological Properties of Polystyrene Made in Suspension Polymerization. *Procedia Engineering* **2012**, 42, 1045-1052.
158. Xing, Q.; Zhang, X.; Dong, X.; Liu, G.; Wang, D., Low-molecular weight aliphatic amides as nucleating agents for poly (L-lactic acid): Conformation variation induced crystallization enhancement. *Polymer* **2012**, 53 (11), 2306-2314.
159. Gogolewski, S.; Czerntawska, K.; Gastorek, M., Effect of annealing on thermal properties and crystalline structure of polyamides. Nylon 12 (polylauro lactam). *Colloid and Polymer Science* **1980**, 258 (10), 1130-1136.